MASTER OF PHILOSOPHY

An investigation of the dynamic properties of a centreless grinding machine with a view to improving the grinding potential in terms of geometric form

Willmore, J. I.

Award date:
1972

Awarding institution:
Coventry University

"AN INVESTIGATION OF THE DYNAMIC PROPERTIES OF A CENTRELESS GRINDING MACHINE WITH A VIEW TO IMPROVING THE GRINDING POTENTIAL IN TERMS OF GEOMETRIC FORM"

BY

J. I. WILLMORE, C.ENG., F.I.PROD.E., M.I.MECH.E.

" A THESIS SUBMITTED AS PARTIAL REQUIREMENTS FOR THE DEGREE OF MASTER OF PHILOSOPHY TO THE COUNCIL FOR NATIONAL ACADEMIC AWARDS FOLLOWING WORK CARRIED OUT IN THE DEPARTMENT OF PRODUCTION ENGINEERING, FACULTY OF ENGINEERING, LANCHESTER POLYTECHNIC, COVENTRY. "

JANUARY, 1972

ACKNOWLEDGEMENTS

The Author wishes to acknowledge continuous encouragement and guidance offered to him throughout the investigations by his Supervisor and Director of Studies, Dr. W. B. Rowe, B.Sc., Ph.D., C.Eng., M.I.Mech.E., M.I.Prod.E., and also to Professor J. Loxham, D.Sc., C.G.I.A., C.Eng., F.I.Mech.E., F.I.Prod.E., F.B.I.M., Supervisor, for his expert advice and encouragement. The kindness of Mr. R. L. Aston, C.Eng., F.I.Mech.E., F.I.Prod.E., F.G.S., Head of Department, in permitting this work to be carried out in the Department of Production Engineering, Lanchester Polytechnic, Coventry.

Thanks are also due to Dr. N. W. Bellamy, B.Eng., Ph.D., C.Eng., M.I.E.E., Head of Department, for the use of the computer facilities in the Department of Electrical Engineering, Lanchester Polytechnic, Coventry, and to Mr. L. J. Hulton, M.A., C.Eng., M.I.E.E., for his assistance in the use of the computer.

To the Science Research Council for their financial support, and to Wickman Limited, Coventry, who sponsored the investigation.

Personal thanks are also due to Mr. C. Callingham, Chief Technician in the Laboratories, and to Mr. K. H. Wright, Technician on the Science Research Council project, who were of considerable assistance in the performance of the tests.

THE AUTHOR

John Innes Willmore commenced his engineering career as a five-year indentured apprentice to toolmaking and general engineering with Standard Telephones & Cables Ltd., of North London.

As a part-time day release student, and by subsequent further part-time studies, he obtained an O.N.C. and H.N.C. in mechanical engineering with endorsements.

From the completion of his apprenticeship in 1939 until 1944, he was employed as a press tool designer with the same company. During 1944, he was directed to a new factory controlled by Standard Telephones & Cables Ltd. in South Wales, where he was given the post of electrical relay assembly workshop foreman.

In 1946, he took up an appointment with De Havilland Aircraft Co., Hatfield, as a senior tool designer and was concerned with the initial production of the "Comet" Aircraft. During his employment with De Havillands, he became an Associate Member of the Institution of Mechanical Engineers.

From 1951 to 1953 he was an engineer with the Ministry of Supply in the Directorate of Aircraft Production.

Whilst in the employ of De Havilland and M.O.S., he was a part-time lecturer at Enfield Technical College, lecturing in Applied Mechanics. In October 1953, he took up a full-time teaching appointment as a lecturer in the Production Engineering Department of Enfield Technical College, Middlesex, and was given three months sabbatical

leave in 1959 to study N.C. Machine Tools in the E.M.I. Ltd., Industrial Laboratory. He also obtained an O.N.C. in Electrical Engineering, by part-time study, whilst he was a lecturer at Enfield Technical College.

In May 1960, he joined the Lanchester College of Technology, Coventry, as a senior lecturer in the Production Engineering Department and soon after, obtained the position of Principal Lecturer, Deputy Head of the Department of Production Engineering in the same college.

The successful running of the degree course at Lanchester College, brought about the disposing of the Deputy Head of Department post and the introduction of the posts of Senior Course Tutor. The author was appointed Senior Course Tutor to the B.Sc. Production Engineering Course in September 1968; a position he now holds in the recently formed Lanchester Polytechnic.

Published Papers

(1) "Plunge Grinding and the Accuracy of the Work-piece Geometry", by J. I. Willmore. 6th I.M.T.D.R. Conference, 1965.

(2) "Machine Dynamics and the Centreless Grinding process", by J. I. Willmore, W. B. Rowe and J. Loxham. To be published.

Relevant Advanced Study Courses Attended

(1) Course of lectures on Hybrid Computing. Lanchester College of Technology, February 1967.

(2) Mechanical Vibration. Lanchester College of Technology, January 1968.

CONTENTS

LIST OF ILLUSTRATIONS

NOMENCLATURE

α Angle between the grinding wheel contact normal OA and the workblade contact normal OB. (See fig. 41)

α_1 Angle between the line joining the wheel centres and the inclined face of the workblade. (See figs. 1 and 41)

β Included tangent angle between the grinding wheel contact normal and the control wheel contact normal. (See fig. 1)

λ Static stiffness

A Cross Sectional Area

$A_{MAX.}$ Resonance amplitude

$A(t)$ Apparent depth of cut when the workpiece is in the position indicated by t.

C Compliance

c Damping

c_c Critical damping

D Damping factor

E Young's Modulus of Elasticity

F Force

f	Frequency
f_o	Natural frequency
Δf	Difference between the frequencies at phase 135° and at phase 45°
G	Modulus of Rigidity
I	Second moment of area
K	Machining - elasticity parameter
K_1	Depth of cut factor for workblade position
K_2	Depth of cut factor for control wheel position
K_s	Chip thickness coefficient
M	Mass
P	Force
Q	Dynamic amplification factor
r	Reduction in radius from the workpiece reference circle
$S(t)$	True depth of cut
t	Time for work to revolve through angle θ
T_1	" " " " " " " α
T_2	" " " " " " " $\pi-\beta$
T	" " " " " " " 2π
W	Load
$x, \dot{x}, \ddot{x}$	Machine deflection and time derivatives

SUMMARY

A centreless grinding machine has been investigated to determine the nature of machine deflections under the influence of the grinding force.

The static deflections were analysed into the contributions from the various major elements of the machine, including the control wheel, bearings, spindle and housing, the grinding wheel bearings, spindle and housing. It was found that the most compliant elements were the control wheel bearings.

The dynamic deflections were analysed and as far as possible identified with those elements mainly involved in the vibration. Equivalent dynamic parameters were obtained from the lower frequency resonances. It was found that the resonance at 82 Hz was of dominant importance in the formation of the workpiece profile. This mode was largely associated with the nature of the constraint of the control wheelhead by the tray.

The process was simulated on a hybrid computer and it was shown that the results correlated well with grinding experiments and provides a realistic tool for further investigations.

Some limitations of other existing methods of analysis have been discussed.

In practical grinding tests, the influence of varying wheel conditions on the roundness and sizing were observed. Suggestions have been made for improved design of the machine.

The investigations were restricted to plunge grinding operations.

CHAPTER I

1.1 INTRODUCTION

Whereas in cylindrical grinding between centres there is a rotational axis of the workpiece which is the basis for producing a cylinder, this is not the case in centreless grinding.

Considering the various forms that the centreless grinding process may take, it is very doubtful if the workpiece, during the grinding operation can ever rotate continually on one centreline and it is generally accepted that the instantaneous centre of rotation of the workpiece moves in relation to the cutting edge of the grinding wheel (1).

It has been substantiated by many people (1, 2, 3) that this workpiece movement relative to the grinding and control wheels is a principal cause of errors in roundness on the ground workpieces. To reduce this inherent inaccuracy of the centreless grinding process, substantial investigations have been carried out (4, 5, 6) to determine the optimum position of the nominal workpiece centre relative to the grinding and control wheel centres and the best support blade angle which will minimise the errors in roundness. The inherent mechanism by which the process tends to produce workpiece movements may be described as the "Geometric Effect". Referring to figure 1, it can be concluded that if variations in the component radius takes place, there may sometimes be a fluctuation in the forces between the grinding wheel, workpiece and the control wheel, which will act as vibration, forcing the machine structure.

Depending upon the machine structure characteristics this induced vibration will most likely produce further errors in roundness on the ground component, which will in some form modify the forced vibration.

It is therefore possible to consider the centreless grinding process as a closed loop system in which the geometric effects and the machine structural characteristics are an integral part of a system. Furthermore, if it may be considered as a closed loop system, it should be possible to simulate the system on a computer.

1.2 The Aims and Scope of the Investigation

The broad objectives of the research were as follows:-

(i) To investigate an existing machine structural behaviour with a view to making recommendations for structural improvements in relation to the rounding ability in grinding.

(ii) To determine the predominant structural characteristics of the machine which were affecting errors in roundness and hence to simulate the machine and process employing a hybrid analogue/digital computer.

(iii) To deduce if a correlation exists between the waviness predicted from the model and waviness measured from experiments.

The aims have been achieved in so far as:-

(i) From static tests it has been shown where the main compliances arise so that it may be concluded where design improvement is required. The static tests are described in Chapter III.

(ii) Dynamic tests have revealed the vibration mode of critical importance and are described in Chapter IV.

(iii) A simplified model has been constructed for a hybrid computer as described in Chapter V.

(iv) Grinding tests were carried out with simultaneous recording of machine deflections. The influence of the process variations was investigated and the extent of correlation with the simulation model is discussed in Chapter VI.

CHAPTER II

2.1 Review of Other Work

Although the centreless grinding process in its present form, had been in operation since before 1920, the first analytical study of the process did not appear until 1939 when Sachsenberg and Kreher (7) recognized the importance of the workpiece position relative to the grinding wheel and control wheel centres. The term "Gleichdicke" (equal diameter lobing) then came into usage to describe shapes arising from centreless grinding.

In 1946, A. H. Dall (8) of the Cincinnati Milling Machine Company, U.S.A. published a paper in which he gave details of a mathematical analysis of the workpiece movement during the centreless grinding process. His work described how errors in roundness supposedly decayed as the process progressed. The correcting effect being obtained by the "geometry" of the process, however no account was taken into consideration concerning the machine characteristics in his main hypothesis. Dall, in his concluding remarks referred to other factors which contributed to the "rounding" effect during the process namely:-

(1) Centre of workpiece shift.

(2) Wheel interference.

(3) Elasticity of the wheels.

He also stated that these factors did not submit to a mathematical analysis, because their effects varied greatly with the magnitude and character of the errors in roundness.

Commenting on the effect of the elasticity of the wheel surfaces he stated that wheel deformation would cause a decrease

in the errors in roundness, also that the frequency at which chatter often occurred, coincided with the natural frequency of one or other of the structural members which either supported the regulating wheel, grinding wheel or the work support blade.

Dall also postulated that a rigid machine structure, having high natural frequencies, would prevent self induced vibrations, because the arc of contact of the wheel would cover more than one flat on the workpiece. This condition he described as that of a damped vibration.

It is interesting to note that Colwell (9) did in fact conduct grinding tests with a high frequency vibrating grinding wheel.

Dall's work was elaborated upon by Yonetsu (3) who produced a very complicated mathematical technique to predict "Geometric" errors, based on a vibration free centreless grinding process. In further work by the same author (10) he introduced the effect of the elastic deformation of the regulating wheel, and stated that the actual depth of cut was smaller than the apparent depth of cut. He also defined a constant "K" relating these two depths of cuts, and then proceeded to show that the constant "K" varied according to the magnitude of the depth of cut.

It is interesting to note that Yonetsu used a dial gauge as a measuring instrument to detect errors in roundness, when he used findings from practical grinding tests to verify his theory.

The introduction of instruments capable of detecting

small errors in roundness, such as the "Talyrond", accelerated the progress of research on centreless grinding especially the theory relating the errors generated on the workpiece, to the magnitude of the workpiece movements.

The theory presented by Rowe (11) appears to be representative of the general theory on geometric effects in centreless grinding.

During the period 1960-1965 the following publications were presented; Rowe and Barash (2) described a method for simulating the centreless grinding process using a digital computer, which took into account the geometric considerations and had an assumption for the elastic deflection of the machine. A term "K" the machining elasticity parameter, was introduced into the theory, and was defined as a ratio between the true depth of cut and the apparent depth of cut. This technique took into account the long time delay terms in the geometric process, but did not take account the machine resonances.

Rowe and Koenigsberger (6) discussed the work regenerative effect in centreless grinding, and represented the dynamic characteristics of the machine by a single degree of freedom system. It should be noted that they stated, "Although it is considered that the inertia and damping associated with the motion of the workpiece may play a significant part in the occurrence of chatter, these have been neglected. This is because no satisfactory method of including their effect has yet been found.

Rowe and Koenigsberger devised charts of limiting sta-

bility, based on the near classical, steady state linear analysis technique, employed by Tobias and Fishwick (12) for drilling chatter. While this analysis illustrates some interesting features of the process its usefulness was severely limited. This is because a geometrically unstable process may be unstable for all speeds and depths of cut. As a special case, Rowe and Koenigsberger analysed geometrical instability.

Unfortunately, it was found that the theory always predicted instability for some workpiece shape. It was concluded that any useful technique should indicate the degree of instability. This is an objective which had never been attempted.

Whilst these investigations were being carried out at Manchester, Becker (4) in Aachen was conducting similar experiments; determining the various characteristics of the structure of a centreless grinding machine and formulated an analogue computer model to study the limits of stability of the process. In his thesis, Becker stated; "the frequency responses of the machine tool are too complicated to justify the time that would be involved in simulating them on the analogue computer", and he then reasoned that it was simpler to obtain the impedance of the significant elements of the machine structure, by referring to the impedance locus diagram, obtained from the machine, from which the amplitude and phase of the impedance could be measured for a <u>given</u> frequency. His analogue model included the machine impedance constants, so derived, and had two time delays incorporated into the

model. The time delays were effected by the time-constants of an operational amplifier, which were adjusted to produce the desired phase shift. Accordingly, his model was simulating the steady state of the process, and neglected the tansient behaviour of the process.

Kaliszer and Singhal (13) proposed a method of establishing a relationship between the vibration marks generated on the workpiece periphery and the rigidity of the grinding wheel-workpiece-grinding machine system for a cylindrical grinding machine. Their analysis of the structure was based on two dynamic systems representing the headstock and tailstock of the machine respectively. Each system was considered to have two degrees of freedom. Dynamic tests were applied to the systems and the dynamic characteristics were obtained.

Gurney (1) presented details of a purely theoretical simulation whereby an analogue computer could be used to examine whether a centreless grinding process was dynamically stable or whether self excited oscillation (chatter) would build up. He also stated that the significance of the dynamic characteristics of the machine structure could be examined, and if need be modified, to improve the roundness of the workpiece. In his simulation of the process he used a sinusoidal signal together with a Transfer Function Analyser to generate the depth of the grinding cut, which excited an analogue one degree of freedom model. The output from the model was the vibration of the machine structure. However, Gurney's model was in fact an open loop system generating the depth of cut in isolation from the dynamic properties of

the machine, also by utilising a T.F.A. in the model, the time delay was not representative of the true time-delay, and therefore did not allow the transient period of the vibration to operate.

In practice the depth of cut is continuously being modified by the amplitude and phase of the structural vibrations, and in this respect Gurney's model, although a link in solving centreless grinding problems is restricted for the same reasons as the dynamic analysis by Rowe and Koenigsberger.

Furukawa, Miyashita and Shiozaki (14) in their study of the process, recently published a paper, in which the process was considered as a closed loop system, having geometric errors and equivalent structural machine elements as an integral part of the system. Their analysis however did not allow for the transient part of the vibration to take place.

Rowe and Richards (5) presented a geometric analysis from which geometric stability charts were derived. The most unstable operating conditions were inferred by correlation with grinding results as described by Richards, Rowe and Koenigsberger (15).

Reviewing previous work, it appears to the writer that the present situation regarding further investigation into centreless grinding process required:

(1) A realistic method of determining the significant machine structural characteristics.

(2) A theory which takes into account the transient part of the process.

Concerning (1) Kennedy and Pancu (16) described a method of uncoupling certain multi-degree of freedom vibrating systems, into a number of equivalent one-degree of freedom systems, and this method has been used in this investigation (see Chapter V).

CHAPTER III

STATIC TESTS

3.1 Aims of Static Tests

Static tests were conducted:-

(i) To determine the static stiffness of the various elements of the machine structure to assist in the analysis of the dynamic response locus of the machine (see Chapter IV).

(ii) To determine the structural deflections of the machine during the grinding process and provide a basis for increasing machine stiffness by improvement of the design.

(iii) To derive deflection/load data to assist in the assessment of certain grinding forces.

3.2 Description of Apparatus and Calibration

The machine was tested with the spindles rotating at their normal speeds, in order that the bearings should contribute their usual operating compliances. The grinding wheel and the control wheel were therefore removed to avoid the necessity for loading against moving abrasive surfaces. Each wheel was replaced by solid aluminium discs of equal weight and equal width.

Figure 2 shows the simple weight/lever rig which was used for applying static loads on to a central position on the replica wheels.

Incorporated in the design of this rig was an aluminium push-rod sliding in an air-bearing to minimise stiction. The push-rod was connected at its end to a ball bearing which made contact with the replica wheel under test. To avoid cold welding taking place between the loaded ball bearing and the

surface of the rotating replica wheels, it was found necessary to provide a track, hence a small steel ring was inserted into the surface of each of the replica wheels.

In order to measure deflections of the grinding wheel spindle in situ in the machine, three horizontal holes were drilled, reamed and tapped into the grinding wheel spindle housing at intervals along its length and into which were fitted spring loaded displacement probes. The probes made contact with the spindle and had nylon inserts in the ends at the points of contact with the spindle (fig. 3). Parallel motion spring steel strips were incorporporated in the design of the probes to minimise measuring cosine errors, also the steel strips provided the light loads necessary to maintain the pressure between the spindle and the probe.

Modifications were also made to the control wheel housing (see Fig. 4a and b) with an additional rig to house two displacement transducers to measure the housing deflections at points 5 inches either side of the replica control wheel position. To provide a datum surface when investigating the deflections of the grinding wheel housing the spindle displacement probes were removed and flat ended plugs were inserted into the tapped holes.

Taylor Hobson variable inductance contacting transducers Type 112/497 were used with their associated amplifiers and recorders to measure the deflections of:-

(1) The grinding wheel spindle via the probes.

(2) The grinding wheel spindle housing via the plugs.

Variable inductance frequency modulated proximity transducers made by Southern Instruments, Type G.323, were used to measure deflections of:-

(1) The replica grinding wheel in situ in the machine.

(2) The replica control wheel in situ in the machine.

(3) The control wheel spindle via the probes.

Wayne Kerr variable capacitance proximity transducers were used to measure deflections of the control wheel housing deflections.

A special test rig to receive the grinding spindle (see Fig. 5) was designed and had clamps which approximated to the normal restraints on the grinding wheel spindle when in situ in the machine. A second test rig (see Fig. 6) was designed and made to enable stiffness tests to be conducted on the control wheel.

Measurement of the grinding spindle deflections and the penetrations of the load bar into the control wheel, using the respective tests rigs, were obtained by using Taylor Hobson variable inductance contacting transducers, type 112/497.

All the transducers were individually calibrated statically, using special adaptors, a vertical comparator stand, and a set of reference slip gauges.

3.3 Experimental Procedure

Before commencing the static tests on the machine spindles, when they were in situ in the machine, a warming up period of two hours was allowed. With the spindles rotating and under

their normal operating conditions, static loading of the grinding and control wheel spindles took place, by applying the loads in the horizontal plane of the machine, and at the grinding point (See Fig. 2).

The total displacements of the spindles relative to the workpiece position were recorded at the grinding point on the replica wheels and at other positions along the spindles as shown in figures 3 and 4b.

Deflections of the grinding wheel spindle housing and that of the control wheel spindle were similarly conducted, by applying static loads at the grinding point, and measuring the displacement of the respective housing at the position indicated in figures 3 and 4b.

To obtain the stiffness of the grinding wheel spindle, it was removed from the machine and fitted into a special test rig (fig. 5). Again the spindle was statically loaded at the reference grinding point, and deflections of the spindle noted at the grinding point and at a point midway between the clamps. During this test a check was made to ascertain whether or not the clamping points were rigid with respect to the table on to which the test rig was clamped.

Finally a test was conducted to determine the order of magnitude of the control wheel stiffness. Having fitted the control wheel on to a close fitting parallel mandrel, it was mounted into a special test rig (see fig. 6). Static loads were applied to the steel bar and its penetration into the control wheel measured. All static tests were repeated at least three times to obtain true representative values of deflection.

3.4. Discussion of Results for Static Loading.

3.4.1. Grinding Wheel Spindle, bearings and housing.

(a) Contributions to combined compliance.

Fig. 7 summarizes the contributions to the total deflection resulting from each of the elements when a load of 100 lbf was applied at the grinding position. The results show that the spindle, the bearings and the housing all have compliance to the same order, when assessed with respect to deflection at the grinding point (position 1).

Grinding point compliances:-

Spindle compliance = 1.9×10^{-6} in/lbf

Overall bearing compliance = 1.0×10^{-6} in/lbf

Housing compliance = 1.2×10^{-6} in/lbf

This illustrates a principle of economical design in that there is no weak link in the chain. Neither is one element over-designed in isolation which would have a small effect on the total result. This principle is confirmed from consideration of bearing spacing, since it has been shown by Honrath that maximum combined stiffness is obtained when the deflection due to the bearings is equal to the deflection due to the spindle (ref. 17).

The order of deflections to be expected in grinding may be deduced from the normal grinding force. Results described in section 6.2 reveal that the maximum force experienced in normal grinding practice with the type of operation involved would be 25-40 lbf. Therefore the overall deflection of this unit for 23 lbf would be approximately 1×10^{-4} in.

(b) Grinding wheel housing.

The grinding wheel housing deflections with load are illustrated in detail in fig. 8, from which, as would be expected, it is apparent that these deflections are proportional to load. The grinding wheel head is a very solid block cast integrally with the tray which is of rather shallow proportions. This part of the machine would be improved by making the tray of deeper section and involving deeper ribs.

(c) Grinding wheel spindle.

Fig. 9 illustrates the total deflections of the spindle which include the contributions from the bearings and housing. These measurements also appear linear over the load range tested in spite of the plain bearings. Such bearings cause non-linearity over a wide load-range as apparent from the results obtained for the control wheel bearings, but the effect is negligible for this application.

The contribution of the spindle deflections may be deduced from the experimental results by drawing a new datum line through the deflected spindle positions at the bearings. Thus the deflections at the bearings yield the contribution from bearing deflections and the deflections relative to the new datum line may be attributed to the spindle. The spindle deflections were checked by two methods:-

(i) Spindle compliance by Calculation. The spindle compliance calculation was approximate since it would not be a simple matter to include the constraint from the axial thrust bearing or from the journal bearings. The spindle was assumed

to be uniform and solid. The effect of the grinding wheel adaptor was also neglected. The error from the assumptions acts in opposite sense to the error from assuming a uniform spindle. The use of the above assumptions are as recommended for general design in reference (24) Referring to fig. 10:-

Bending deflection $A_T P = \frac{Pa^2(b+a)}{3EI}$ = 0.00021 in.

Shear deflection $A_T P = \frac{\alpha Pa(b+a)}{G.A.b}$ = 0.00004 in.

where α varies from 1.11 to 1.33 and is taken here as = 1.2. Total deflection = 0.00025 in. for an applied load of 100 lbs. Spindle stiffness at grinding point = 400,000 lbf/in. Spindle compliance at grinding point = 2.5×10^{-6} in/lbf.

(ii) Spindle compliance measured out of the machine.

The spindle deflection was also checked experimentally out of the machine and supported by clamping in vee blocks at the bearing positions. The result of this measurement was:-

Spindle compliance measured out of machine = 1.5×10^{-6} in/lbf. Thus the simplified calculation yields a compliance thirty per cent larger than estimated from the measurement in the machine and the simplified measurement out of the machine underestimated the compliance by twenty per cent. The stiffness of the spindle would be greatly increased by the addition of an extra "outboard" bearing. Figs. 11 and 12 give details of this test.

(d) Grinding Wheel Bearings.

It is of interest to the designer to know the bearing compliance at the bearing which is independent of the bearing separation and the spindle overhang. By taking moments about position 4 (fig. 13a) the reaction at position 2 in terms of a load W at position 1 is $W\frac{(a+b)}{b}$ (see fig. 13b). Thus the compliance at position 2 is:

Front bearing compliance $= \frac{\delta_2 b}{W(a+b)}$

$= 0.69 \times 10^{-6}$ in/lbf

The reaction at position 4 is $W\frac{a}{b}$

Rear bearing compliance $= \frac{\delta_4 b}{Wa}$

$= 0.35 \times 10^{-6}$ in/lbf.

The stiffness of the bearings would be increased by designing the bearings for hydrostatic support with valve compensation (18). An additional "outboard" bearing would increase the effective stiffness of bearings and spindle at the grinding point.

3.4.2. Control Wheel, Spindle, Bearings and Housing

(a) Contributions to combined compliance

The contributions from each of the elements to the total compliance of the control wheel unit are summarised in fig. 14. The compliances measured at the grinding point were found to be:-

Spindle compliance $= 4.0 \times 10^{-6}$ in/lbf

Overall bearing compliance $= 14.0 \times 10^{-6}$ in/lbf

Housing compliance = 2.5×10^{-6} in/lbf

Wheel compliance = 8.5×10^{-6} in/lbf

Thus the bearings have a predominantly strong influence on the order of the deflection. For a grinding force of 25 lbf the total deflection of the control wheel unit is therefore 7.25×10^{-4} in.

(b) Control wheel

The deflections obtained by loading the full width of the control wheel working face (3 in.) were approximately linear over the range of the normal grinding loads imposed on to a control wheel (see fig. 15) and produced a stiffness of $.107 \times 10^{6}$ lbf/in. This stiffness will no doubt vary according to the length of the workpiece being ground and will be reduced for shorter workpieces. The value of $.107 \times 10^{6}$ lbf/in is comparable with the machine structural stiffness, and is not a weak link in the machine system. The effective stiffness of the control wheel will also be reduced for smaller workpiece diameters.

(c) Control Wheel Spindle

The control wheel spindle deflections are larger than the grinding wheel spindle deflections principally due to the reduced diameter. The experimental value for spindle compliance was deduced by geometrical elimination of the bearing compliance as shown in fig. 14. A comparison with a calculated value at the grinding point gives:-

Experimental compliance = 4×10^{-6} in/lbf

Calculated compliance = 2.8×10^{-6} in/lbf

It is considered that the large deflections of the bearings do not allow an accurate assessment of the control spindle by measurement in situ in the machine. The calculated compliance is more likely to be reliable.

(d) Control Wheel Bearings.

The control wheel bearings deflect to a much greater degree than the grinding wheel bearings although of a similar construction. This difference largely results from the difference in operating speeds. At the low control wheel speeds it appears that the oil film is very quickly collapsed and at this point the stiffness is very low. The bearing compliance is approximately fourteen times as large as the grinding wheel bearings and three-and-a-half times the control wheel spindle compliance.

It was found (figs. 6 and 7) that as load increases, there is a reduction in the bearing stiffness up to a load of approximately 100 lbf. For loads in excess of 100 lbf it was found that stiffness is increased again and it is suggested that this is caused by partial metal contact in the bearings. In an investigation of a similar control wheel unit, (18),it was shown that vertical loadings on the spindle give rise to horizontal deflections. However, since the vertical forces on the control wheel are very small, it was decided to neglect this effect.

A very much improved stiffness would be obtained by application of a pre-load equal to 100 lbf. However, this would be at the expense of increased wear and therefore hydrostatic bearings are preferable. Stiffness would also

be improved by addition of an "outboard" bearing at the end of the spindle nearest the control wheel. The compliances of the individual bearings were calculated and may be compared with the previous results for the grinding wheel bearings. The results for the control wheel bearings were:-

Front bearing compliance = 4.5×10^{-6} in/lbf

Rear bearing compliance = 1.0×10^{-6} in/lbf

(e) Control Wheel Housing

The deflection resulting from the housing (see figs. 14 and 18) were approximately twice the housing deflection on the grinding wheel side. This result is not surprising when considered with reference to the differences in the construction. The control wheel head is supported on a slideway which is displaced horizontally from the line of the grinding action by a distance of $7\frac{1}{2}$ in. and displaced vertically by a distance of 6 in. (see fig. 19) Thus, in addition to the direct displacements, there are considerable twisting displacements about the line of drive. A further explanation is the reduced stiffness of the tray in the area under the control wheel head.

3.5 CONCLUSIONS

The static deflections of the critical elements have been measured. The stiffnesses corresponding to the more critical elements referring to their effect at the grinding point were:-

Grinding wheel bearing stiffness = 1.0×10^6 lbf/in.

Grinding wheel housing stiffness = 0.83×10^6 lbf/in.

Grinding wheel spindle stiffness = 0.53×10^6 lbf/in.

Control wheel housing stiffness = 0.4×10^6 lbf/in.

Control wheel spindle stiffness = 0.25×10^6 lbf/in.

Control wheel stiffness = 0.107×10^6 lbf/in.

Control wheel bearings stiffness = 0.075×10^6 lbf/in.

It is concluded that the machine would be improved by attention to the following design changes:-

(i) The application of an improved type of bearing.

(ii) Elimination of Abbe offsets on the control wheel head drive.

(iii) Application of "outboard" bearings.

CHAPTER IV

Dynamic Tests

4.1 The aims of the dynamic tests were:-

(a) To determine the vibration characteristics of the machine acting relatively between the grinding and control wheels in order to relate these to the errors in roundness on the ground workpieces.

(b) To investigate the modes of vibration of the machine structure in order to determine areas of possible improvement.

(c) To obtain parameters of the machine for use in the simulated model; described in Chapter VI.

4.2 Description of Apparatus and Calibration

The apparatus listed below was used during the dynamic tests:-

(1) A Philips electro-dynamic exciter (Type PR 9270) used to produce a sinusoidal exciting force on:

(a) The replica grinding wheel

(b) The replica control wheel

(c) The machine tray

(2) A Philips excitation amplifier (Type PR 129043) used to provide the necessary current to the exciter (PR 9270). The exciter and amplifier used together have been calibrated and yield a constant force for a given current over the operating frequency range.

(3) A Servomex Controls Ltd. low frequency wave-form generator and variable phase unit (Type LF 141/VP142) was used

to provide:-

(a) a sinusoidal voltage of variable frequency to the excitation amplifier.

(b) a second sinusoidal voltage of variable frequency for assessing phase changes that took place between the transducer and its associated measuring equipment.

(4) Frequency Counters

Because of the coarse frequency control on the waveform generator, precision frequency counters were used, as follows, to ensure greater accuracy of setting the frequency.

(a) Venner frequency counter Type TSA 336. This instrument monitored the input signal to exciter amplifier.

(b) Racal Instruments Ltd., Digital frequency Meter, Type SA 520. This instrument was used for monitoring the reference frequency for the phase change calibration.

(5) Vibration Transducers

(a) Wayne Kerr Ltd. capacitance proximity transducers Type C1 were used to measure:-

(i) Vibration amplitudes of the replica grinding wheel.

(ii) Vibration amplitudes of the replica control wheel.

The Wayne Kerr transducers were connected to their associated displacement and amplitude measuring equipment (Type B 731A).

(b) Bruel and Kjaer accelerometer Type 4330 Serial No. 92760, was used to investigate the structural modal displace-

ments, that took place when the machine was force excited. The output from the accelerometer was fed to a Bruel and Kjaer Vibration pick-up preamplifier (Type 1606).

(c) A Philips electromagnetic vibration pick-up (Type PR 9261) was used as a complementary method of investigating the modal displacements of the machine structure. This velocity contact transducer was used in conjunction with a Philips direct reading meter (Type 922) and an oscilloscope.

(6) Frequency Analysis

A Bruel and Kjaer frequency analyser (Type 2107) which incorporated in its design:-

(a) A signal amplifier

(b) A valve-Voltmeter for measurement of the accelerometer signals.

(c) A selective or automatic sweep frequency discriminator.

Also combined with the frequency analyser was a pen recorder (Type 2305).

(7) Phase Meter

An AD-YU Electronic INC precision phase meter (Type 406L-1) was used to compare signal phase relationships.

(8) Oscilloscope

A Solartron double beam oscilloscope (Type M977) was used throughout the tests as a secondary means of assessing the amplitudes, frequency and phase of the signals concerned.

4.3 Experimental Procedure

To obtain the parameters of the structure under normal operating conditions the machine was allowed a warming up period of two hours before commencing any of the tests, whether static or dynamic.

The dynamic tests which commenced with the excitation of the replica grinding wheel took two forms.

(1) Excitation on the face of the replica wheel on to which the cutting force acts (see figs. 20 and 21). To conduct this test it was necessary, because of the bulk of the exciter, to remove the complete control wheel housing.

(2) Excitation on to the face of the replica wheel from the position which was diametrically opposite the point which was excited in the previous test.

During this test, the control wheel housing was back in its normal position on the machine.

The object of this second test was to ascertain whether or not the results from the previous test were valid, bearing in mind that the mass of the control wheel housing had been removed. Throughout these two vibration tests on the grinding wheel, the vibration transducer was placed in the workpiece position, and hence any change in distance between the nominal centre of the workpiece and the surface of the grinding wheel was measured.

The output signals from the capacitance transducer, via the Wayne Kerr associated measuring equipment (basi-

cally an operational amplifier), was fed to the frequency analyser.

By manually setting the frequency analyser to the frequency of the exciting force, it was possible to filter out from the transducers signal:-

(a) the signal obtained from the errors in roundness on the replica wheel.

(b) the noise in the signal; possibly due to the surface texture of the replica wheel, and other pick-up noise.

It was considered that errors in waviness on the workpiece would be attributed to machine vibrations below the 100 Hertz range, however, to explore fully the characteristics of the machine, the dynamics tests on the grinding wheel were conducted to a frequency of approximately 600 Hertz.

Because low frequencies were involved, precautions were taken to account for phase changes which took place in the measuring equipment. A reference sinusoidal signal was fed through the measuring equipment and checked for phase changes, by the use of a phase meter. This tedious calibration test took place at each frequency at which force excitation took place. Having carried out these dynamic tests on the machine wheels, it became evident that further dynamic tests were necessary to analyse the vibration modes and to identify the critical frequencies with the various modes of vibrations. The modal vibration

investigations took two forms:

(1) An accelerometer (Bruel and Kjaer) was used to measure vibrations.

(2) A Philips absolute vibration pick-up was used to measure vibration amplitudes.

The exciting force in each case of these modal vibration tests was applied to the grinding and control replica wheels respectively, again on the face of the wheel which would normally make contact with the work-piece (see fig. 22). Considering test 1, a lattice of tapped holes was drilled in three planes, in the control wheel housing and the grinding wheel housing. These tapped holes served to attach the accelerometer to the housing being examined (see fig. 21).

Test 1 was conducted by exciting the replica wheel at known critical frequencies obtained from the previous tests, and measuring the amplitude and phase of the vibration at the selected points on the housing. Also to assist in the analysis of modes, the accelerometer was attached to the side face of the replica control wheel and then by rotating the wheel and the accelerometer, the position of the maximum amplitude of the critical vibrations was observed.

The second modal vibration test, using the Philips absolute displacement pick-up, was a supplementary method of assessing the modes of vibration of the previous tests.

Arising from these modal vibration tests it became

apparent that the machine "tray" was dominantly involved in vibrations, mainly apparent on the control wheel housing.

It should be appreciated that the grinding wheel housing was an integral part of the "tray" casting and that the tray provided the necessary dovetail slide on to which the control wheel housing infeed movement took place.

A tray vibration test was therefore carried out in which the dovetail slide was excited; the excitation being in the vertical plane of the machine and therefore normal to the slide. Measurements of the amplitude of vibration were made in a similar plane, alongside the exciter, using a Philips absolute pick-up and measuring meter.

4.4 Dynamic Test Results

4.4.1 Grinding Wheel Spindle, Bearings and Housing

Figs. 23 and 24 illustrate the results obtained for amplitude and phase response due to an exciting force of 5.46 lbf. applied horizontally at the grinding point.

The results were also plotted as a harmonic response which gives a better indication of the important resonances. The harmonic response locus is shown in fig. 25 from which it is apparent that there are significant resonances at 154 Hz, 240 Hz, and 280 Hz.

The principle elements involved in the 154 Hz mode of vibration were the grinding wheel spindle and its bearings. The modal shape is illustrated in fig. 26 and is similar to the classic case of a rotating mass on a shaft supported in two bearings (22). The mode is situated between the two

bearings. In the mode analysis of Chapter V the classic analysis is used to obtain the equivalent mass of the wheel and the spindle. Clearly it would be possible to eliminate this mode by addition of an outboard bearing on the grinding wheel end of the spindle. The modal shapes relating to the resonant frequencies at 240 Hz and 280 Hz are illustrated in figs. 27 and 28. Both modes involve a swinging motion of the grinding wheelhead on the tray. However, while the resonance at 280 Hz involves a pure swinging, the motion at 240 Hz involves also a degree of twisting. The stiffness in these modes is largely dependent on the constraint at the base of the wheelhead which is integral with the tray. This constraint would be improved if the tray was made deeper in section with deep ribs at right-angles to the housing axis.

4.4.2. Control Wheel Spindle, Bearings and Housing

Amplitude and phase responses obtained by horizontal excitation at the mid point of contact on the control wheel revealed five resonances which might be of major importance, (figs. 29 and 30). The frequencies of resonance were 82 Hz, 105.5 Hz, 150 Hz, 175 Hz, and 410 Hz. The results are also illustrated in harmonic response locus form, (fig. 31).

(1) 82 Hz Resonance. The mode of vibration at 82 Hz was found to be of dominant influence on grinding performance and the vibration behaviour of the machine under grinding conditions. At frequencies below this resonance the grinding wheel and control wheel move together in

phase, although not necessarily with equal amplitude. However at 82 Hz and above, the vibration amplitudes act in opposition and give rise to large relative vibrations in the line of grinding.

The modal shape at resonance is illustrated in fig. 32 and it is evident that the control wheel spindle housing swings about the constraint at its base where it is attached through the infeed slideway to the tray. The spring stiffness in this mode is largely derived from the tray, and again it is found that the stiffness would be improved if the tray were of deeper and stiffer construction. The effect of the slideway also reduces the stiffness of the control wheel-head restraint. Redesign of the slideway for increased stiffness would be worthwhile.

(2) 105.5 Hz Resonance. A rocking mode of the control wheel spindle housing on its infeed slideway appears at 105.5 Hz (see fig. 33). The main contributing factor to this modal vibration is the nature of the restraint offered to the control wheel by the slide and the tray.

The amplitude of this vibration, at the grinding point is proportional to the vertical distance between the slideway and the grinding point, and its effect can be minimised by having the infeed slideway and the control wheel spindle in the same horizontal plane.

(3) 150 Hz Resonance. The modal shape of this resonance is illustrated in fig. 34, and it has a relative large amplitude in the vertical plane of machine at the grinding

point, however, its amplitude in the horizontal plane is considerably reduced.

An accurate assessment of the horizontal amplitude at the grinding point due to the 150 Hz was not possible because of the coupling effect of the twisting mode at 175 Hz.

Thus introducing a pair of infeed guideways straddling the grinding point would considerably reduce the amplitude of this vibration.

(4) 175 Hz Resonance. The modal shape at this resonance is illustrated in fig. 35 and it is evident the control wheel spindle housing twists on the slideways which guides the infeed motion of the control wheel spindle housing.

The effect of the slideway constraint on the amplitude of vibration at the grinding point is dependent on:-

(a) The ratio between width and length of the slide on the housing.

(b) The distance the grinding point is from the centre of the slideway.

(c) The stiffness of the bearing surfaces, between the slideway and the slide in the housing.

To improve the design is an obvious solution; to remove this undesirable mode of vibration the slideways should be positioned either side of the control wheel and the infeed drive force applied centrally between the slideways, directly in line with the grinding force.

(5) 410 Hz Resonance. From the modal shape illustrated

in fig. 36, the resonance at 410 Hz may be primarily identified with the control wheel, spindle and bearings. Although this frequency corresponds to a higher order than any lobing on the workpieces which may be produced on this machine, it is possible that it has an effect on the nature of the surface texture.

4.4.3. The Machine Tray

Having observed from the previously described tests that the tray was of critical importance it was decided to carry out a test by direct vertical excitation on to the tray at a point where the work support blade is located. The resulting harmonic response locus is shown in fig. 37. The first resonance occurs at 60 Hz, a frequency at which the grinding wheel and the control wheel do not vibrate in opposition. Thus at first sight this vibration is not greatly important. However, the vertical vibration of the workblade might be expected to lead to roundness errors, a proposition which was not confirmed by later grinding tests.

Much larger amplitudes were experienced at 82 Hz revealing the importance of the tray in this dominant mode.

4.4.4. Proposed Structure for Improved Static and Dynamic Stiffness

Fig. 64 is a sketch of a layout for a centreless grinding machine and incorporates the principles specified in Chapter 7.1.

4.5. Conclusions from Dynamic Tests

(1) The modes of vibration have been investigated and the critical frequencies determined for amplitudes of

relative vibration between the two wheels at the grinding point.

(2) The machine tray is of insufficient depth and rigidity.

(3) The control wheelhead infeed slideway is incorrectly positioned and lacks sufficient stiffness.

(4) The infeed drive involves Abbe offsets which should be avoided.

(5) Additional bearings for each spindle would greatly increase stiffness.

CHAPTER V

SIMULATION BY HYBRID COMPUTER

5.1 Determination of Machine Parameters

5.1.1. Introduction

A single degree of freedom lightly damped vibrating system produces a harmonic response locus which closely approximates to a circle. Furthermore, if the magnitude of the exciting force is known, it is possible to deduce from the harmonic response locus of such a system the following dynamic parameters of the system for the mode of vibration under consideration:-

(a) The resonant frequency.

(b) The damping factor.

(c) The amplication factor.

(d) The spring constant or the equivalent static stiffness for a single degree of freedom system.

(e) The mass.

(f) The damping coefficient.

Kennedy and Pancu (16) described how the analysis of a complex lightly damped vibrating system, having multiple degrees of freedom could be resolved into a number of equivalent single degree of freedom systems.

Tobias (19) gives an account of this theory and gives details of how the equivalent parameters may be determined from a harmonic response locus containing two resonances. This technique, known as superposition of uncoupled coordinates, enables one to study the contribution of each

mode to the total response of the system.

The principle of uncoupling from the harmonic response locus was used to determine the parameters of equivalent systems that may have had a significant effect on the errors in roundness on the workpiece.

Fig. 39 shows the harmonic response locus obtained from the control spindle bearing and housing; showing in position two best fitting single mode response circles.

From these single mode response circles, the various parameters of the equivalent systems were determined as follows:-

5.1.2. First Control Wheel Mode

(Equivalent mass with a resonant frequency at 82 Hz)

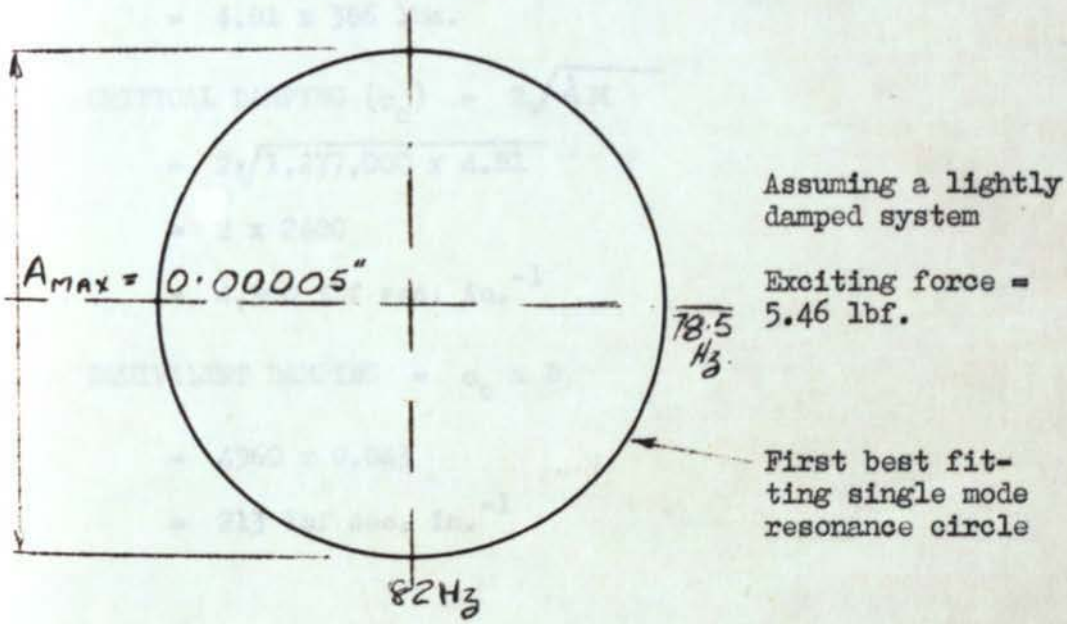

DAMPING FACTOR (D) = $\frac{82 - 78.5}{82}$ = 0.043

DYNAMIC AMPLIFICATION FACTOR (Q) = $\frac{f_o}{\Delta f} = \frac{82}{7} = 11.7$

EQUIVALENT STATIC STIFFNESS (λ) = $\frac{P.Q}{A_{Max.}}$

= $\frac{3.46 \times 11.7}{0.00005}$ lbf/in.

= 1,277,000 lbf/in.

$$f_o = \frac{1}{2\pi}\sqrt{\frac{\lambda}{M}}$$

Therefore MASS OF EQUIVALENT BODY (M) = $\frac{1,277,000}{(2\pi)^2 \times 82}$

= 4.81 lbf. sec^2/in.

= 4.81 x 386 lbm.

CRITICAL DAMPING (c_c) = $2\sqrt{\lambda M}$

= $2\sqrt{1,277,000 \times 4.81}$

= 2 x 2480

= 4,960 lbf sec. $in.^{-1}$

EQUIVALENT DAMPING = $c_c \times D$

= 4960 x 0.043

= 213 lbf sec. $in.^{-1}$

SECOND CONTROL WHEEL MODE

(Second equivalent mass with resonant frequency at 105.5 Hz)

Exciting force (P) = 5.46 lbf

Assuming lightly damped system

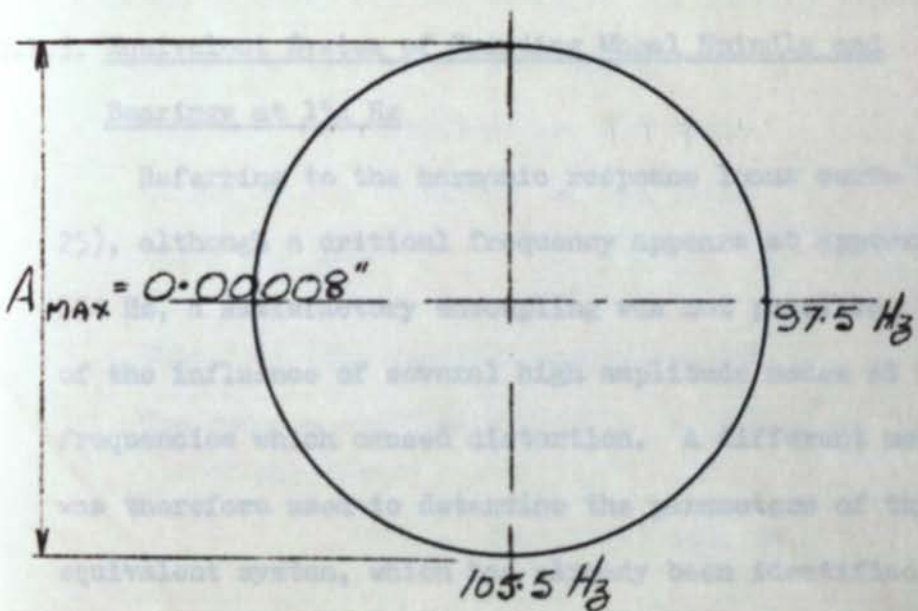

DAMPING FACTOR (D) = $\frac{(105.5 - 97.5)}{105.5} = \frac{0.076}{}$

DYNAMIC AMPLICATION FACTOR (Q) = $\frac{f_o}{\Delta f} = \frac{105.5}{16}$

= 6.6

EQUIVALENT STATIC STIFFNESS (λ) = $\frac{5.46 \times 6.6}{0.00008}$

= 450,000 lbf in.$^{-1}$

EQUIVALENT MASS (M) = $\frac{450,000}{(2\pi)^2 \times 105.5^2}$

= 1.04 lbf sec. in.

= 400 lbm.

DAMPING EQUIVALENT $= c = 2D\sqrt{m\lambda}$

$= 2 \times .076 \times \sqrt{450{,}000 \times 1.04}$

$= 104$ lbf sec. in.$^{-1}$

CUTTING FORCE

For the determination of the grinding coefficient (K) for a depth of cut, see section 6.3.5.

5.1.3. Equivalent System of Grinding Wheel Spindle and Bearings at 154 Hz

Referring to the harmonic response locus curve (fig. 25), although a critical frequency appears at approximately 154 Hz, a satisfactory uncoupling was not possible, because of the influence of several high amplitude modes at higher frequencies which caused distortion. A different method was therefore used to determine the parameters of this equivalent system, which had already been identified as being largely associated with the grinding wheel spindle and its bearings (see chapter IV). The following data on the spindle and bearings was known:-

(1) The weight of the grinding wheel, 28 lbf.

(2) The static stiffness at the grinding point obtained from experiments (Chapter III)

(3) The weight of the spindle together with the grinding wheel adaptor; 37½ lbf.

(4) The position of centre of gravity of spindle with the adaptor in position (see Fig. 40).

(5) The resonant frequency of system; 154 Hz.

The equivalent weight acting at the grinding point

$$= 28 + 37\tfrac{1}{2}\left[\frac{5\tfrac{1}{16}}{10\tfrac{1}{4}}\right]^2 \qquad \text{(reference 20)}$$

$$= 37.6\ 16 \text{ (weight)} \quad \text{or Mass} = \frac{37.6}{386} \text{ lb(f) Sec}^2 \text{ in.}$$

A sharp blow was imparted to the dummy grinding wheel to obtain the damping factor of the system, and from the recorded decaying sinusoidal curve the damping factor of the system was determined as follows:-

Height of 1st amplitude = 2.2 units

Height of 2nd amplitude = 1.1 units

Hence $\log \frac{2.2}{1.1} = 2\pi D$

Therefore (the damping factor) = .11

The damping coefficient (c) of the system $= 2D\sqrt{\lambda M}$.

$$= 23.2 \text{ lb(f) sec. in.}$$

5.1.4. Resultant Equivalent Static Stiffness

It is important that any equivalent model of the machine should take into account the total compliance of the system and should not be restricted to those compliances which may be associated with the selected resonances. This is one advantage of the model proposed in the following chapter over a conventional linear analysis which would be restricted to some equivalent dynamic systems.

The resultant static stiffness obtained from the measurements and analysis in Section 3 was found to be $\lambda_R = 0.03 \times 10^{-6}$ lbf/in. The value of λ_R employed for

the purposes of constructing the model was obtained from the harmonic response loci, which yielded $\lambda_R = 0.038 \times 10^6$ lbf/in. The effect of the stiffnesses which were apportioned to the various equivalent dynamic systems may be allowed for by subtracting the equivalent compliances.

$$\frac{1}{\lambda_R} = \frac{1}{\lambda_1} + \frac{1}{\lambda_2} + \frac{1}{\lambda_3} \text{ etc.} + \frac{1}{\lambda_0}$$

where λ_0 is a static stiffness in series with

λ_1 = Equivalent static stiffness in Mode 1

λ_2 = Equivalent static stiffness in Mode 2

An implicit assumption is involved here that all deflections are vectorially additive. From Section 5.1.2.

82 Hz $\lambda_1 = 1.28 \times 10^6$ lbf/in.

105.5 Hz $\lambda_2 = 0.45 \times 10^6$ lbf/in.

However, from preliminary investigations it was found that the second Mode system confused the picture by introducing higher frequency vibrations. Hence the model was investigated as a single resonance system together with a parallel compliance, $C_o = \frac{1}{\lambda_o}$.

5.2. The Hybrid Computer Model

The simulation of the centreless grinding process was conducted on the Lanchester Polytechnic Hybrid Computer.

The machine consists of a Honeywell DDP 516 digital computer, coupled by a high speed data and control interface to a purpose-built analogue computer. The details are given in Appendix A.

5.3. Design of the Model for Centreless Grinding

Before proceeding with the computer simulation the following decisions were taken and assumptions were made:-

(a) That the frequency of vibrations which would affect waviness on the workpiece that could be ground on the machine, would be no greater than 100 Hertz. Hence, only equivalent parameters having a critical frequency below 100 Hertz were considered in the simulation.

(b) That the investigation would be confined to the case of plunge grinding.

(c) That the relationships for geometric errors by Rowe and Koenigsberger (6) should be used as the basis for generating irregularities on the workpiece.

(d) That the process would be simulated for the case of zero blade angle and zero β angle.

(e) That no slip took place between the workpiece and control wheel.

The object of the simulation was to design an analogue computer system to represent the critical structural characteristics, and to consider errors in roundness on the workpiece as the source of a regenerative force on the vibratory analogue system.

Investigations had already shown that only one equivalent mass had a significant effect on the waviness of the workpiece (21). Hence, a standard one degree of freedom analogue system was used to represent this system.

The following diagram indicates the relevant analogue computer system.

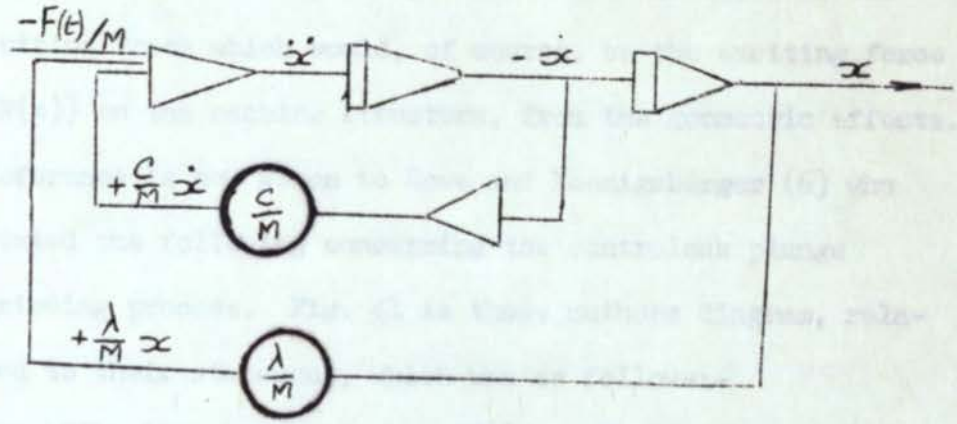

The above circuit is obtained from the standard expression:- (assuming viscous damping)

$$M\ddot{x} + c\dot{x} + \lambda x = F(t)$$

$$\ddot{x} = \frac{F(t)}{M} - \frac{c\dot{x}}{M} - \frac{\lambda x}{M}$$

Although only one vibrating system was considered, the effect of the other equivalent parameters were not totally disregarded; this overall equivalent compliance was determined and placed in parallel and the simulation was as follows:-

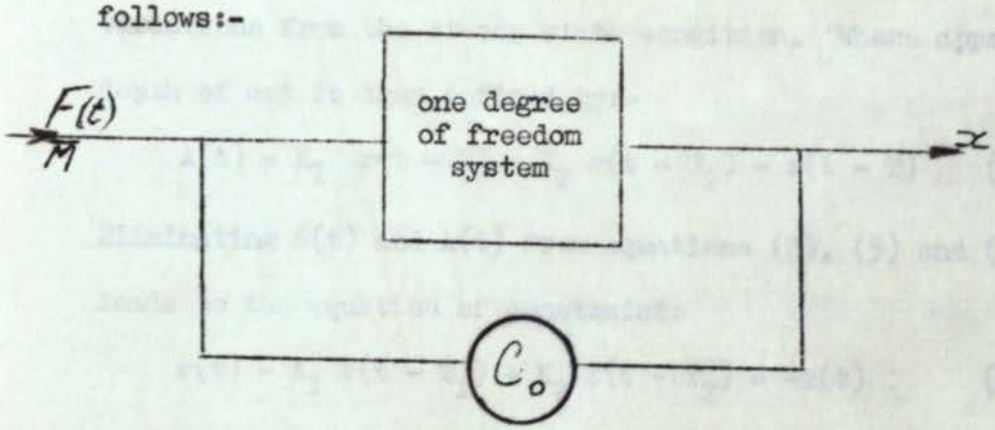

Having devised a model for the machine structure, it then became necessary to synthesize the variation in the cutting force which would, of course, be the exciting force (F(t)) on the machine structure, from the geometric effects. Reference is now given to Rowe and Koenigsberger (6) who stated the following concerning the centreless plunge grinding process. Fig. 41 is those authors diagram, related to their statement, which was as follows:-

"The true depth of cut, S(t), at any instant indicated by t is the difference between the apparent depth of cut A(t) and the machine deflection x(t)"

i.e. $S(t) = A(t) - x(t)$ (2)

also $S(t) = r(t) - r(t - T)$ (3)

where these equations are true for the steady state or for small variations from the steady state. In this discussion the constant steady state terms related to the average depth of cut and the average deflection of the machine are neglected because in purely theoretical considerations they are inconsequential to the onset of chatter. The terms are therefore taken to mean small variations from the steady state condition. Where apparent depth of cut is then defined by:-

$$A(t) = K_1 \, r(t - T) - K_2 \, r(t - T_2) - r(t - T) \quad (4)$$

Eliminating S(t) and A(t) from equations (2), (3) and (4), leads to the equation of constraint:

$$r(t) - K_1 \, r(t - T_1) + K_2 \, r(t - T_2) = -x(t) \quad (5)$$

The force F is assumed to be proportional to the depth of cut but to have opposite sense:

$$F = - K_s \left[r(t) - r(t - T) \right] \qquad (6)$$

For a single degree of freedom system the equation of motion is then:-

$$m\ddot{x}(t) + C\dot{x}(t) + x(t) = Ks \left[r(t) - r(t - T) \right] \qquad (7)$$

Considering the case of zero blade angle and zero angle equation (5) can be re-arranged to obtain:-

$$-x(t) - r(t - \tfrac{T}{2}) - r(r - T) = r(t) - r(t - T) = S(t) \qquad (8)$$

Fig. 42 illustrates in block diagram form how the true depth of cut $S(t)$ was generated from equation (8) for the particular case when $K_1 = 0$ and $K_2 = 1$.

The physical method of obtaining the results shown in Fig. 42 was to utilize a core storage unit containing 512 bits into which the analogue values of $r(t)$ for one complete revolution of the workpiece were fed, via an analogue to digital converter.

Sequential scanning of the core storage unit was made simultaneously at two places in the store.

(1) Commencing at bit No. 255 which gave a time lag of $\frac{T}{2}$. The output from the scanner was fed to a Digital to Analogue Converter.

(2) Commencing at bit No. 512 which gave a time lag of T (one revolution of the workpiece).

The output from this scanner was fed to a digital to analogue converter.

As scanning of the core storage took place, fresh values of $-\delta R(t)$ were fed into the core storage at the same rate at which the scanning took place. It was also arranged that the time taken to scan 512 bits in the core storage was equal to the time of one complete revolution of the workpiece. Finally, an initial condition was necessary to set the simulated model in motion.

An initial condition was arranged by setting the values of the core storage unit to zero with the exception of bits 45 to 58 which had five volts in each. This information approximated to a small flat on the workpiece prior to grinding.

The numerical values in the model were as follows:-

Mass (M) = 1800 lbm.

Damping (c) = 200 lbf sec. $in.^{-1}$

Stiffness (λ) = 1,250,000 lbf $in.^{-1}$

Parallel Compliance (C_o) = 2.36×10^{-5} in/lbf

Grinding Coefficient (K) = 500,000 lbf $in.^{-1}$

5.4. Discussion of Results from the Hybrid Computer Model

The schematic diagram (Fig. 43) gives details of the simulation model. The system was set in motion by feeding in the initial conditions, as described in Chapter 5.1. The parameters of the system listed below were monitored and recorded on a U.V. Recorder (See figs. 44 and 45).

Monitor 1: the amplitude of vibration of the equivalent mass system = $x(t)$

Monitor 2: the apparent depth of cut = $s(t)$

Monitor 3: the reduction in radius from the workpiece reference circle after successive half revolutions of the workpiece = $r(t - \frac{T}{2})$

Monitor 4: the reduction in radius from the workpiece reference circle after successive revolutions of the workpiece = $r(t - T)$

The initial conditions which were set in the analogue computer system simulated a small flat on an otherwise cylindrical workpiece. In practice, if this small flat on the workpiece came into contact with the control wheel, at the commencement of a plunge grinding operation, there would be a movement of the workpiece away from the grinding wheel which would produce a sudden reduction in the depth of cut, which would be accompanied by a sudden reduction in the grinding force.

This sudden reduction in the grinding force and depth of cut would produce an increase in the radius of the reference circle of the workpiece, at a point on the periphery of the workpiece diametrically opposite to the position of the initial flat.

It can be appreciated that the sudden reduction in the grinding force would produce a decaying oscillatory vibration in the machine elastic structure, and evidence of this

effect taking place can be seen by examining the trace of x(t) in Figs. 44 and 45.

It is observed that the increase in radius one-half revolution after the initial disturbance is less than the initial disturbance, a fact which is largely explained by the elasticity of the machine structure. This difference between the true depth of cut and the apparent depth of cut was referred to by Rowe and Barash (2) from which they derived a term the "Machining elasticity parameter K."

The monitoring of $r(t - \frac{T}{2})$ clearly shows this effect; indicating by a change in sign, that an increase in the radius had taken place, also showing that the magnitude of the increase in the radius is relatively small when compared with the negative initial decrease in radius due to the flat on the workpiece.

If the grinding cycle is allowed to progress through a further half revolution of the workpiece, the generated small rise on the workpiece will make contact with the control wheel and the initial flat will be at the grinding position. Bearing in mind that a constant feed rate is assumed to be operating, there will be a reduction in the depth of cut of the workpiece radius at this point.

As grinding proceeds, there is a gradual reduction in the initial error accompanied by a slowly increasing lobe generated on the opposite side of the workpiece.

The effect of these changes are clearly seen on the monitoring of either $r(t - \frac{T}{2})$ or $r(t - T)$, and shows that

this action takes place until the two errors on the workpiece are of equal magnitude. At this stage, the machine deflection x(t) and the depth of cut S(t) have both decayed to a very small amplitude.

Whilst these changes were taking place on the simulated workpiece periphery, their effects were being transmitted to the vibrating equivalent system, the result of which is shown on the monitor of x(t), and the monitor of the depth cut S(t).

5.5. Conclusion, from Hybrid Computer Model

The behaviour of the model as described, agrees very well with experience from grinding experiments. It is useful in that it demonstrates two principles which apply in all grinding operations, but are rarely included in a discussion of dynamic performance. The principles which emerge are as follows:-

(i) The static compliance of the machine system is shown to be of primary importance in the process of shape generation even when the effect of a machine resonance is freely allowed to operate. This is because no error can be rapidly removed or built up. Hence, there is a prolonged period in which transient behaviour is exhibited.

(ii) A linear analysis of dynamic variations as described in references 1, 4, 11 and 12, makes no distinction between a phase shift which occurs within one cycle or a phase shift which extends over many cycles. The regenerative effects of a disturbance occurs in this example after

one-half of a revolution and after one revolution. The transient effects of the resonant system have completely decayed before the regenerative impulse occurs. Thus the long time delay between an impulse and its regenerative effect changes the nature of the transient behaviour and extends the period over which shape generation takes place.

Thus, from the model, it is possible to demonstrate why the process of shape generation occurs very slowly in grinding operations. No previous model has included all the factors which are inherent in the hybrid computer model. It is suggested that the hybrid model will allow detailed examination of more complex grinding systems and accordingly reveal the importance of parameters under investigation such as forced vibrations.

CHAPTER VI

Grinding Tests

6.1. Aims of the Practical Grinding Tests

The aims of the practical grinding tests were as follows:-

(1) to obtain an order of magnitude of a radial grinding force during a normal plunge grinding operation.

(2) to determine the grinding force coefficient under practical grinding conditions.

(3) to investigate frequency levels of the vibrations induced on to the grinding wheel during a plunge grinding operation.

(4) to investigate frequency levels of the vibration induced on to the control wheel during a plunge grinding process.

(5) to obtain a statistical sample of plunge ground workpiece for examination.

(6) to obtain samples of plunge ground workpieces for waviness comparison with the predicted waviness obtained from the computer simulation.

6.2. Description of Apparatus and Calibration

(1) Transducers

Southern Instrument Ltd., Miniature proximity vibration transducers (Type 324) were used to:-

(a) Measure grinding wheel displacement and amplitudes of vibrations. (See fig. 46)

(b) Measure control wheel displacement and amplitudes of vibrations.

(c) To indicate the speed of rotation of grinding wheel.

(d) To indicate the speed of rotation of control wheel.

(e) To indicate the speed of rotation of workpiece.

(f) To measure the rate of in-feed on the control wheel.

} see fig. 46

The output from the transducers via the transducer oscillator (Type 1822, were fed to the Southern Instrument (frequency modulated) measuring equipment (Type M1800).

(2) Recorders

(a) Two SE Laboratories Ultra-violet recorders (Type SE3006) were used for recording the signals from the various transducers, together with a time pulse signal from a signal generator. (See Fig. 47)

(b) A Philips portable instrument recorder (Type EL 1020/02/04/07) in which is incorporated seven recording channels, and an eighth channel which may be used as a "voice channel" which is used for speech, cues and similar purposes.

(3) Signal Generator

A Servonex Controls Ltd. low frequency waveform generator and variable phase unit (Type LF141/VP142).

(4) Filter

A Dawe Instrument Ltd. variable bandwith filter

(Type 1462) was used as a low pass filter on the signal from the grinding wheel spindle.

(5) Frequency Analyser

A Bruell and Kjaer frequency analyser (Type 2107) and its associated Recorder.

The following equipment was made:-

Two aluminium discs which were made and one was attached on to the end of:-

(a) the grinding wheel spindle

(b) the control wheel spindle

The discs were trued up in situ on the spindles and the gaps variation between the discs and their proximity transducers indicated the displacement of the spindle, also the force acting on the spindle.

The aluminium discs together with their transducers are clearly seen in Fig. 46.

A removable aluminium adaptor was made, so that it could be secured on to the end of a workpiece specimen. Four drilled holes in the side of this adaptor provide the means, via a transducer, of recording the speed of rotation of the workpiece.

6.3. Discussion of Results from Grinding Experiments

Fig. 48 illustrates the shape of the workpieces which were used throughout the plunge grinding tests. Each workpiece was numbered or lettered for identification purposes.

Details of the grinding, control wheels and coolant used during the tests are given in Appendix B.

The grinding tests were conducted using nickel chrome molybdenum steel (EN 30 B) workpieces in the soft condition and in the hardened state. All workpieces were prepared initially by cylindrical grinding between centres and checked for uniformity of size to within $\pm$ 0.0001 inch, and errors in roundness, which were always less than ten micro-inches (M.Z.C.). A plunge feed rate of 0.010 inch per minute was considered as a reasonable practical feed, and was used throughout the various grinding tests.

6.3.1. Results for $\alpha = 0^{\circ}$, $\beta = 0^{\circ}$. As grinding proceeded, chatter developed which was followed in some cases by loss of speed control.

When the workpieces were measured for roundness, the most common shape was a continuation of three and five lobes, with signs of higher order lobing as in Fig. 49(a). The low order lobing is not surprising in view of the geometric setting. However, in one outstanding case there was a large amplitude of twenty waves around the workpiece shown in Fig. 49 (b).

As the assumption that the waviness was generated at the workpiece speed prior to loss of control, the chatter frequency was 77 Hz. During the tests, the displacement of the grinding wheel and the displacement of the control wheel were monitored on magnetic tape for subsequent analysis. Fig. 50 shows a frequency analysis of the control wheel displacement which reveals the peak amplitude at approximately 82 Hz. The resonance at this frequency

has previously been discussed in Chapter V.

In view of the lack of speed control at the completion of grinding, it is surprising that the frequency calculated from the normal operating speed is so close to the resonance.

The mechanism of chatter in this test is not fully understood. However, frictional constraint is lower at this setting than with other settings, which is no doubt contributory to loss of speed control.

To overcome the low frequency limit of twenty Hertz of the frequency analyser, the play-back speed of the magnetic tape recorder was increased by a factor of eight, thereby enabling an analysis down to low order frequencies to be obtained. Fig. 51 shows a recording obtained by this method from these initial tests. Referring to the initial tests previously described, it was thought that the soft workpieces, together with the condition of the surface of the support blade, may have in some way contributed to the chatter experienced in these tests.

6.3.2. Further tests were carried out using the same process configuration of $\alpha_1 = 0^\circ$ and $\beta = 0^\circ$, but with the exception that hardened workpieces were ground instead of soft workpieces. In this test, the hardened workpieces were ground, assessed for size, roundness and the magnetic recordings were frequency analysed. Chatter was again experienced throughout these tests, and roundness errors and the frequency analysis conformed to the results obtained previously from grinding soft components.

6.3.3. Results for $\alpha_1 = 20^\circ$, $\beta = 8^\circ$

Because the two grinding tests, in which $\alpha_1 = 0^\circ$ and $\beta = 0^\circ$ were unsatisfactory, further tests were conducted for $\alpha_1 = 20^\circ$ and $\beta = 8^\circ$. This condition is the best known setting in the working range of the machine for stability and the problems previously described were not experienced at this setting. It was decided to record the order in which each component was ground, hence detecting any trends or repeatable effects in the process. This procedure was adopted because of the saw-tooth pattern of size variations observed by Loxham (23), (25).

Although grinding forces were not directly measured, an indication of force variations was obtained from records of machine deflections. This condition is geometrically unstable in theory for twenty-two waves, but with the workpiece speed set to coincide with the machine resonance, it appears from experiments that the geometric instability is not highly pronounced (21). Specimens were identified by numbering them from 14 to 40 after which they were cylindrical ground between centres and individually checked for errors in roundness. The grinding wheels and control wheels were dressed and three unidentified samples were ground so that the initial sharpness of the grinding wheel was removed.

The results presented are the first of the series of such grinding tests, and all measurements were completed and recorded before comparison or analysis, thus obviating

the risk of prejudicial bias. The deviations from size of successively ground components are illustrated in Fig. 52. The overall trend correlates with the reducing size of the grinding wheel, an effect which may be compensated on many machines by feedback after measurement of size. However, there are also cyclic variations which would cause greater problems of size control. The results appear to follow an approximate saw-tooth pattern which for a number of cycles are quite well defined. There is increasing size for several components followed by a reduction in size. The record of roundness errors, Fig. 53, shows several results which are outstanding in that their magnitude is greater than the majority of components. In a number of cases, examination of the records revealed coincidence between the component with poor roundness and reduced size. Also, it has been possible to observe in some cases the apparent onset of this condition illustrated by an obvious change in the static deflections in the machine and the vibration level of the machine. A very good example with deflections and vibrations was provided by specimens 19, 20 and 21. From the Talyrond traces, (Fig. 54) it is observed that specimen 20 has a roundness error of 100 mic. in M.Z.C. whereas the roundness errors of specimen 19 and 21 are only 30 mic. in. In the course of grinding specimen number 20, the vibration level was initially normal. It was then observed to build up, an effect which was accompanied by reduction in the static component of the

deflection under the influence of the grinding forces. The reduced deflection accounts for the reduced component size for specimen 20 evident in fig. 52. The corresponding vibration traces, fig. 55, were measured from the machine structure relative to the grinding wheel spindle and illustrate several interesting features, when compared with the Talyrond traces, fig. 54.

(1) The maximum vibrations while grinding specimen 20 are worse than for specimens 19 and 21.

(2) The high frequency vibration corresponds to a frequency just below a resonance of the control wheel head at 82 Hz, which is transmitted by the grinding forces to the grinding wheel. This also coincides with the geometrically unstable condition which gives rise to 22 waves.

(3) The low frequency vibration corresponds to the 3-lobeshape apparent.

The surface roughness records of Fig. 56 do not show such strong correlation with roundness errors as were apparent between size and roundness errors. If there is a saw-tooth pattern with surface roughness, it appears that the tendency is for slight improvement when forces decrease and roundness deteriorates. The overall tendency is for surface roughness to increase with time, which may be attributed to generally increasing irregularity of the grinding wheel surface to be expected with wear and dislodgement of grits.

In order to explain the effects which occurred while grinding specimens 19, 20 and 21, it is desirable to

distinguish the cause and effect. It is not absolutely clear whether there is an external cause of occasional vibration which leads to the associated effects or whether there is a natural instability of the grinding wheel surface leading to increased vibration. An hypothesis for such an instability is that as the grinding progresses there is a dulling of the cutting edges of the grinding wheel grits. The dulling is accompanied by an increase in the radial cutting force which has the effect of deflecting the grinding wheel spindle and thereby increasing the diameter of the ground workpiece. The action progresses to a point at which the grits become sufficiently dull so that they are either dislodged from the grinding wheel or fractured. During this period, there is a consequent increase in vibration level which is associated with increased roundness errors. The increase of roundness errors with reduced forces would be expected for the geometrically unstable condition.

This explanation requires that the self-dressing effect once initiated accelerates for a short period until a stable situation is achieved. Otherwise, if the self-dressing effect were steady, the process would not be cyclic. The occurrence of these phenomena, i.e. the almost instantaneous change in the grinding conditions has been observed, grinding both soft and hard specimens. It appears that the frequency of occurrence depends on the type of grinding operations and in our experiments the process

appears to be accelerated with soft specimens leading more rapidly to a condition where the grinding wheel requires redressing.

In order to investigate the low-frequency content of the grinding wheel deflections, the magnetic tape play-back speed was increased by a factor of eight. The output was analysed by means of a frequency analyser yielding the result shown in Figs. 57 and 58. The peaks indicated correspond approximately to lobing on the workpiece. The orders of lobing corresponding to the frequencies were 1, 2, 3, 4, 5, 9, 18 and 22. On the corresponding chart, three waves and twenty-two waves may be positively identified. (Figs. 57 and 58)

6.3.4. Results for $\alpha_1 = 30^\circ$, $\beta = 0^\circ$ Specimens Hardened with Initial Flat (Correlation with simulation model)

The depth of the initial flat on the periphery of the otherwise circular workpiece is 0.0009 in. Fig. 59(a) illustrates the roundness chart for a typical specimen prior to centreless grinding. The grinding test was conducted for the same geometric conditions as were specified on the model simulated on the hybrid computer described in Chapter V. The test commenced by placing the workpiece on the support blade with the flat on the workpiece contacting the surface of the control wheel. The workpiece was held stationary in this position with a wooden probe whilst the control wheel was fed towards the rotating grinding wheel. On making contact with the grinding wheel, the probe was

removed and the workpiece was allowed to rotate.

Subsequent to removing 0.0009 in stock removal the final workpiece shape was as shown in Fig. 59(b). This illustrates that a ridge has been formed opposite the flat and of approximately equal size. The depth of the flat subsequent to grinding was 0.0016 in. and the size of the ridge was 0.00015 in.

This correlates very well with the simulation model Fig. (44) where it is seen that after a shorter length of time the size of the flat is approximately 0.4 of its original size and the ridge is approximately 0.33 of the initial flat.

Figs. 60 and 61 are portions of the recording for the grinding and control wheel deflections. It may be seen that the initial pulses decay away to a small amplitude although the corresponding errors on the workpiece were still large. Unfortunately, the level of noise which arises from various sources in the machine and the reference discs is too high to allow an accurate correlation with the transient vibrations of the simulated resonance. However, a visual examination shows reasonable agreement with the trace from the model, Fig. 43.

6.3.5. Determination of the Grinding Coefficient (K) for a Depth of Cut.

Practical plunge grinding tests were conducted in which the infeed rate and deflections of the grinding wheel spindle were monitored (Fig. 62), whilst normal cutting

was taking place; the spark-out period was not included in the tests. Deflections of the grinding wheel spindle at the monitoring point, had been previously calibrated against known forces.

Fig. 63 illustrates the force/feed rate relationship obtained from the test, from which the grinding coefficient (K) was determined. The resulting values were K = 470,000 lbf/in. for a feed rate of 0.010 in. per minute, and K = 380,000 lbf/in. for a feed rate of 0.0125 in. per minute. These findings concur with the generally accepted theory that the value of K decreases with increasing feed rate.

It should be noted that although the value of K is independant of the machine static parameters, its value is approximately of the same order of magnitude as the various machine structural stiffnesses.

6.4. Conclusions from Grinding Tests.

(1) The grinding results were in agreement with the results from the simulated model and hence confirm the conclusions reached in Chapter V, concerning the critical importance of static compliance.

(2) Vibrations measured in grinding and roundness assessments of ground workpieces have revealed the critical importance of the first resonance in the direction between the two wheels.

(3) The forces and deflections in grinding are affected by the condition of the grinding wheels which is subject to

frequent variations. During periods when the grinding forces were reduced, the roundness errors and the vibrations were increased, while the workpiece sizes were reduced.

(4) Roundness errors may result if the infeed motion gives rise to a small flat on the workpiece at the onset of grinding, or if there is any other sudden disturbance during the grinding process.

CHAPTER VII

Design Recommendations and Final Conclusions

7.1. Design Recommendations Arising from the Research Results

In design of a new machine, careful attention to the following design principles would increase machine stiffness, and improve accuracy with respect to both size and shape.

(1) The tray should be of deep rigid construction and provide constraint to the two wheelheads.

(2) The feed-drive should be in line with the centres of the two wheels, thus satisfying the Abbe Principle for the relationship between the required dimension on the work-piece and the indicated dimension from the feed-drive.

(3) The axis of the infeed slideway should also be in line with the centres joining the two wheels as clearly as practicable to minimise twisting.

(4) Each wheel should be supported symmetrically in a housing by bearings which straddle the wheel. This would reduce spindle and bearing deflections.

(5) The control wheel bearings which operate at low speed should have inherent accuracy and stiffness both at light grinding loads and at low speeds. This requires either hydrostatic bearings or very high precision preloaded rolling bearings.

(6) The infeed drive characteristics should be designed so as to minimise the sudden penetration which occurs at the onset of grinding which may initiate round-

ness errors.

(7) The machine stiffness should be as high as possible to minimise the amplitude of forced vibrations which inter-act with the geometric process to be a primary cause of roundness errors. The machine stiffness should also be high in relation to the mass in the lowest frequency resonant mode of relative vibration between the two wheels, so that the first important resonant frequency will be as high as possible.

(8) The grinding wheel bearings should be designed for very high accuracy in order to minimise the generation of vibrations at the grinding point. For this application, hydrostatic bearings would be ideal.

Fig. 64 shows a configuration which attempts to incorporate the above features without loss of the practical advantages arising from an open structure. It will be appreciated that other designs are possible which satisfy the listed principles to a greater or lesser extent. However to actually design a new machine was not an objective of this thesis.

7.2. Final Conclusions (Detailed conclusions have been presented at the end of Chapters III, IV, V and VI)

1. The compliances at the grinding point due to the various machine elements have been measured in static and dynamic tests. The findings have been incorporated in a statement of important design principles as listed in Section 7.1.

(2) A model of the grinding process has been developed which simulates both the static and dynamic behaviour of the machine. The model also simulates the geometric process with realistic time delay terms. Good correlation was obtained with grinding experiments.

(3) The grinding tests revealed that the grinding conditions do not remain constant over a period of time. Hence there may be a saw-tooth pattern of process variations. The simulated model cannot take all these variations into account accurately, although the qualitative conclusions do remain valid.

(4) In all the tests it was apparent that both the large static compliance and the lowest frequency resonance were of primary importance in the formation of the final workpiece shape. Thus from the model, it is possible to demonstrate why the process of shape generation occurs very slowly in grinding operations.

CHAPTER VIII

Suggestions for Future Work

8.1.(1)A more comprehensive hybrid computer model should be investigated, which should include:-

(a) A range of geometric conditions to allow a study of the phase relationships and conditions of instability.

(b) Further machine structural parameters.

(c) The effect of the workpiece inertia.

(2)The computer simulation should be used to investigate on the following influences on the final workpiece shape:-

(a) The initial profile of the workpiece.

(b) The initial rate of penetration of the grinding wheel into the workpiece.

(3)The computer simulation should be used to determine an optimum machine stiffness, possibly related to infeed rate and the grinding coefficient.

(4)The conclusions from this thesis should be applied in the design of an open structured centreless grinding machine. The machine should be tested to compare its performance against the performance of other machines.

APPENDIX A

Honeywell DDP 516 Digital Computer

Specification

Core store of 8,000 words of 16 bits with 0.96 μS cycle time. Single address with multi-level indirect addressing and indexing.

Speed -	Add and subtract	1.92 μ S
	Multiply	5.28 μ S
	Divide	10.56 μ S
	Single word I/O transfer	1.92 μ S

Input/output equipment

- Teletype (ASR-33)
- Paper tape reader 500/1000 cps
- Paper tape punch 110 cps

Standard input/output lines (6 V TTL compatible)

- 10-bit address bus
- 16-bit input bus
- 16-bit output bus
- 12 levels of priority interrupts
- External control and sense lines

Off-line equipment

- Teletype (ASR-33)

The computer is to be extended in the future for greater digital capacity.

Analogue Computer

Technology:

100 Volt discrete-component solid state

Complement:

4 patch areas with 50 patch panels

56 operational amplifiers (32 integrators,
16 summer/multipliers, 8 inverters)

32 Servo-set coefficient potentiometers

32 manual coefficient potentiometers

Control:

No manual controls - computer control only

Interface

Functional units:-

8 integrator control groups

16 analogue comparators

16 analogue switches

8 D to A converters (15 bit)

1 A to D converter (15 bit, 30 S Con.)

256 channel solid state multiplexer

1 11 inch CET computer - controlled
4-beam display unit

Logic display panel

Numerical 5-digit display

1 remote control box

16 external monitor points

4 manual switches

2 on-line output control registers

2 on-line input control gates

Software

A comprehensive package of manufacturers programming software is available for digital computation. This has been extended by the addition of special purpose programmes including a hybrid compiler.

Manufacturers Software

DAP-16 mneumonic code assembler

Fortran IV compiler

Maths library

Test routines

Lanchester Software

on-line editor

Hybrid computer software system I

Hybrid computer test routines

On-line process control programmes

APPENDIX B

Grinding Test Conditions

Grinding Machine: Wickman Scrivener No. 0 Model as described in Appendix C

Grinding Wheel: 5A 46/54 - K5 - V50 Initially 11.6 in. x 3 in. x 4 in. bore

Control Wheel: A80 - R - R Initially 6.7 in. x 3 in. x 3 in. bore

Workblade: Zero angle; cast steel hardened and tempered, 30° angle; Tungsten Carbide

Control Wheel Speed: 24 revs/min., inclination $\frac{1}{4}^{\circ}$

Grinding Wheel Speed: 1,800 revs/min

Coolant: Fletcher Miller "Clearedge" water soluble oil (1:40)

Wheel Dressing Procedure: Traverse rate 1.5 in/min. 1 pass with .001 in. depth of cut, return pass .001 in depth. 1 pass without cut return pass .0005 in. in cut. 1 pass and return pass without cut

Stock Removal: .010 in. on diameter

Spark out time: 7 seconds

Infeed: was continuous and controlled by a hydraulic mechanism incorporating a plate cam.

APPENDIX C

The Machine Description

Base and Bed

Contained in this rigid integral casting was the grinding wheel head, the main slideway, the base for the grinding wheel truing device, and the workblade seating.

Grinding Wheel Spindle

The spindle of nitralloy steel ran in two plain phosphor-bronze bearings. Provision for adjustment of clearance was made by pressure pads in the top half of the bearings locating the spindle against the lower half. End thrust was taken by spring-loaded ball-bearings, and the drive from the main motor was by vee belts.

Control Wheel Spindle

The control wheel spindle was of similar design, but independently driven by a separate motor, providing quick change over from working to truing speeds. For through-feed grinding the control wheel was adjustable up to 6° forward tilt and 2° reverse tilt.

Workblade Seating

This seating provided accommodation for both through-feed and plunge-feed workblades. It was mounted on a dovetail slide which could be connected or disconnected with the control wheel slide as required.

Automatic infeed Unit

Basically the controlled-cycle plunge feed unit con-

sists of a hydraulically-operated reciprocating camplate of suitable profile, which is traversed past the control head slide, imparting wheel closing and opening movements to it automatically. The camplate profile embodies rapid approach, stock-removing controlled infeed, dwell during "rounding-up" of the work as size is reached and, on accelerated reversal, rapid wheel opening to complete the cycle. A flow-control valve is provided to permit control over the total cycle time.

Form Truing of Wheels

Separate hydraulically-operated power truing attachments are provided for each wheel, by means of which any desired profile can be obtained by fitting a suitable former plate. On the grinding wheel, this attachment has a ball bearing cross-slide, permitting the more accurate following of extreme forms. The control wheel attachment may be adjusted vertically so that truing may be carried out at the height of contact between the control wheel and the workpiece.

Specifications

Wickman - Scrivener No. 0 Centreless Grinding Machine

Work range (Plunge feed) grinding 0.06 to 1 in.

Work range (Through feed) grinding 0.02 to .625 in.

Maximum opening (new wheels) (controlled cycle) 1.375 in.

Grinding wheel size (dia x width x hole) 12 x 2 x 4 in.

Control wheel size (dia x width x hole) 7 x 3 x 3 in.

Grinding wheel spindle speed	1806 rev/min
Control wheel spindle speeds (working)	23,30 and 39 rev/min
Control wheel spindle speeds (truing)	385,490 & 600 rev/min

Electric Motors

Grinding wheel	5 h.p.
Control wheel	3/4 h.p.
Coolant pump	1/8 h.p.
Hydraulic power unit pump (controlled cycle)	2 h.p.
Coolant tank capacity	40 imp. galls
Coolant pump max. delivery	10 i.g.p.m.

REFERENCES

1. Gurney, J. P., "Analysis of Centreless Grinding". A.S.M.E. Paper No. 63-WA-26, Journal of Engineering for Industry, May 1964, pp. 163-174.

2. Rowe, W. B. and Barash, M. M., "Computer Method for Investigating the Inherent Accuracy of Centreless Grinding". Int. Journal Mach. Tool Des. and Res. Vol. 4, pp. 91-116.

3. Yonetsu, S., "Proceedings of the Fujihara Memorial Faculty of Engineering". KE 10 University, Tokyo, Japan, 1959. Vol. 12, No. 47, pp. 8-26.

4. Becker, E. A., "Krafte Und Kreisformfehler Beim Spitzenlosen-einstechschleifen", 1965. Doktor-Ingenieurs Thesis, Aachen.

5. Rowe, W. B. and Richards, D. L., "Geometric Stability Charts for the Centreless Grinding Process", Journal of Mechanical Engineering Science. To be published, 1972.

6. Rowe, W. B. and Koenigsberger, F., "The Work-Regenerative Effect in Centreless Grinding". Int. Journal Mach. Tool Des and Res. 1965, Vol. 4, pp 175-187.

7. Sachsenberg and Kreher, "Werkstattstechnik Und Werksleiter", 1939, Vol.33, No. 11, p. 280.

8. Dall, A. H., "Rounding Effect in Centreless Grinding", Mechanical Engineering, April 1946, Vol. 58, pp. 325-329.

9. Colwell, L. V., "The Effects of High-Frequency Vibrations in Grinding", Trans A.S.M.E. 1956, Vol. 78 p. 837.

10. Yonetsu, S., "Forming Mechanism of Cylindrical Work in Centreless Grinding", Proc. of the Fujihara Memorial Faculty of Engineering, Keio University 1959. Vol. 12, No. 47, pp. 8-26.

11. Rowe, W. B., "Some Studies of the Centreless Grinding Process with Particular Reference to the Roundness Accuracy". Ph.D. Thesis 1964, Manchester.

12. Tobias, S. A. and Fishwick, W., "Theory of Regenerative Machine Tool Chatter". Engineering (London), 1958, Vol. 205.

13. Kaliszer, H. and Singhal, P. D., "Analysis of the Rigidity of the Grinding Wheel Workpiece - Grinding Machine System". Proc. of I.Mech.E. (Applied Mechanics Group), 1966-67. Vol. 181, part 1, pp 1-11.

14. Furukawa, Y, Miyashita, M. and Shiozaki, S., "Vibration Analysis and Work-Rounding Mechanism in Centreless Grinding". 11th I.M.T.D.R. Conference.

15. Richards, D. L., Rowe, W. B. and Koenigsberger, F., "Geometrical Configuration for Stability in the Centreless Grinding Process", 1971. 12th I.M.T.D.R. Conference.

16. Kennedy, C. C. and Paucu, C. D. P., "Use of Vectors in Vibration Measurement and Analysis", Journal of the Aeronautical Sciences, Nov. 1947. Vol. 14, No. 11 pp. 603-625.

17. Honrath, R., "Uber die Starrheit von Werkzengmaschinen und deren Lagerung". Thesis T.H. Aachen, 1960.

18. Rowe, W. B., "Experience with Four Types of Grinding Machine Spindles", 8th I.M.T.D.R. Conference, 1967.

19. Tobias, S. A., "Machine Tool Vibrations", Blackie 1965, Chapter iA-17. pp. 87-93.

20. Grassie, J. C., "Applied Mechanics for Engineers", Longmans 1962, p. 256.

21. Richards, D. L., "An Investigation of the Centreless Grinding Process with a View to Improving Geometric Stability." M.Phil Thesis 1971, Lanchester Polytechnic, Coventry.

22. Den Hartog, "Mechanical Vibrations", McGraw-Hill, Chapter 6, pp. 225-229.

23. Loxham, J., "The Potentialities of Accurate Measurement and Automatic Control in Production Engineering", Symposium on Machine Tool Control Systems, College of Aeronautics, Cranfield, August 1960.

24. Bell, I. F., "The Design of Machine Tool Spindles", Short Course; Aspects of Machine Tool Design, Lanchester College of Technology, February 1965.

25. Loxham, J. and Purcell, J. "Measurement and Control of the Residual Stress Produced by Grinding Operations", Conference on Properties and Metrology of Surfaces. Oxford. April 1968. Vol. 182.

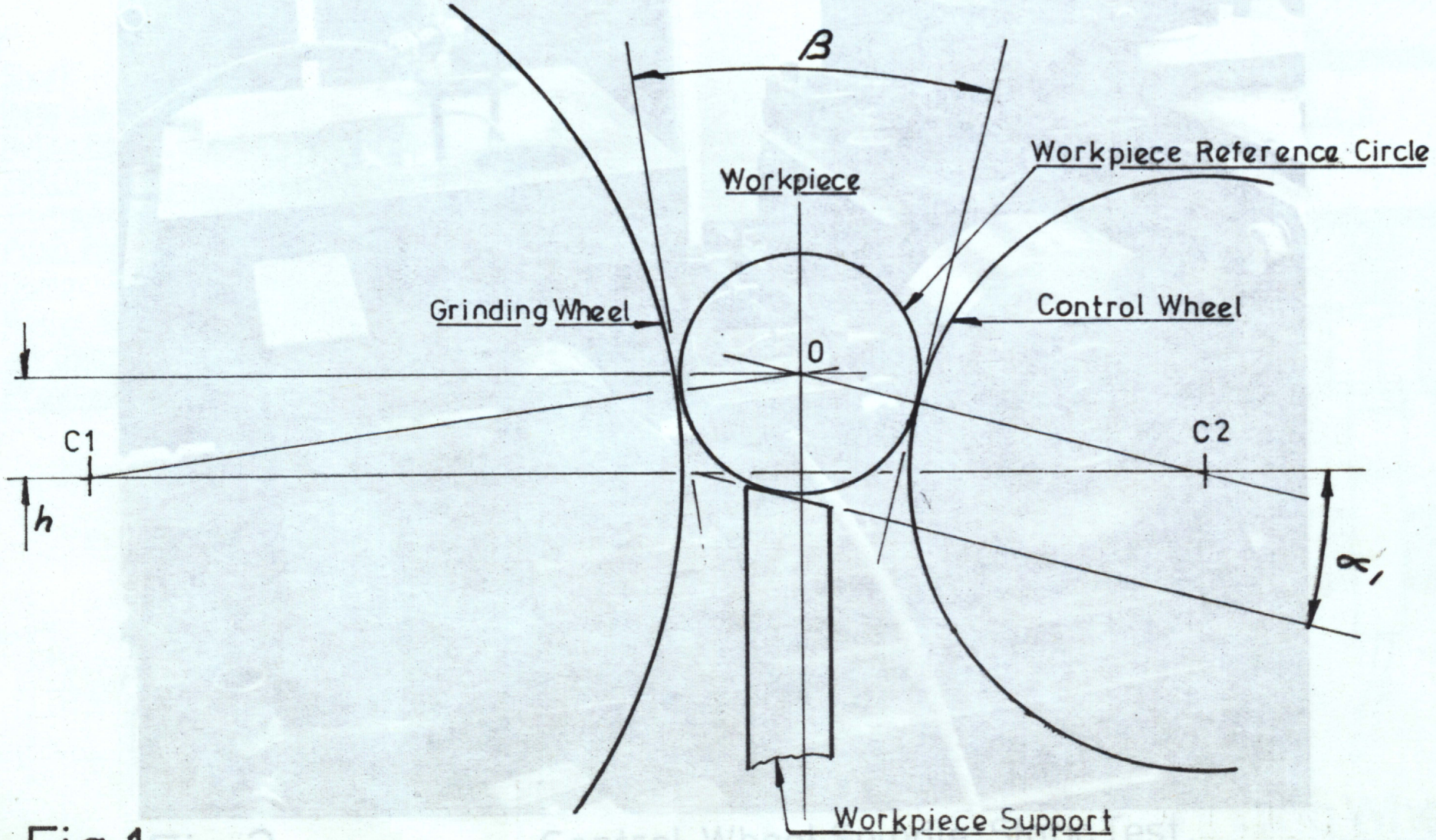
β
Workpiece Reference Circle
Workpiece
Grinding Wheel
Control Wheel
0
C1
C2
h
α1
Workpiece Support

Fig 1

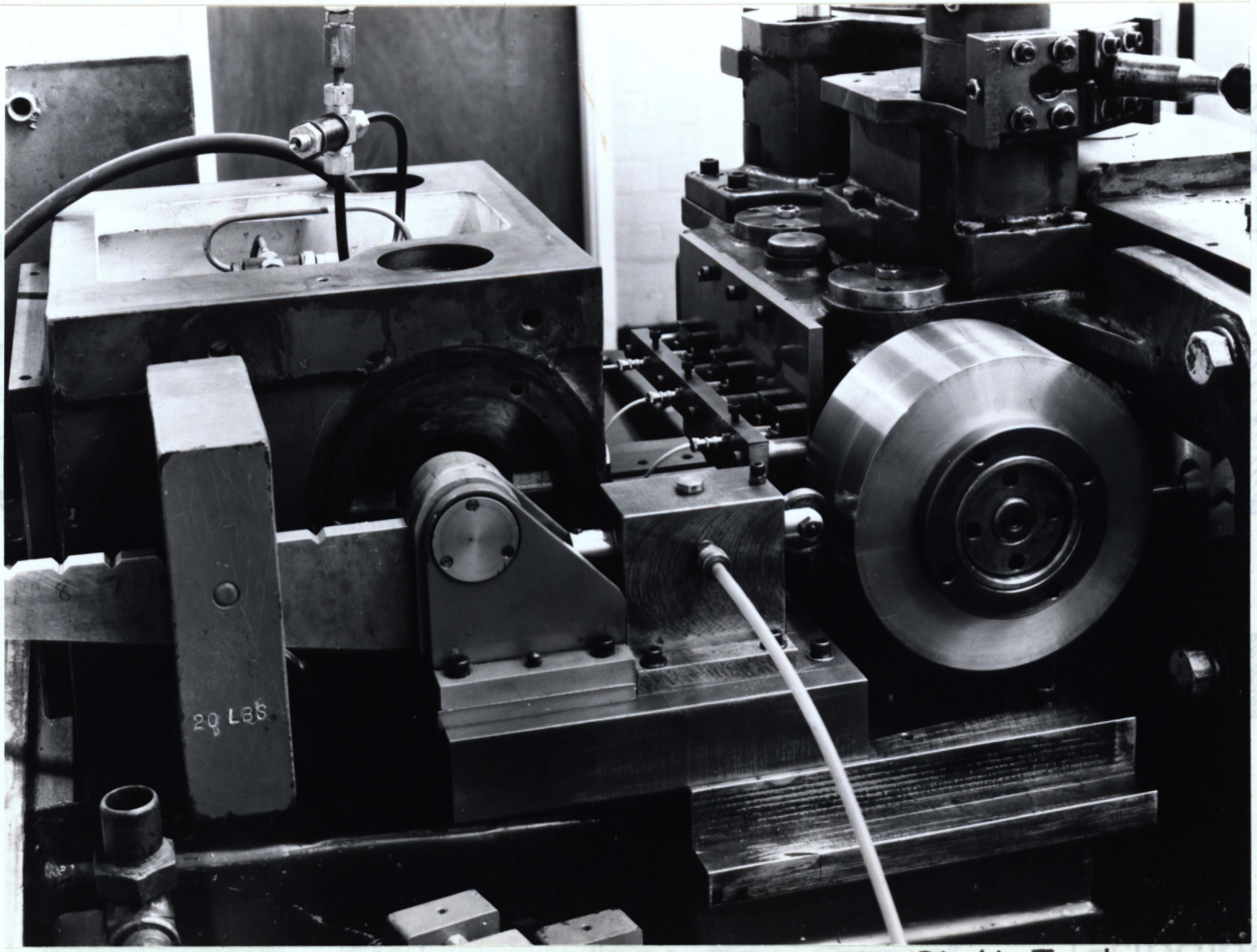

Fig 2 Control Wheel Spindle. Static Test.

Key:

A - Shaft
B - Bearing
C - Nylon Pad
D - Spring
E - Transducer
F - Push Rod
G - Dummy Wheel
H - Roller & Carrier
J - Air Bearing
K - Proximity Transducer

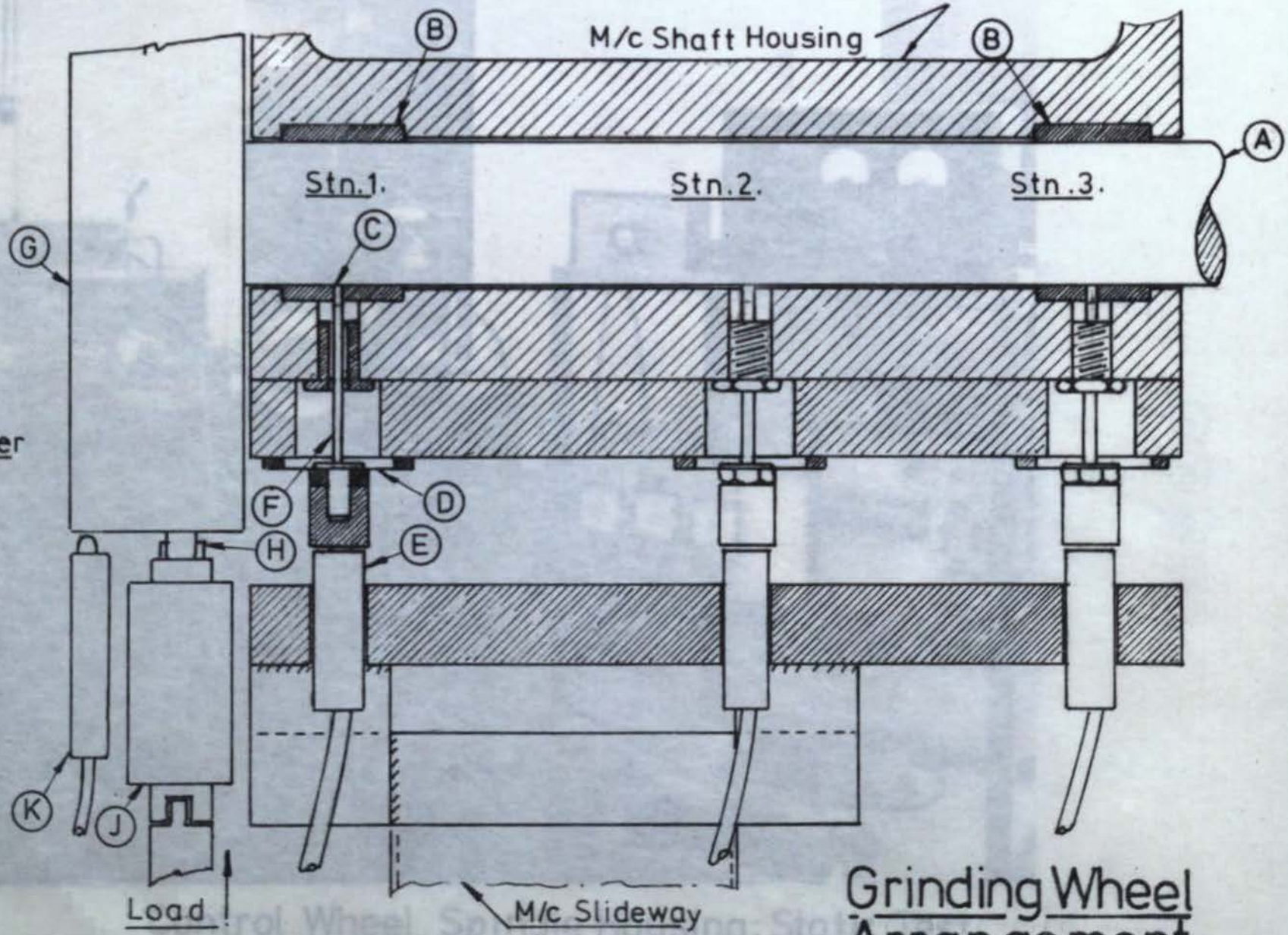

Fig 3

Grinding Wheel Arrangement

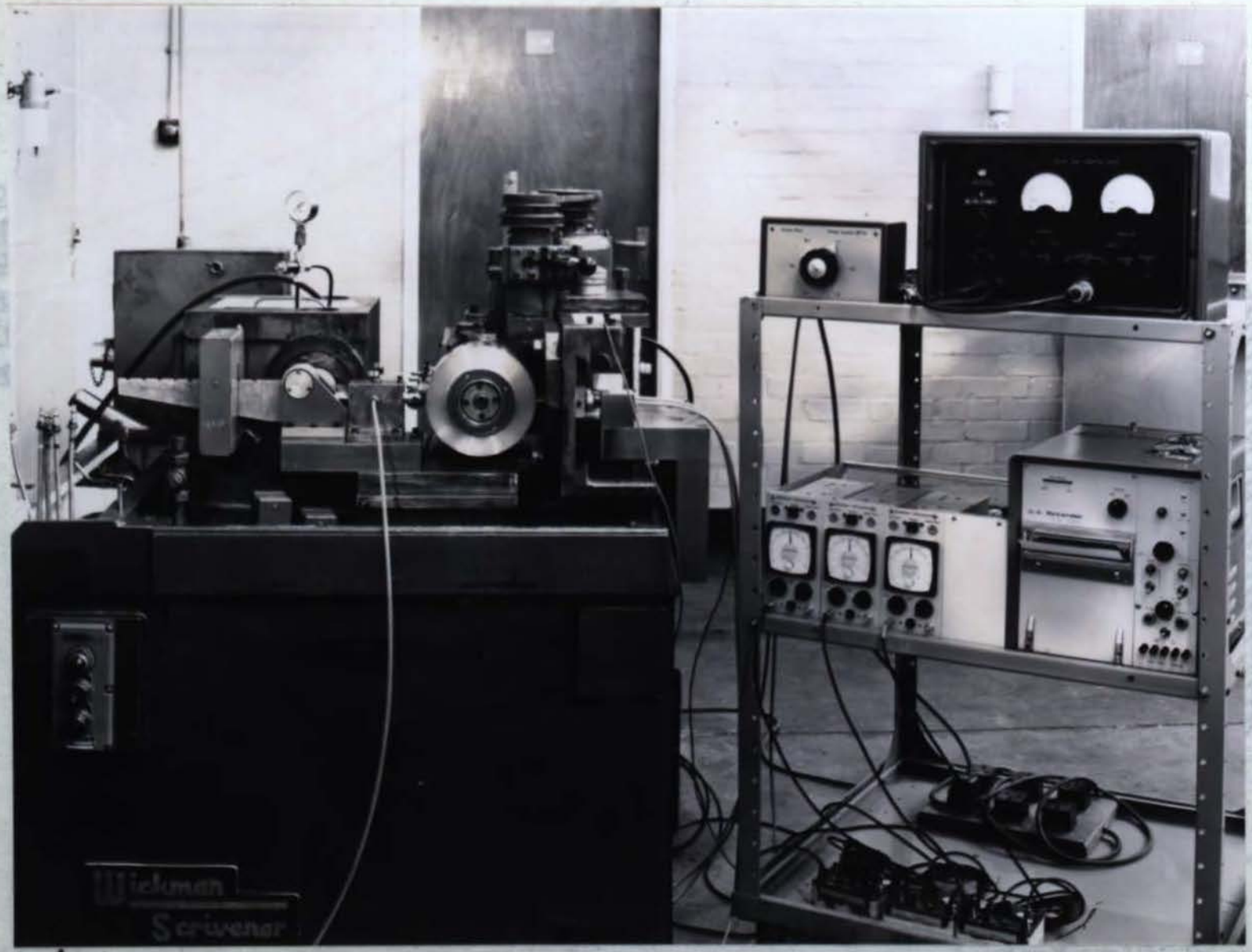

Fig 4 (a) Control Wheel Spindle Housing: Static Test

Key

A: Proximity Transducer
B: Shaft
C: Bearing
D: Housing
E: M/c Base
F: Wheel

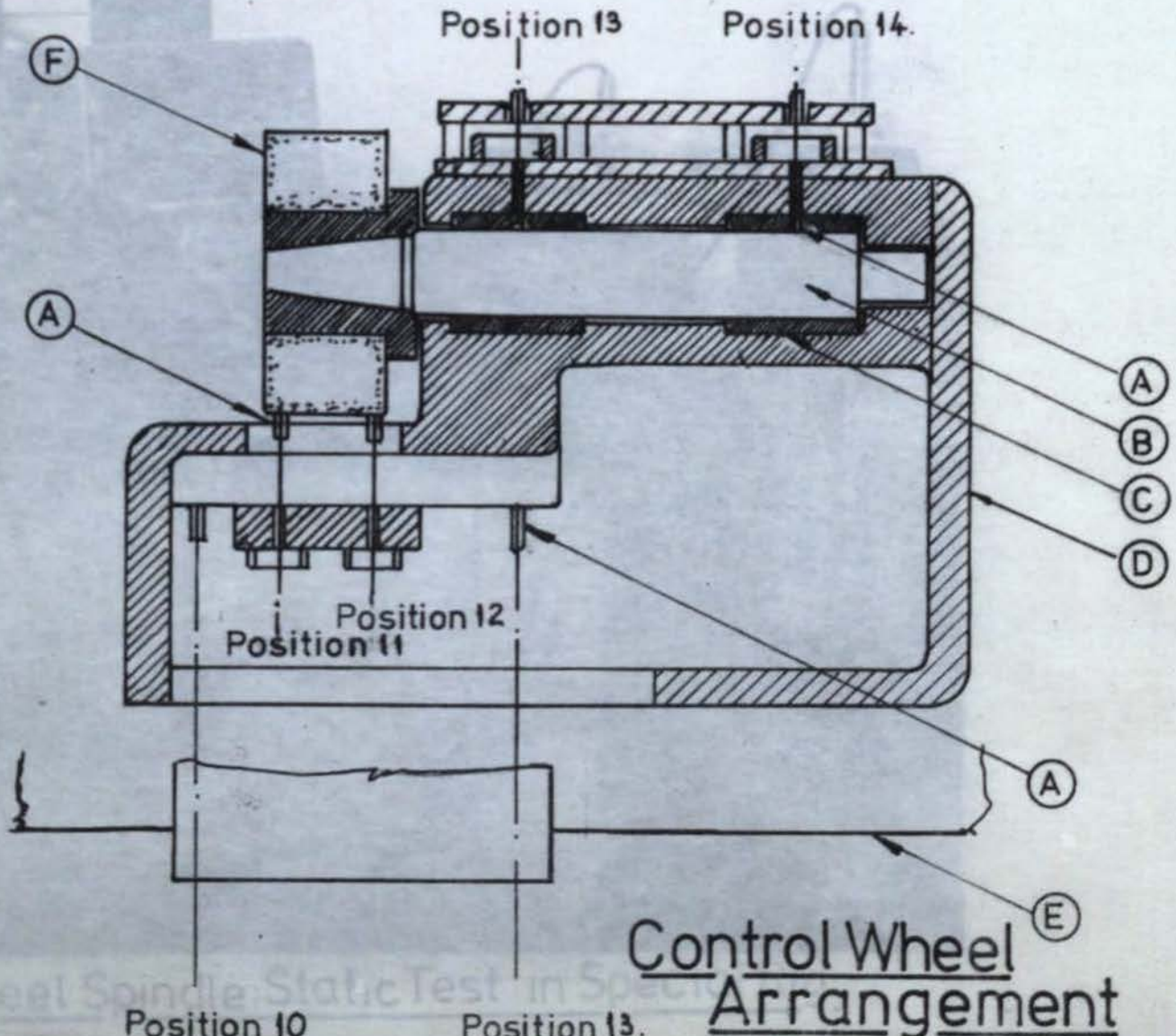

Fig 4 (b)

Control Wheel Arrangement

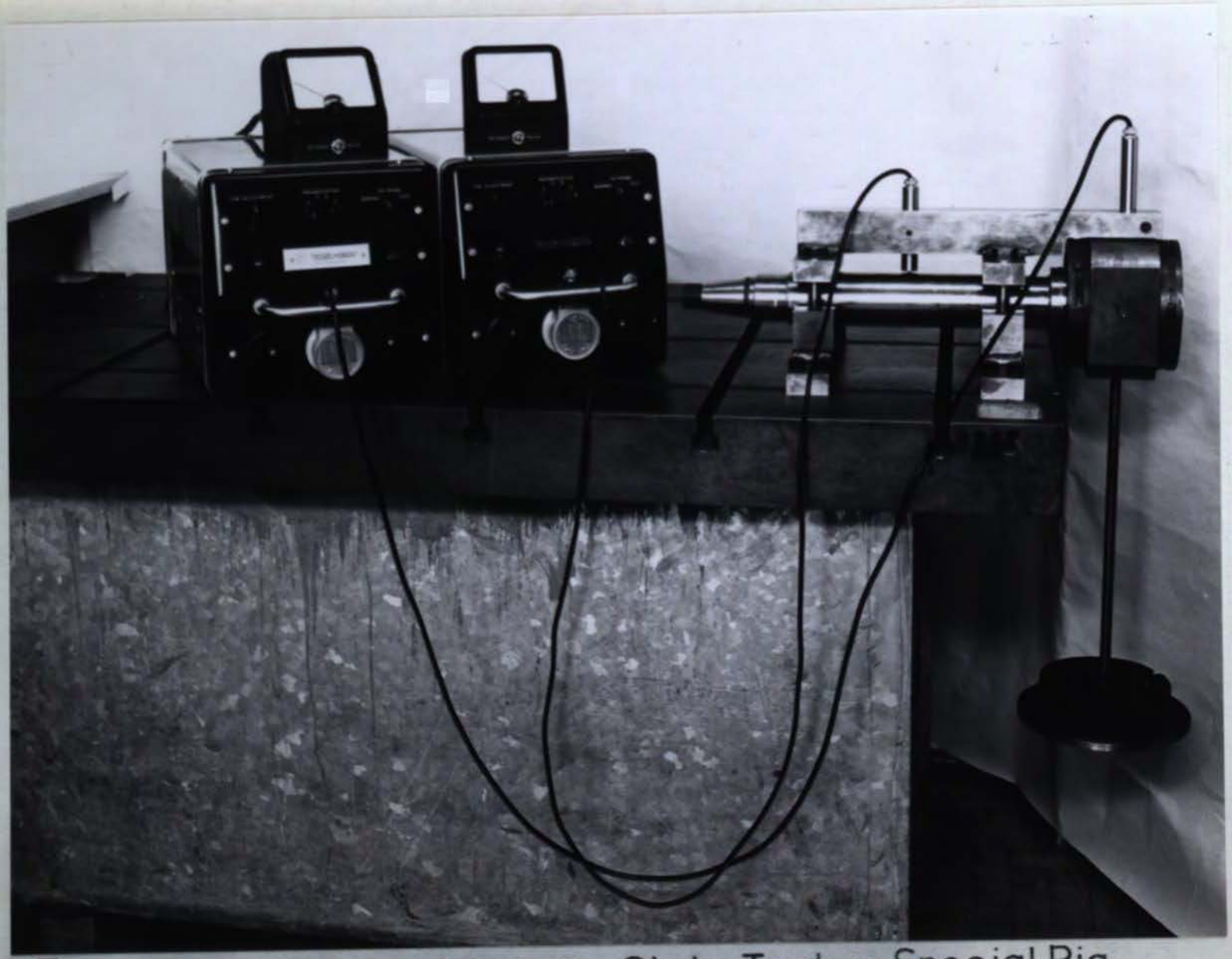

Fig 5 Grinding Wheel Spindle: Static Test in Special Rig.

Fig 6 Control Wheel: Stiffness Test

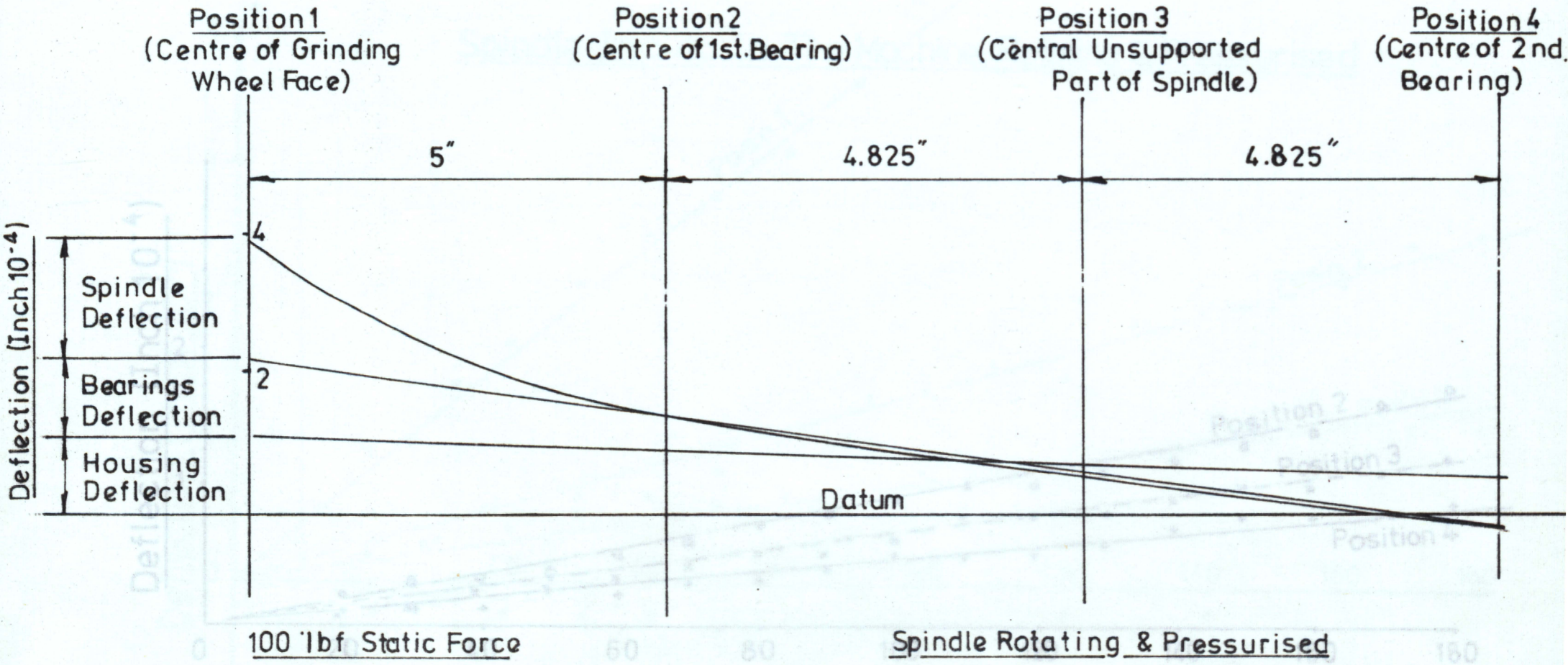

Fig 7 Grinding Wheel Spindle, Bearing, & Housing, Relative Deflections

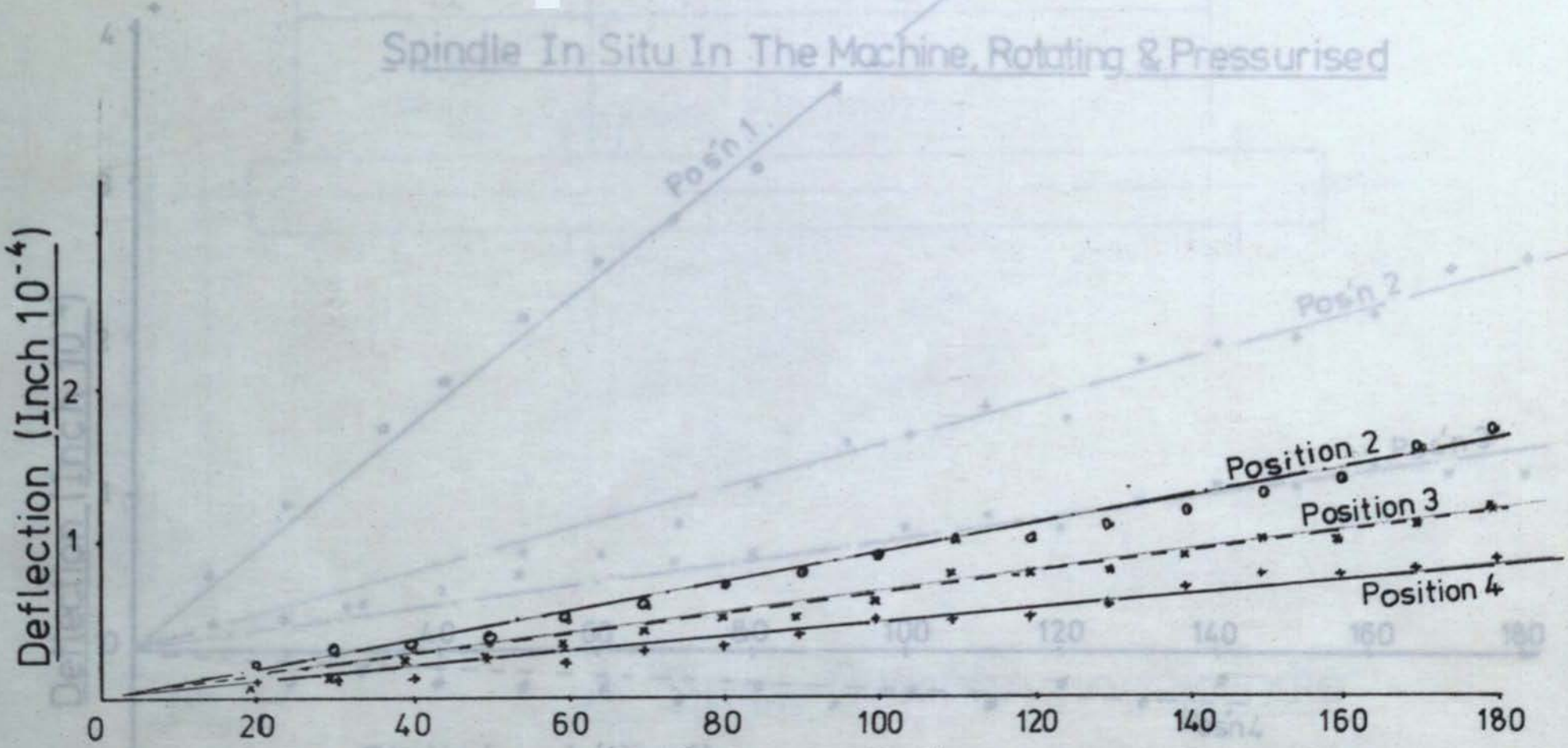

Static Load (lb.f)

Grinding Wheel Spindle Housing Load/ Deflection
At Positions: 2, 3, 4,

Fig.8

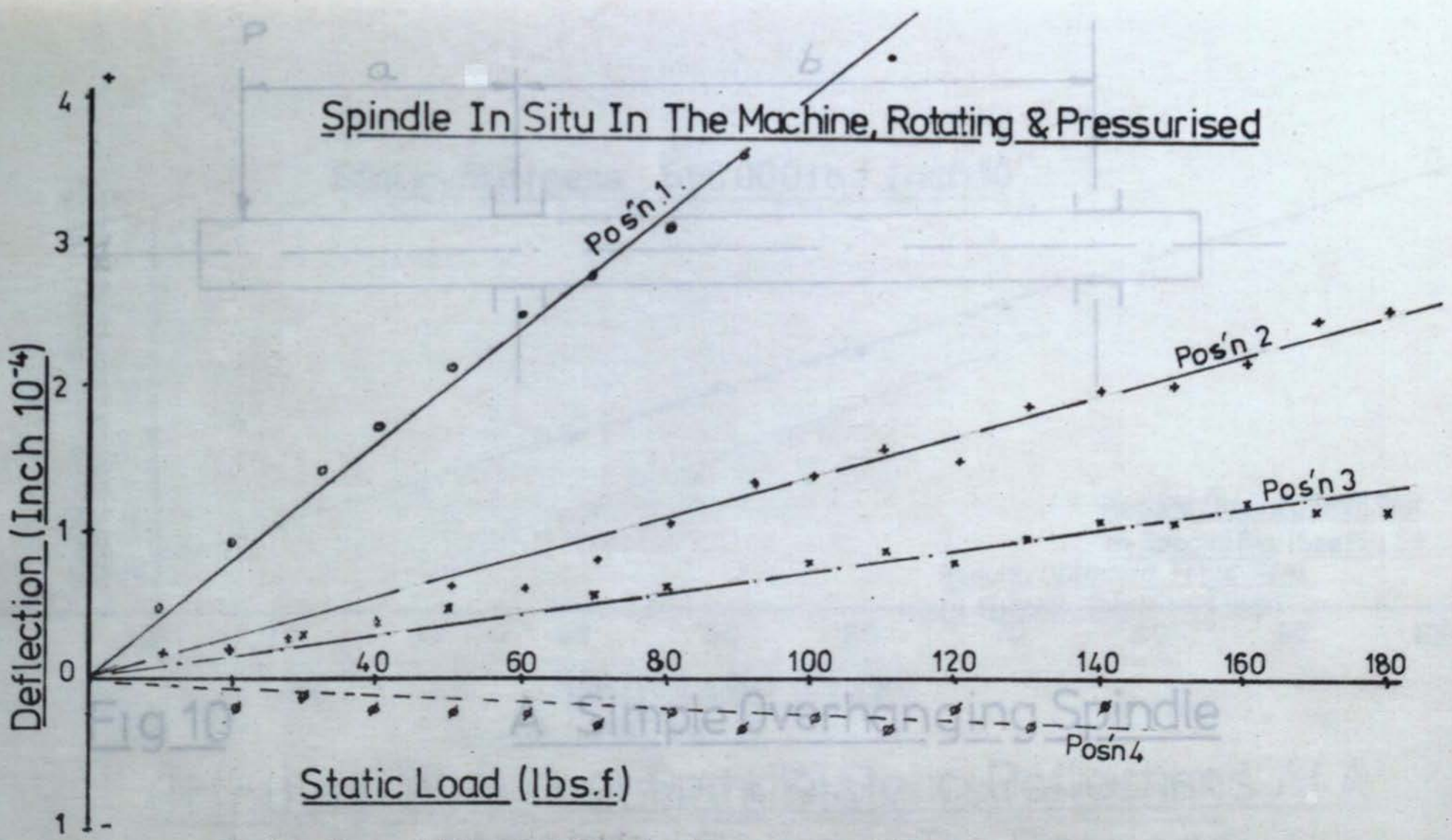

Grinding Wheel Spindle Load Deflection
At Positions 1.2.3.&.4.

Fig.9.

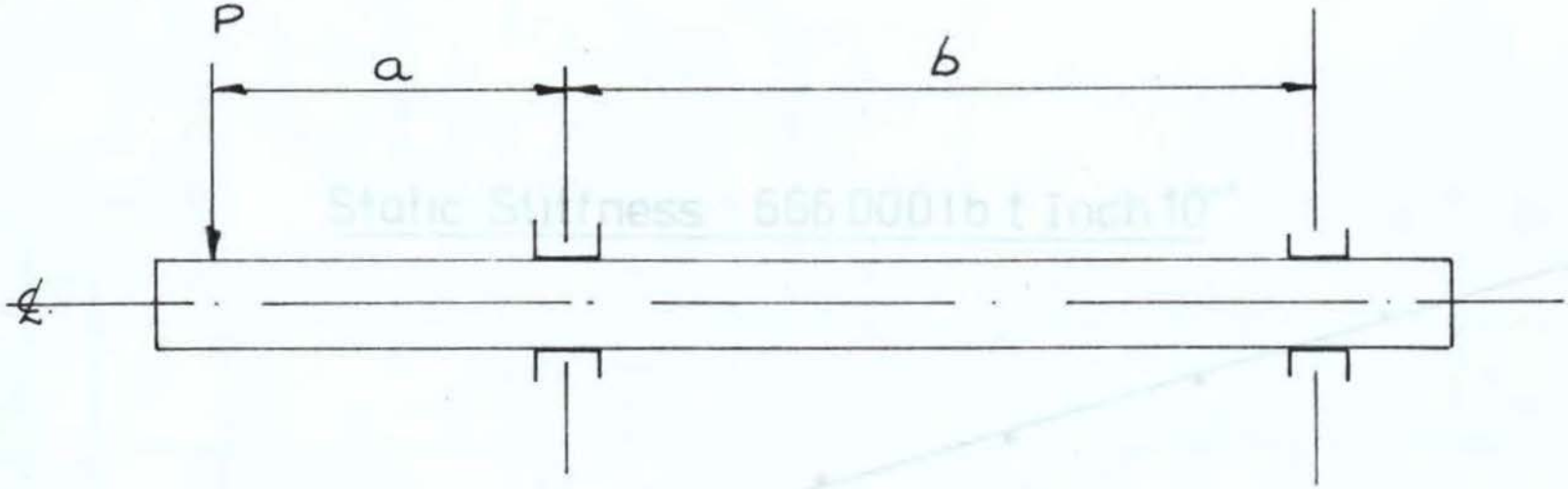

Fig 10 A Simple Overhanging Spindle

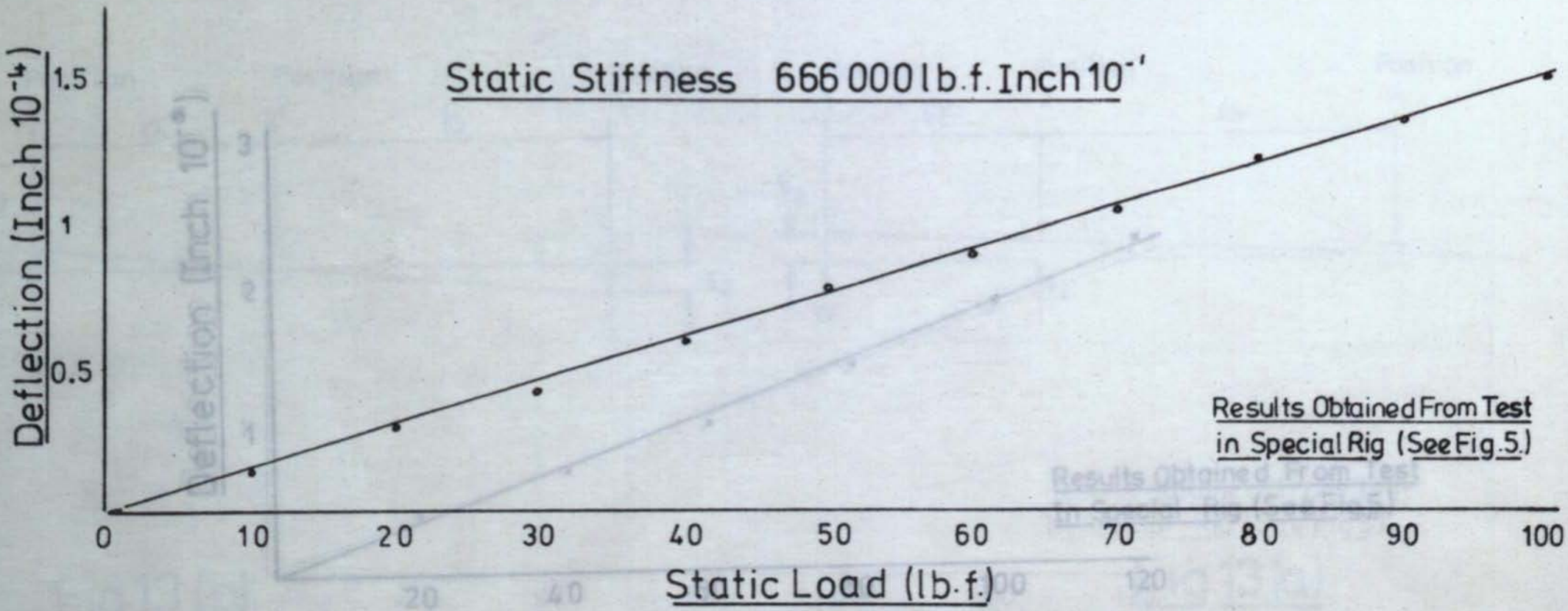

Grinding Wheel Spindle Static Deflections At Position 1

Fig 11

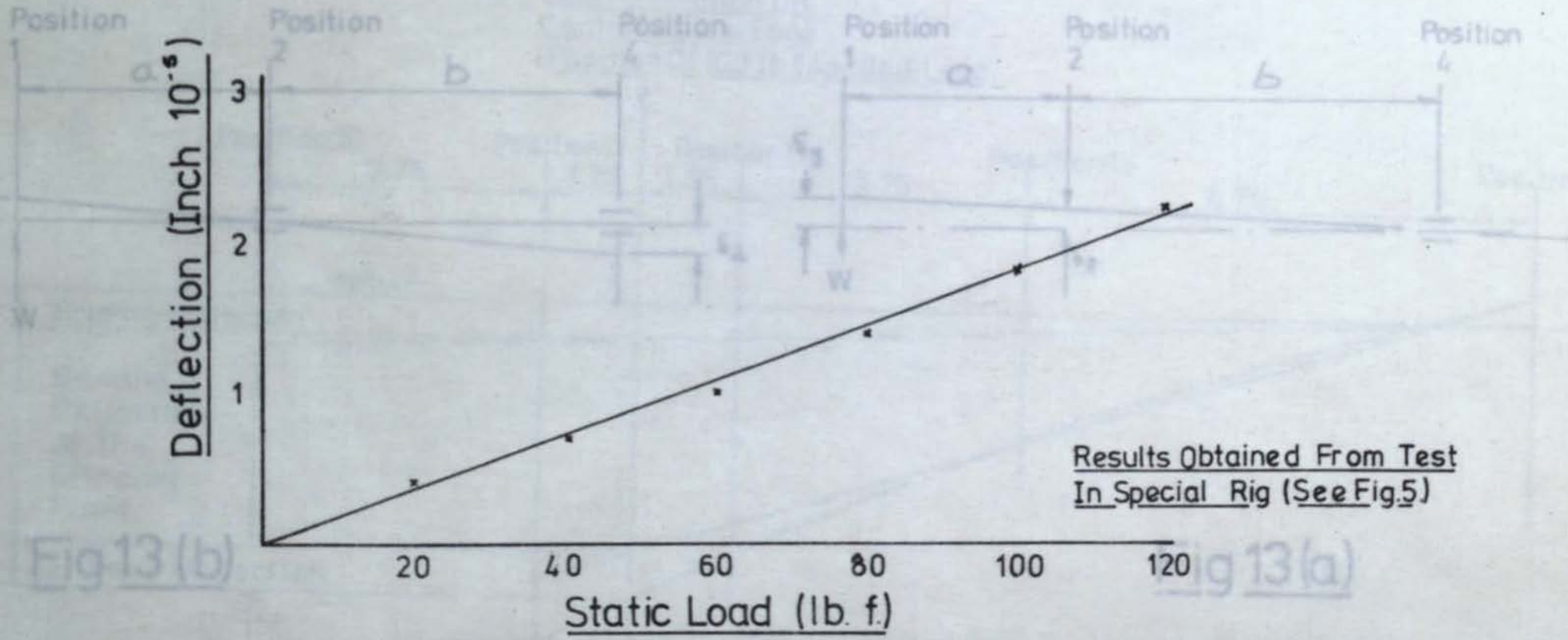

Grinding Wheel Spindle Static Deflections At A Position Mid-Way Between The Bearings

Fig 12

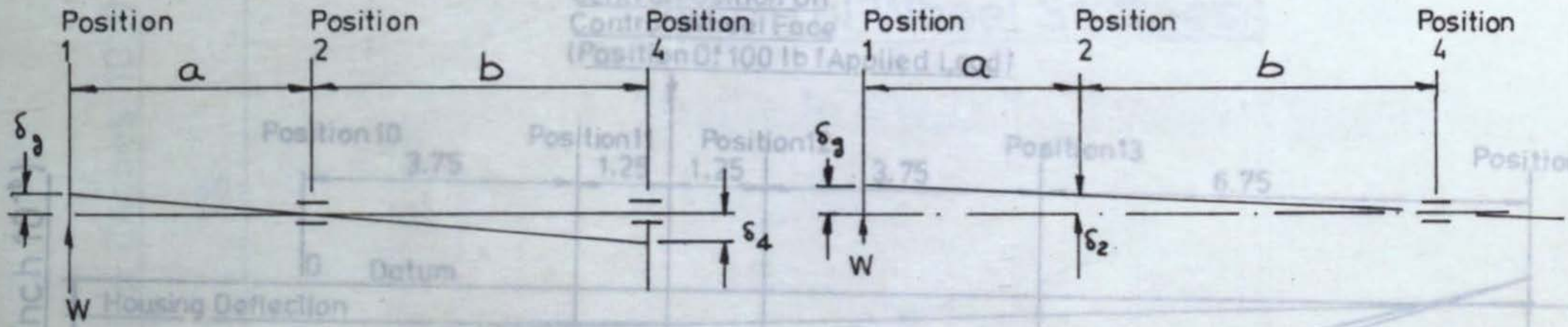

Fig 13 (b)

Fig 13 (a)

Bearing Stiffness Determination

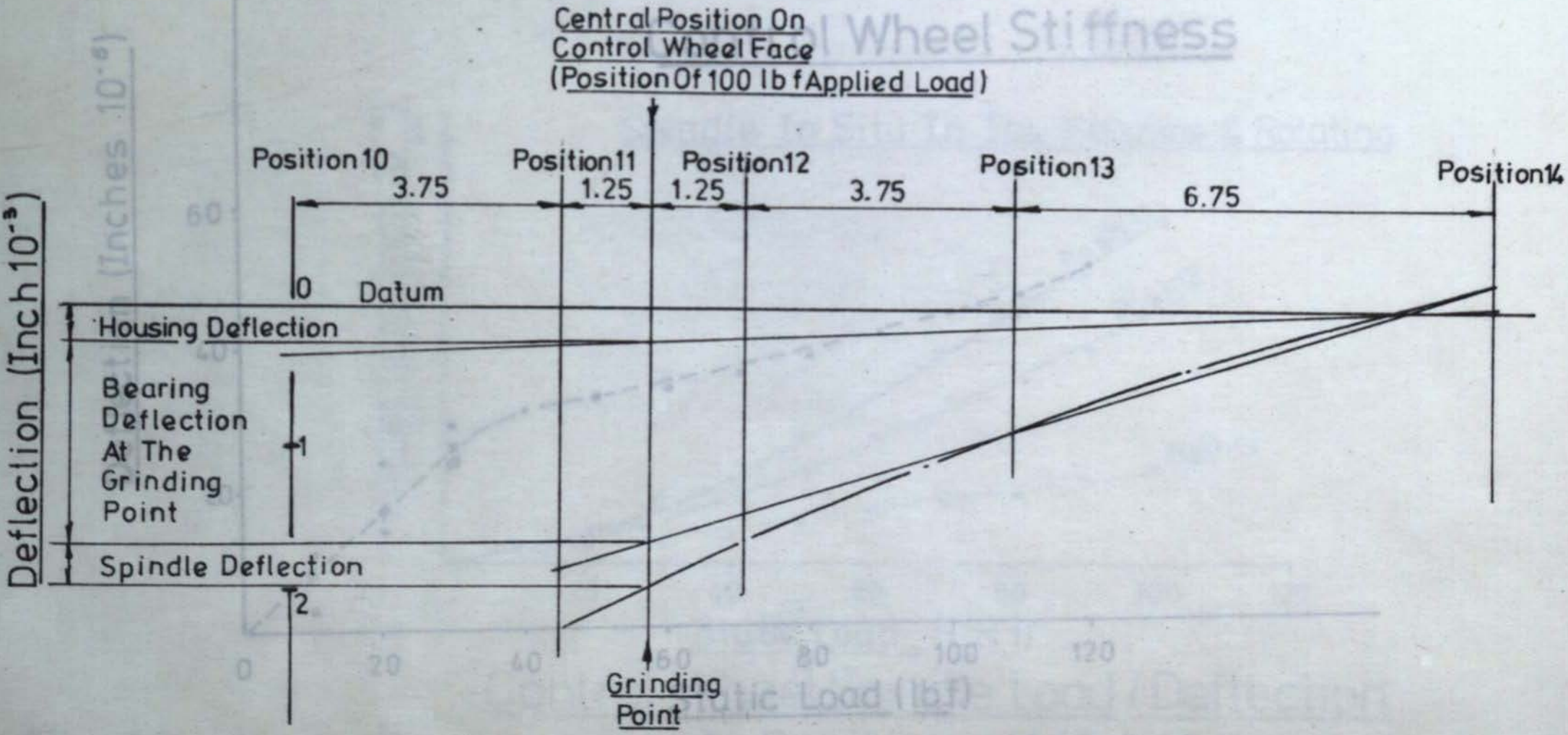

Fig 14 Relative Deflection of Control Wheel Spindle Bearings & Housing

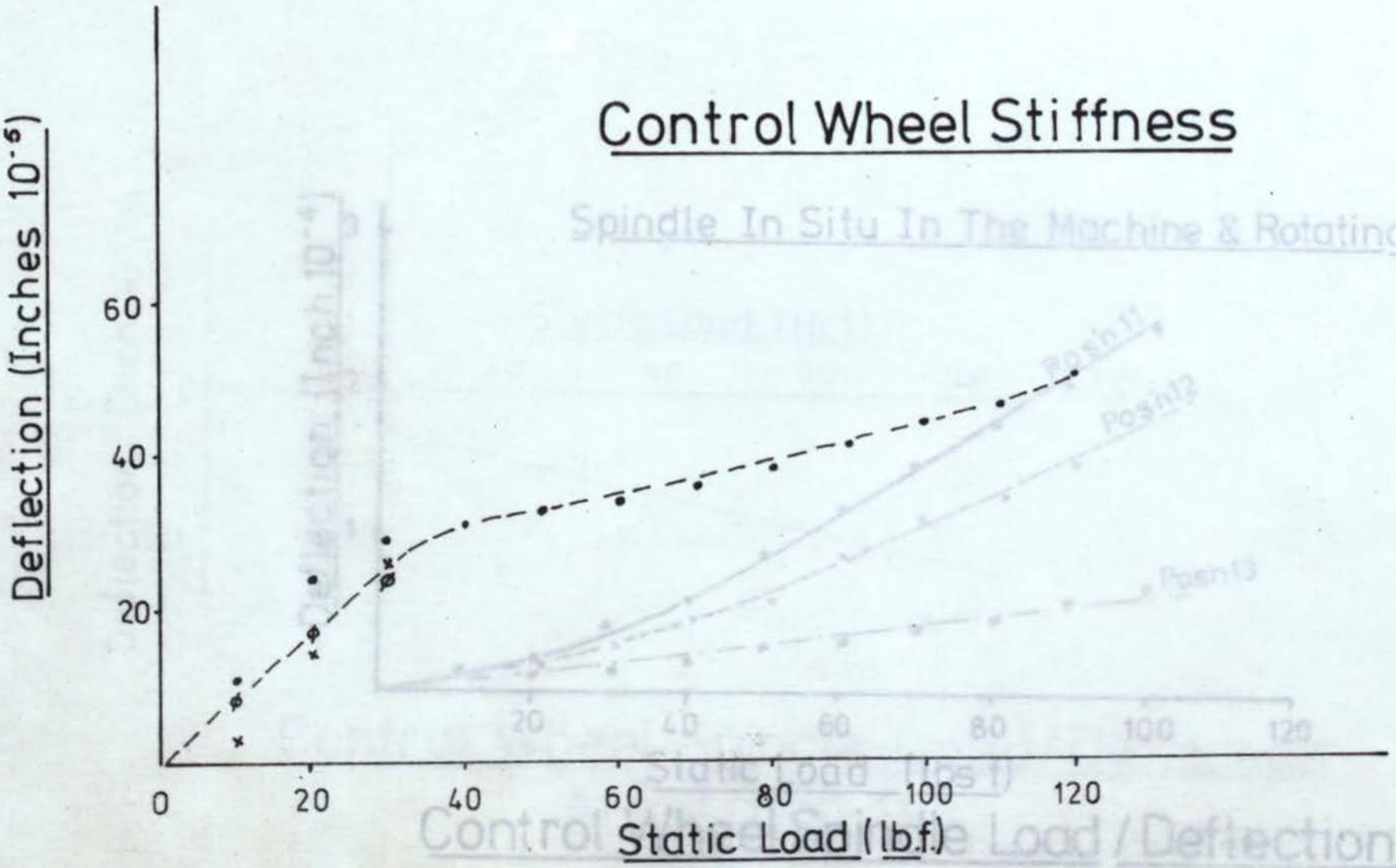
Control Wheel Stiffness
Deflection (Inches 10⁻⁵)
60
40
20
0
20
40
60
80
100
120
Static Load (lb.f.)

Fig.15

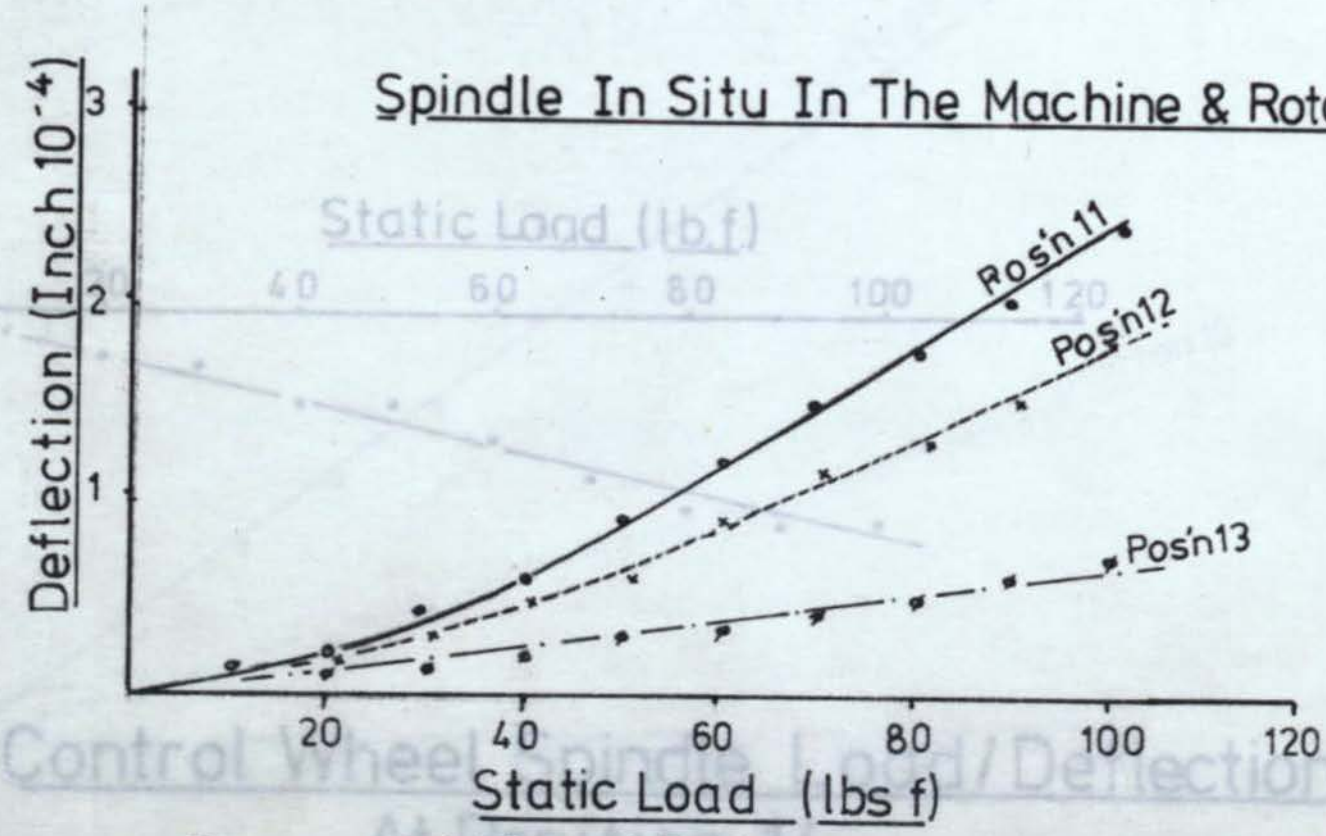

Control Wheel Spindle Load / Deflection
At Positions 11, 12 & 13

Fig 16

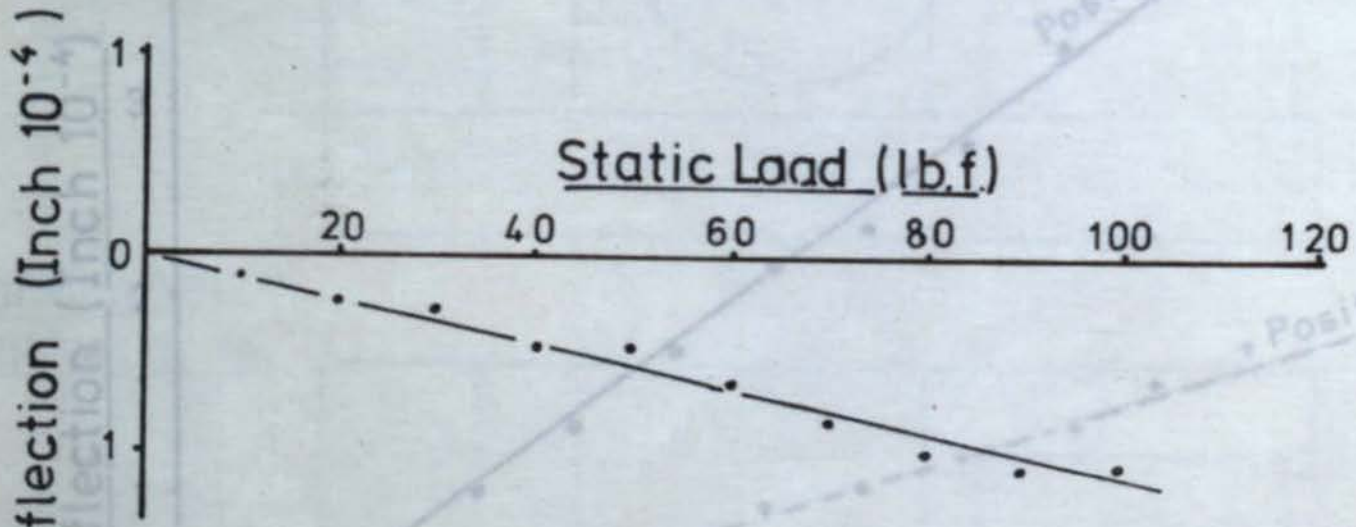

Control Wheel Spindle Load/Deflection
At Position 14

Fig 17

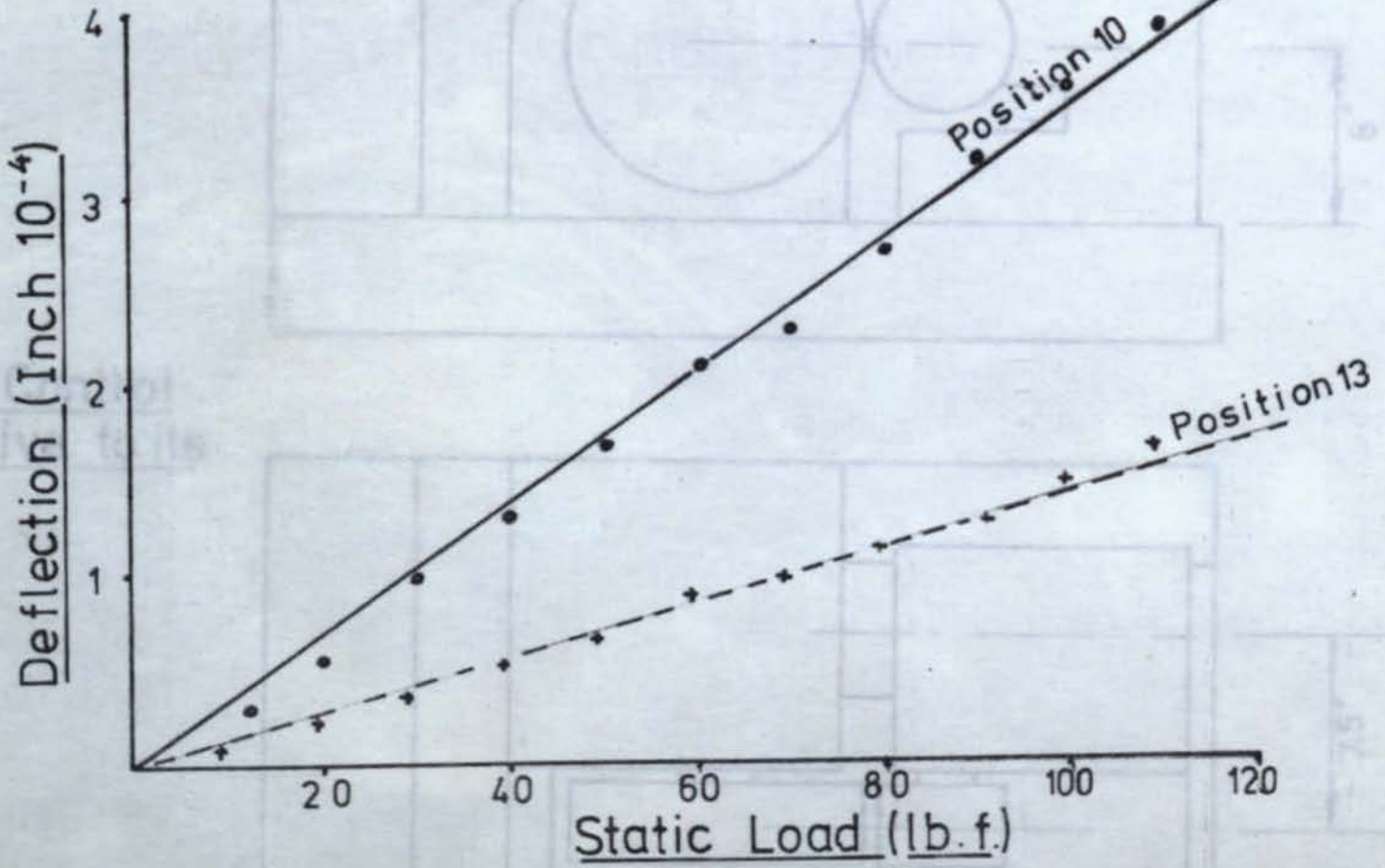

Control Wheel Housing Load / Deflection At Positions 10. & .13.

Fig 18

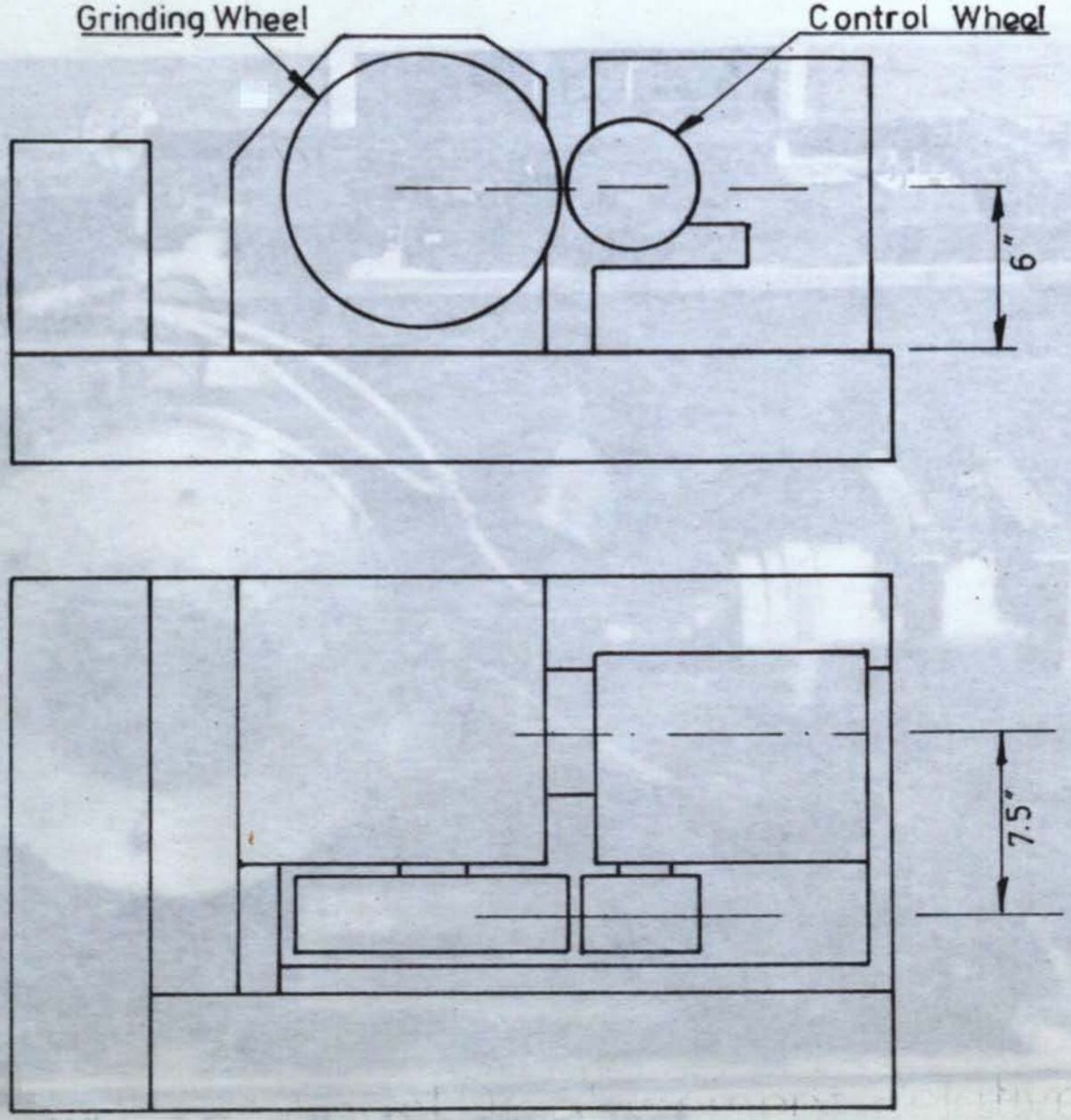

Position of Control Wheel Relative to its Slide

Fig 19

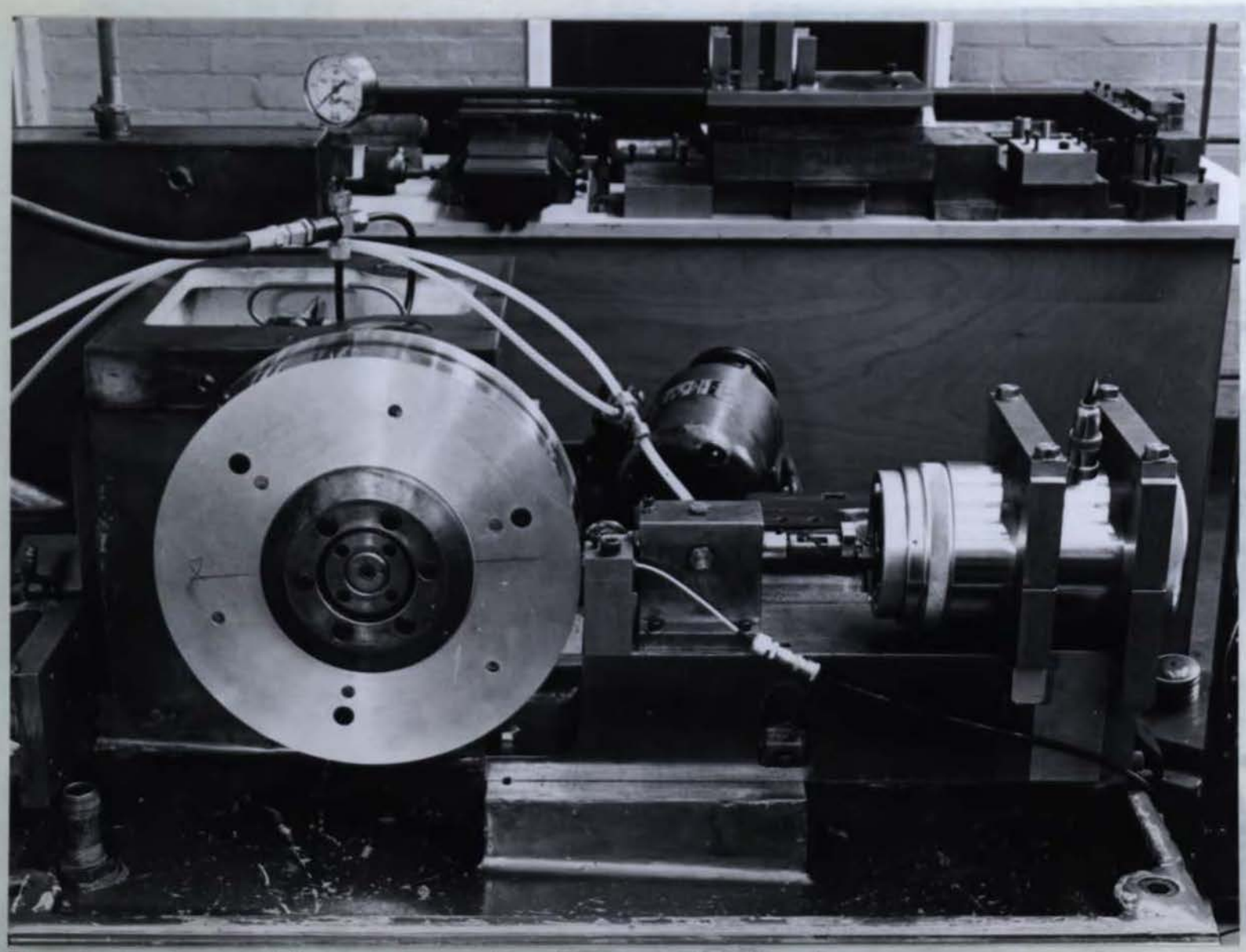

Fig 20 Grinding Wheel Spindle; Dynamic Test

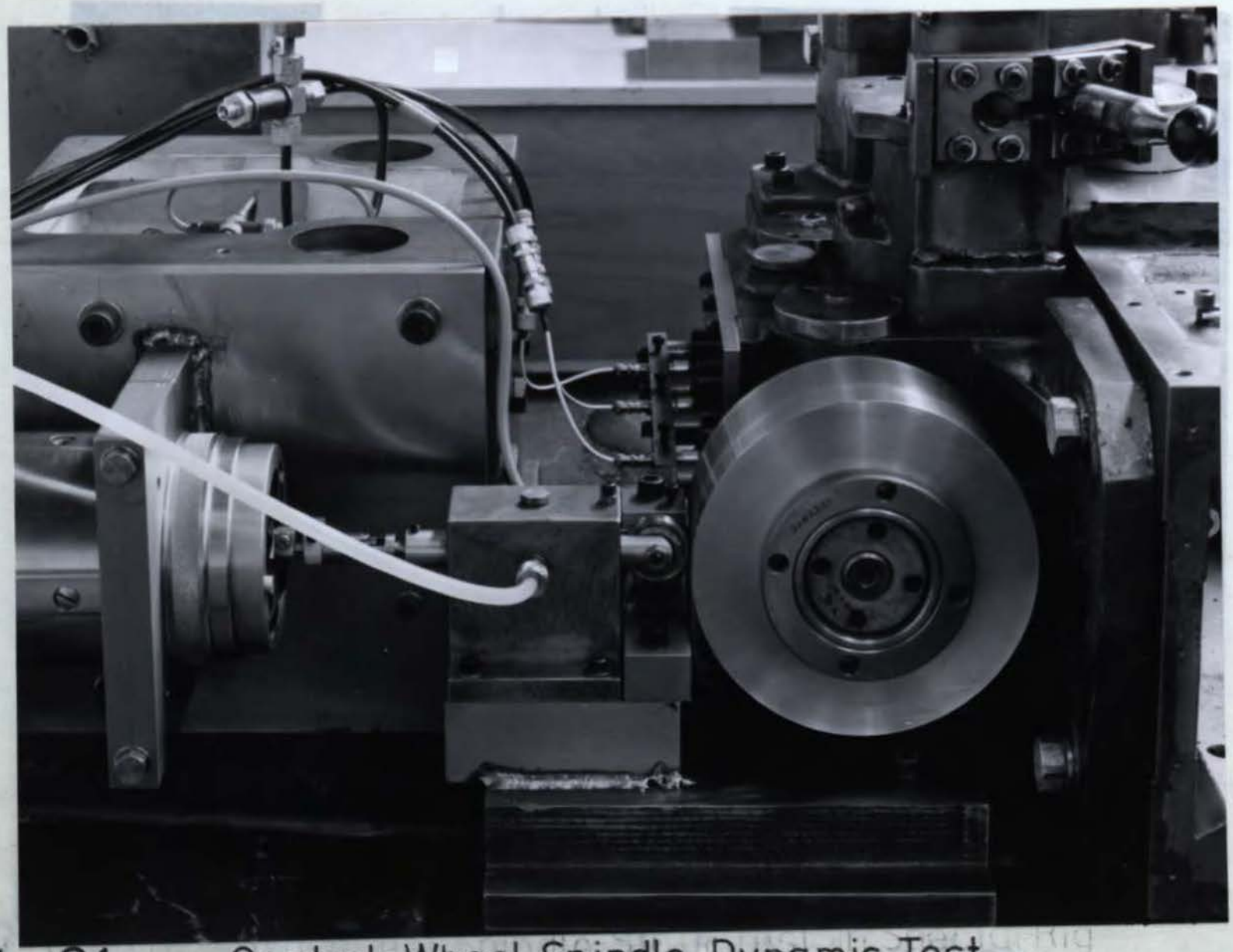

Fig 21 Control Wheel Spindle: Dynamic Test

Fig 22 Control Wheel Housing: Mode of Vibration Test

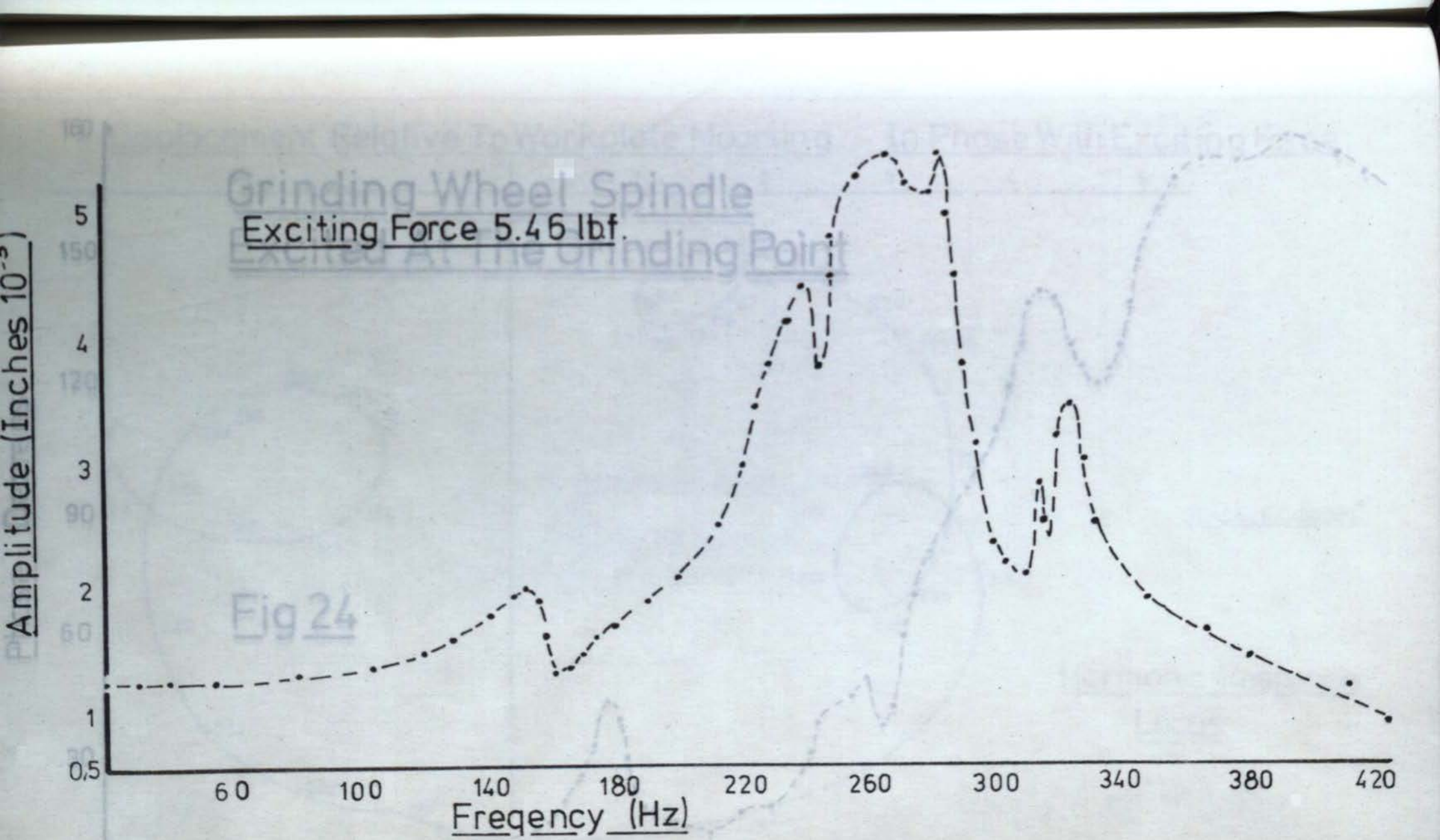

Fig. 23 Grinding Wheel Displacement Relative to Workpiece

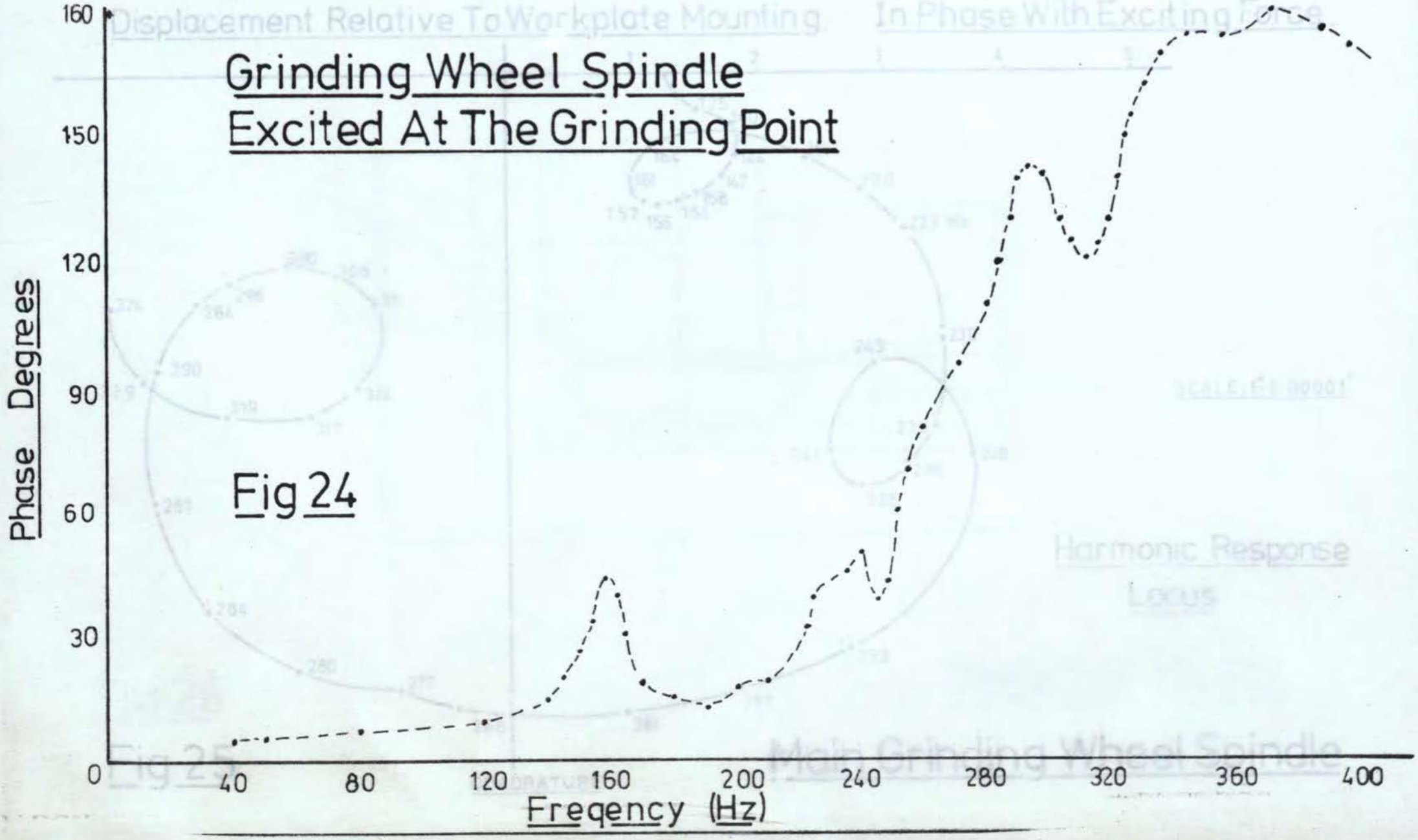
Grinding Wheel Spindle
Excited At The Grinding Point
Fig 24
Phase Degrees
160
150
120
90
60
30
0
40
80
120
160
200
240
280
320
360
400
Freqency (Hz)

Displacement Relative To Workplate Mounting. In Phase With Exciting Force.

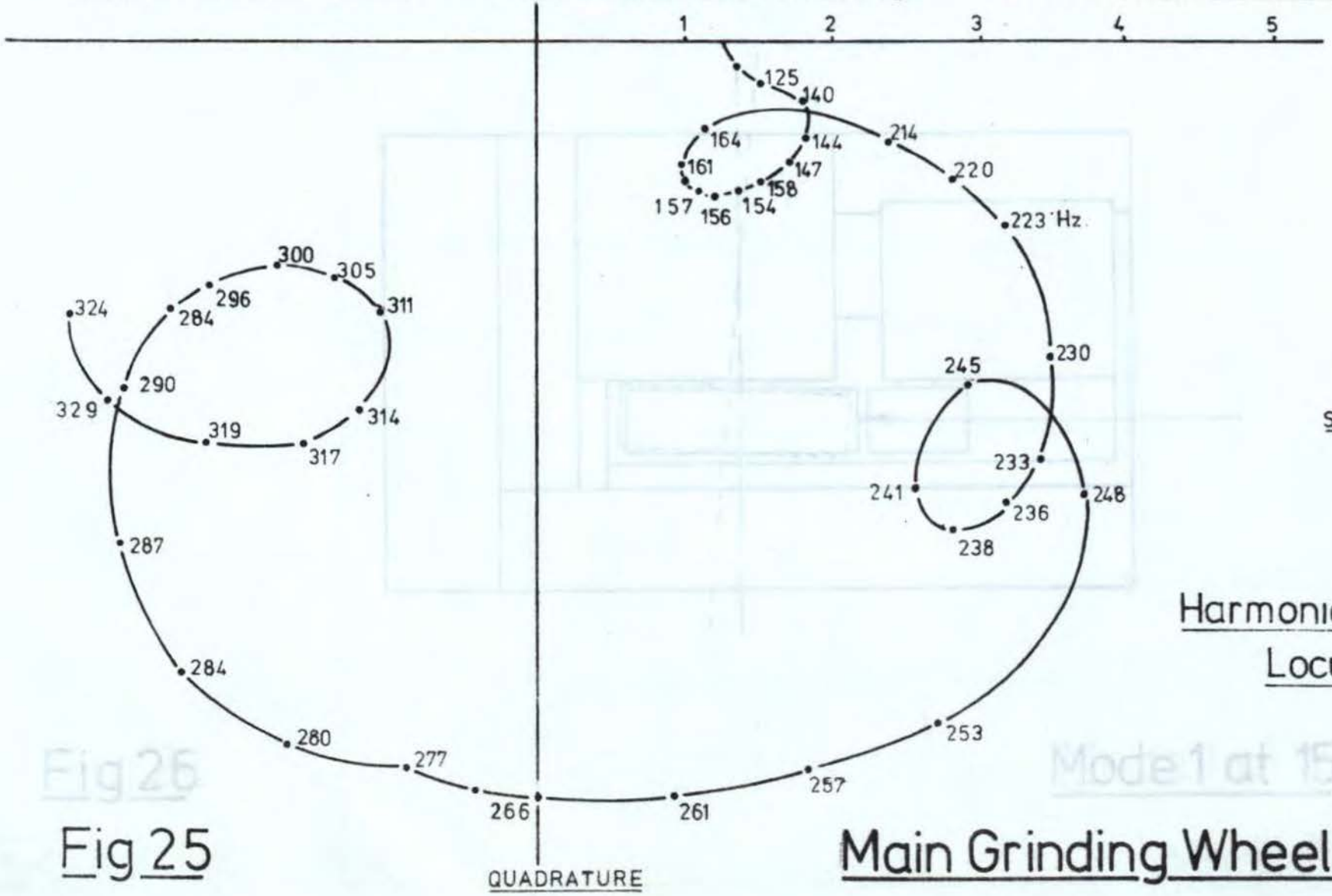

SCALE: 1" = 0·00001"

Harmonic Response Locus

Fig 25

Main Grinding Wheel Spindle.

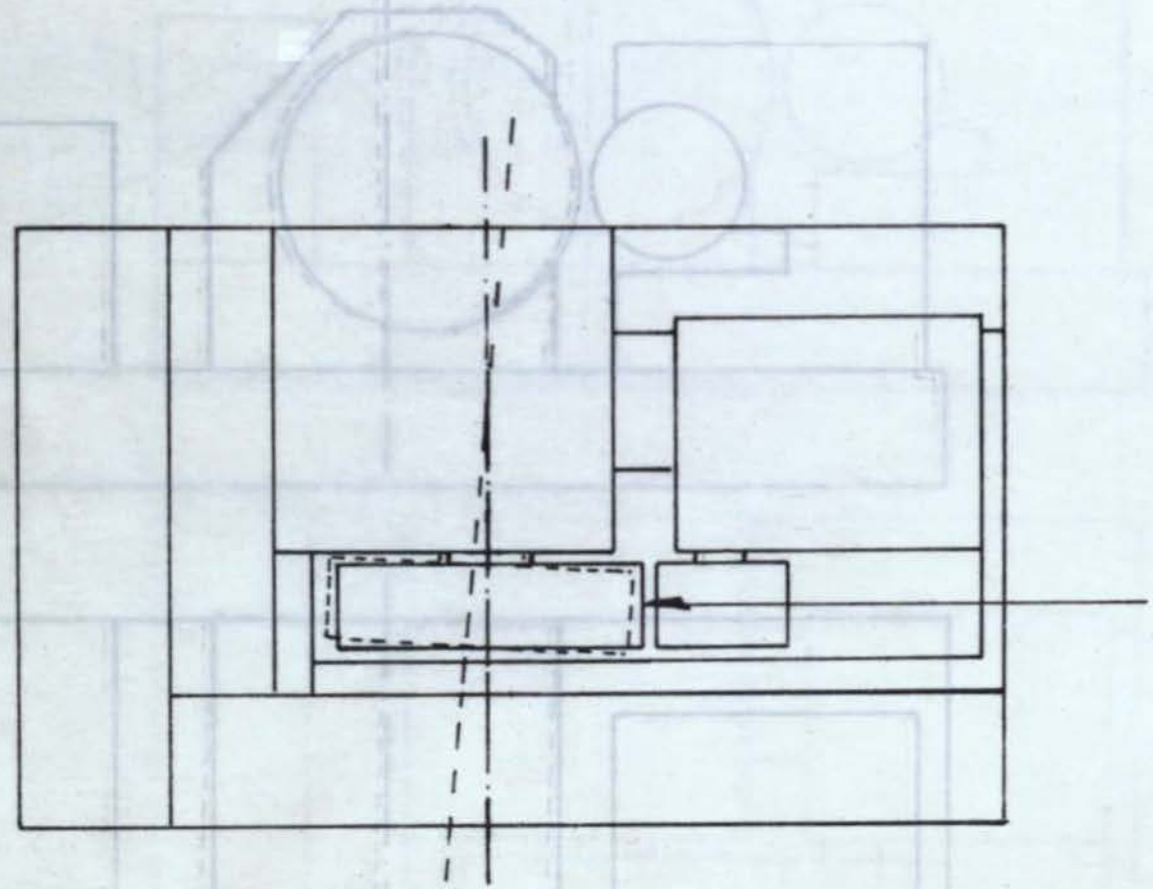

Fig 26

Mode 1 at 154 Hz

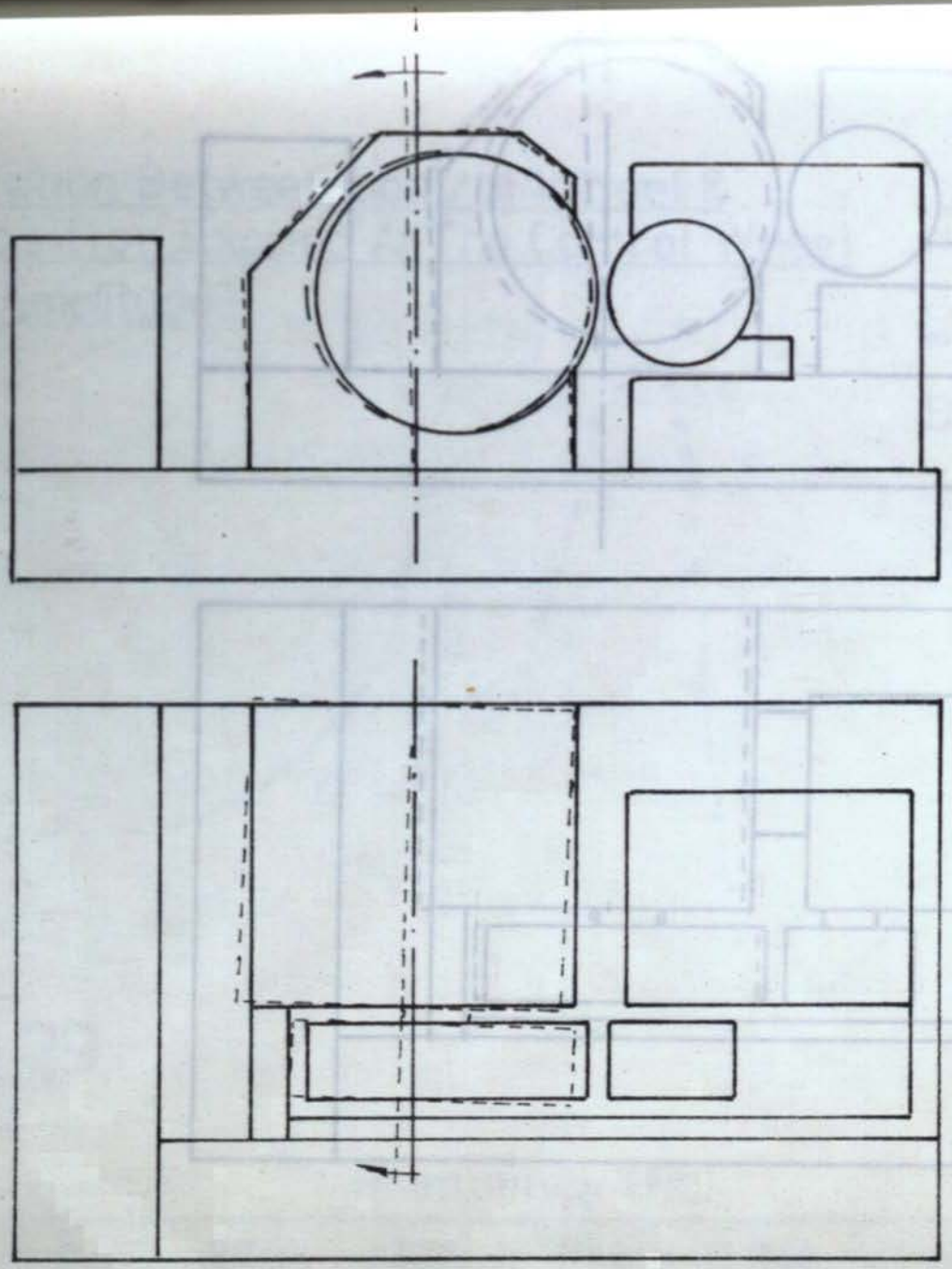

Fig 27

Mode 2 at 240. Hz.

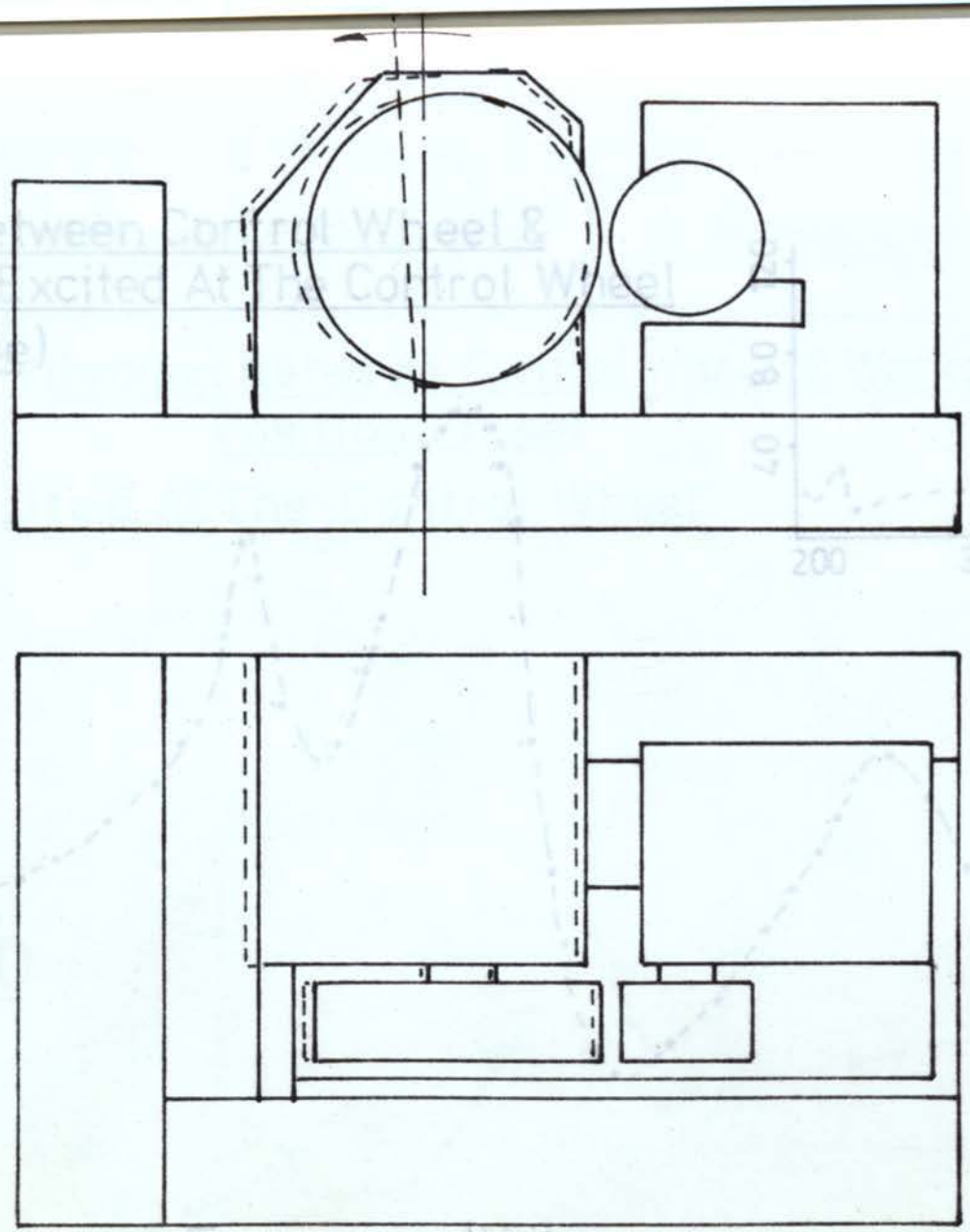

Fig 28

Mode at 280Hz

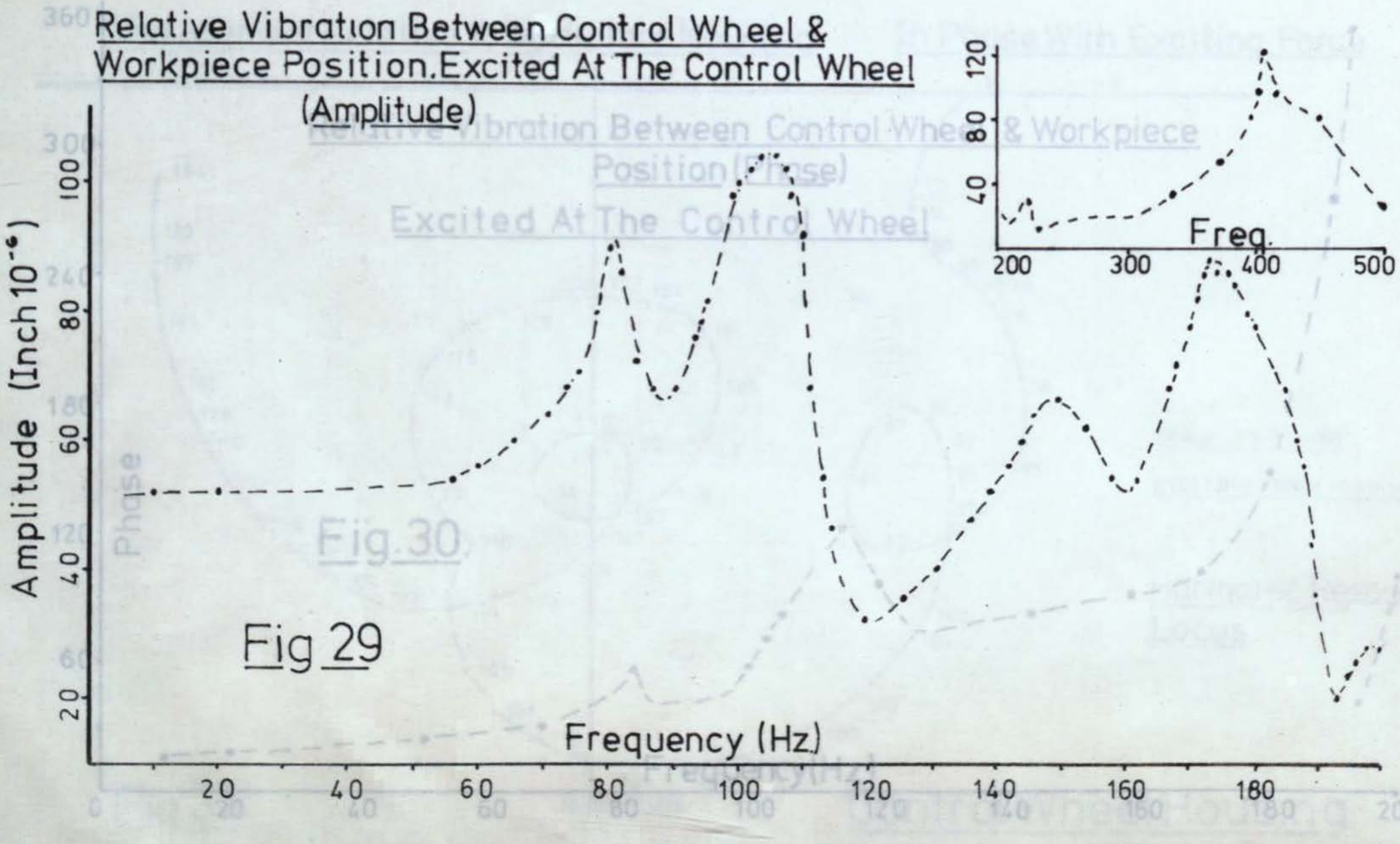
Relative Vibration Between Control Wheel &
Workpiece Position. Excited At The Control Wheel
(Amplitude)
Amplitude (Inch 10⁻⁶)
20
40
60
80
100
Frequency (Hz)
20
40
60
80
100
120
140
160
180
Freq.
40
80
120
200
300
400
500

Fig 29

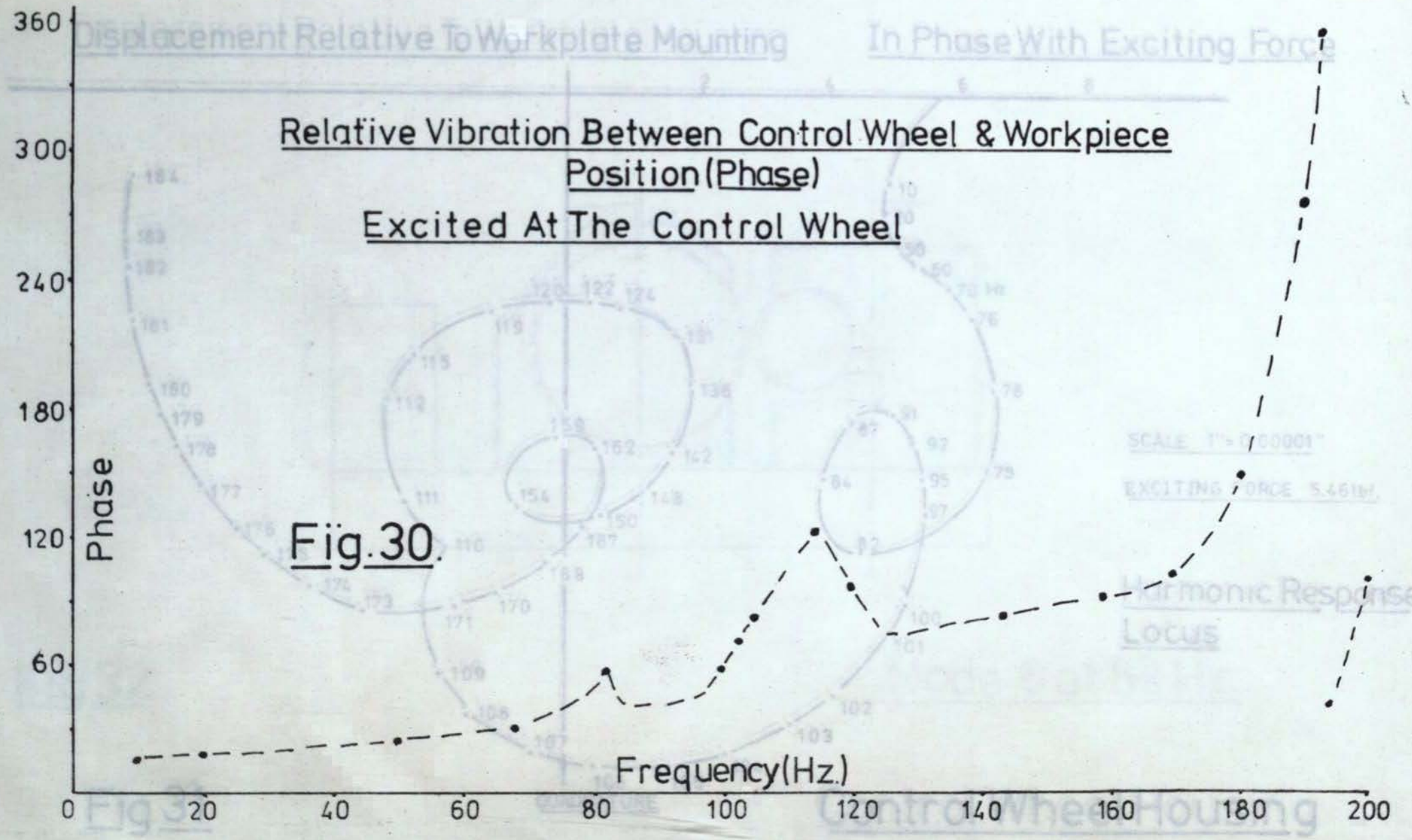
Relative Vibration Between Control Wheel & Workpiece
Position (Phase)
Excited At The Control Wheel
Fig. 30.
Phase
Frequency (Hz.)
360
300
240
180
120
60
0
20
40
60
80
100
120
140
160
180
200

Displacement Relative To Workplate Mounting

In Phase With Exciting Force

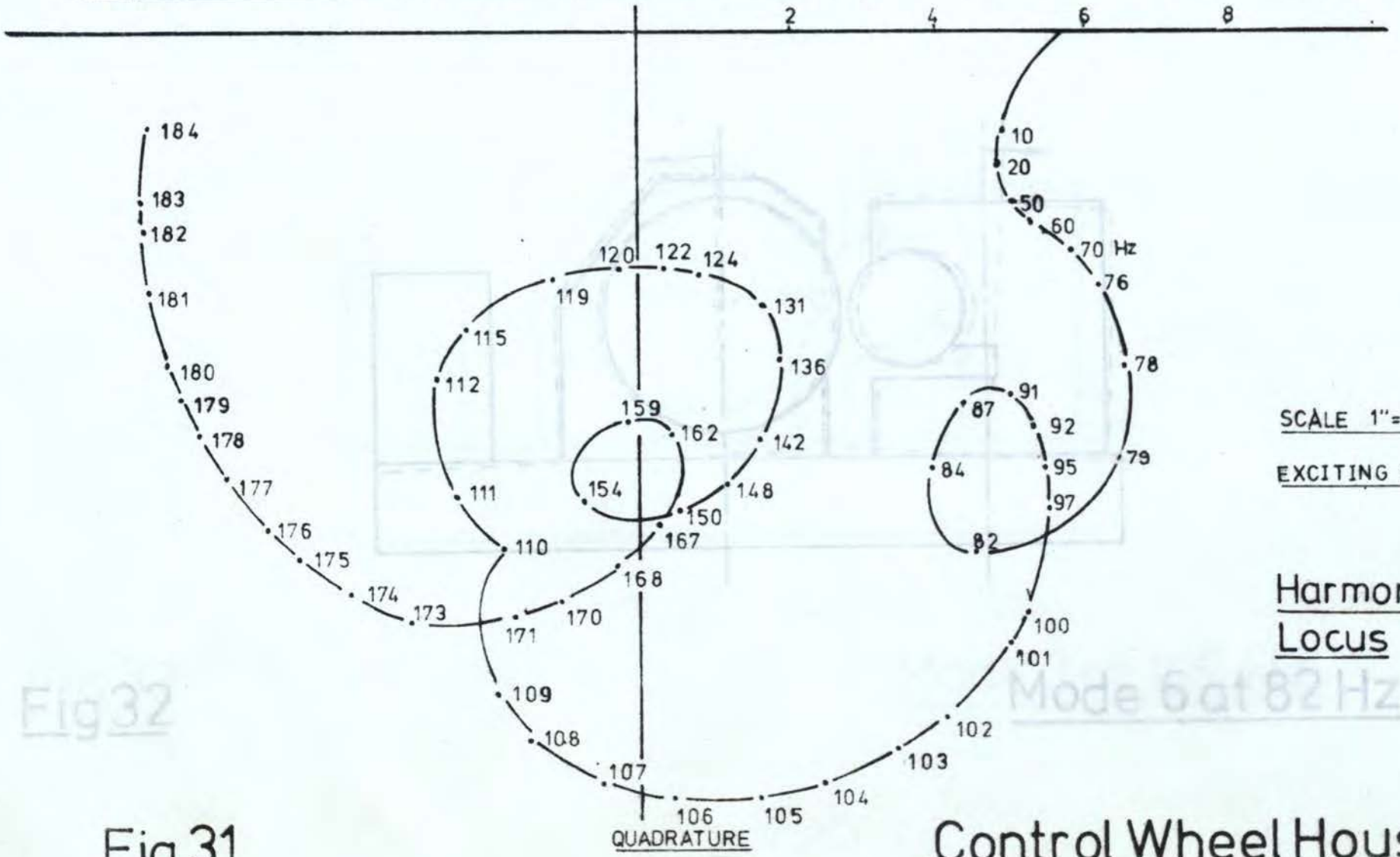

SCALE 1" = 0·00001"

EXCITING FORCE 5.46 lbf.

Harmonic Response Locus

Mode 6 at 82 Hz.

Fig 32

Fig 31

Control Wheel Housing

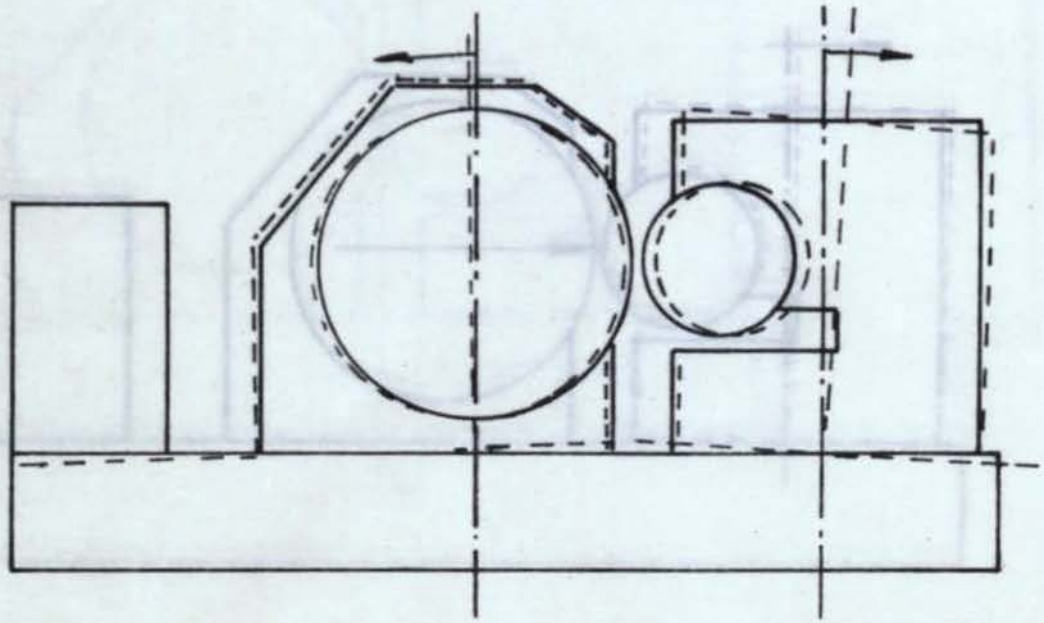

Fig 32

Mode 6 at 82 Hz.

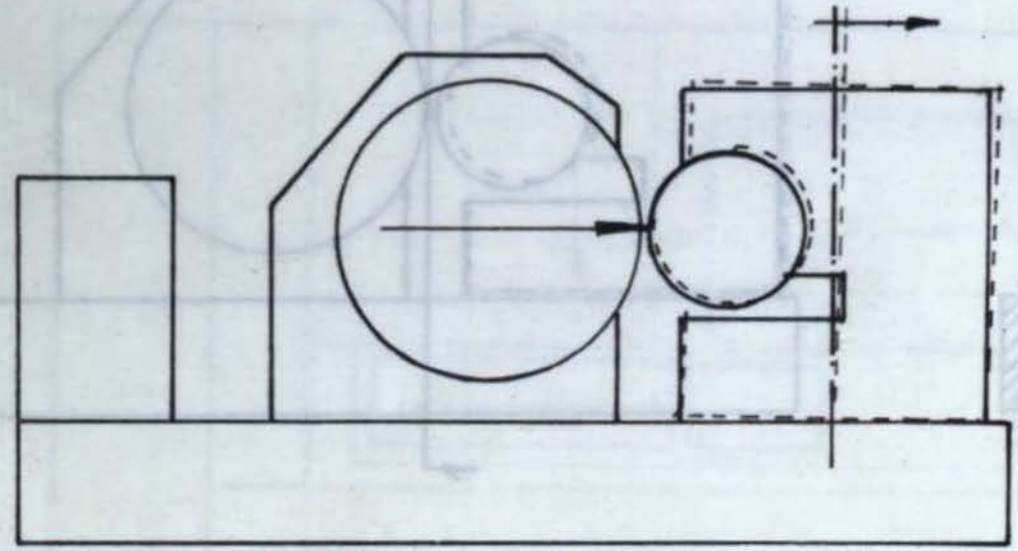

Fig 33

Mode 3 at 105 Hz

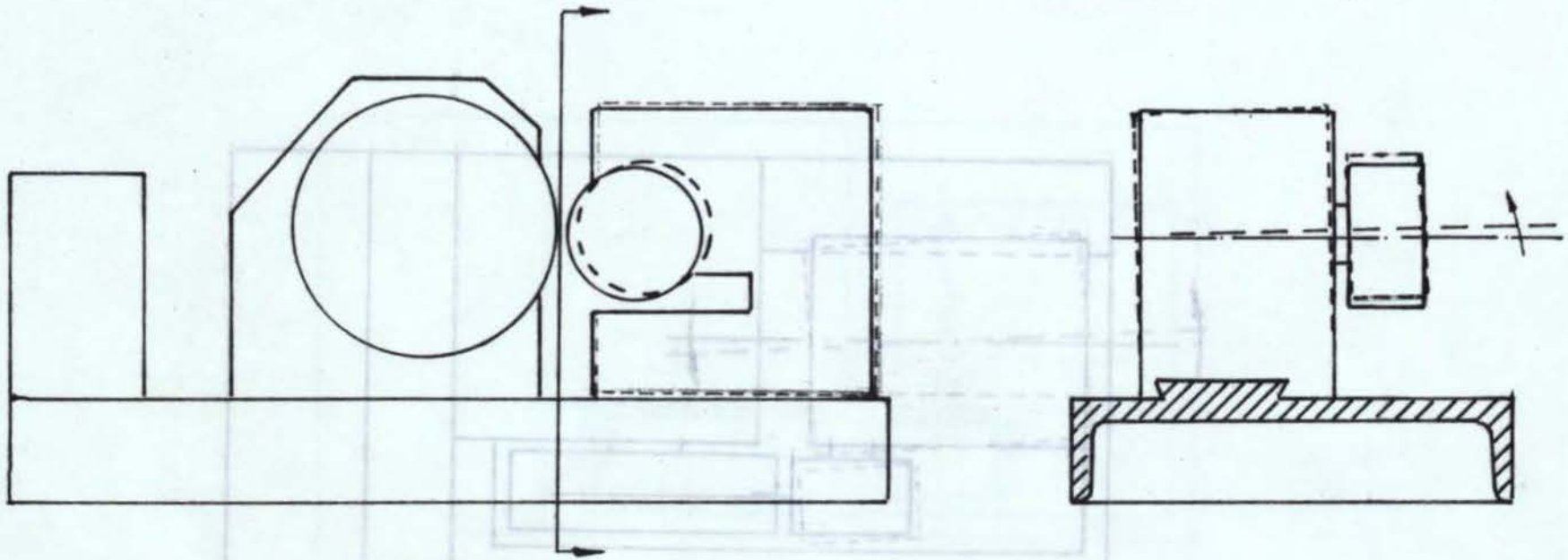

Fig 34

Mode at 150 Hz

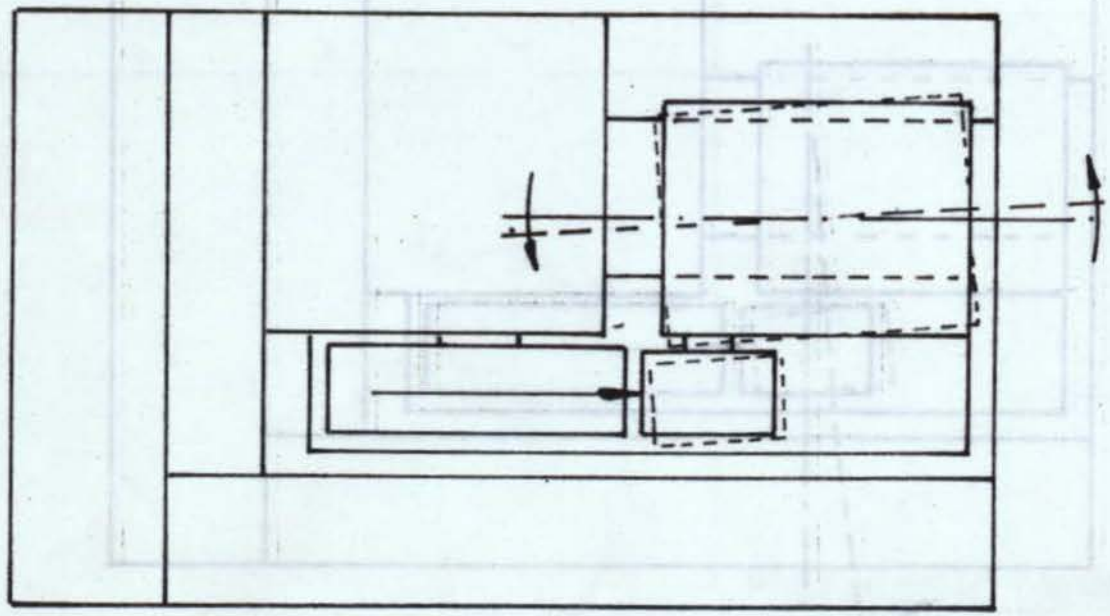

Fig.35.

Mode 4 at 175 Hz

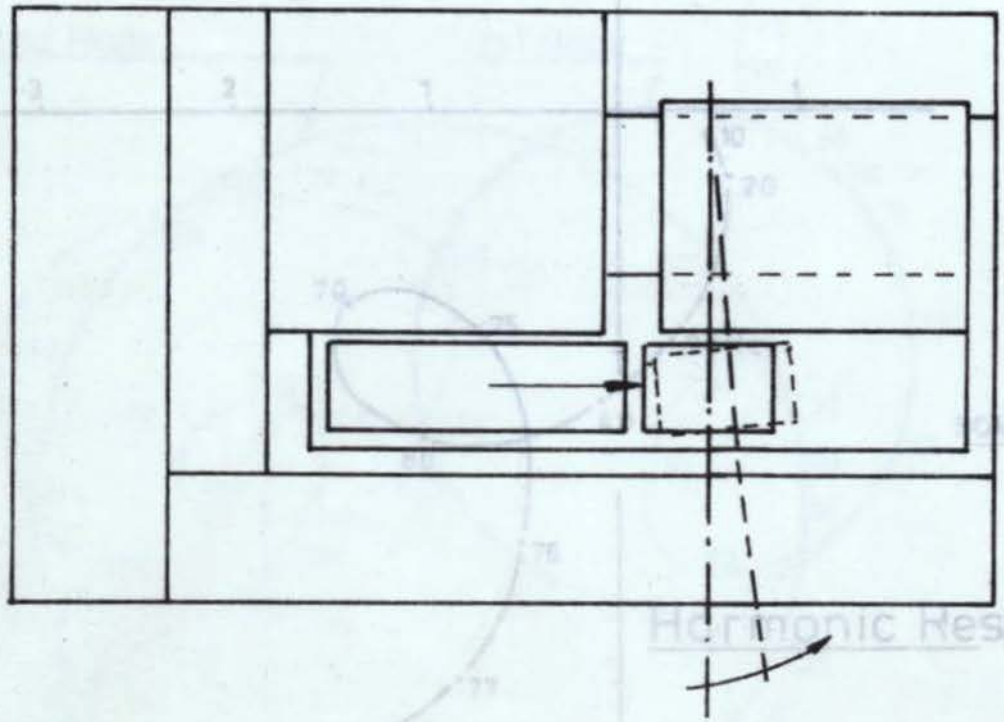

Fig 36

Mode 5 at 410 Hz.

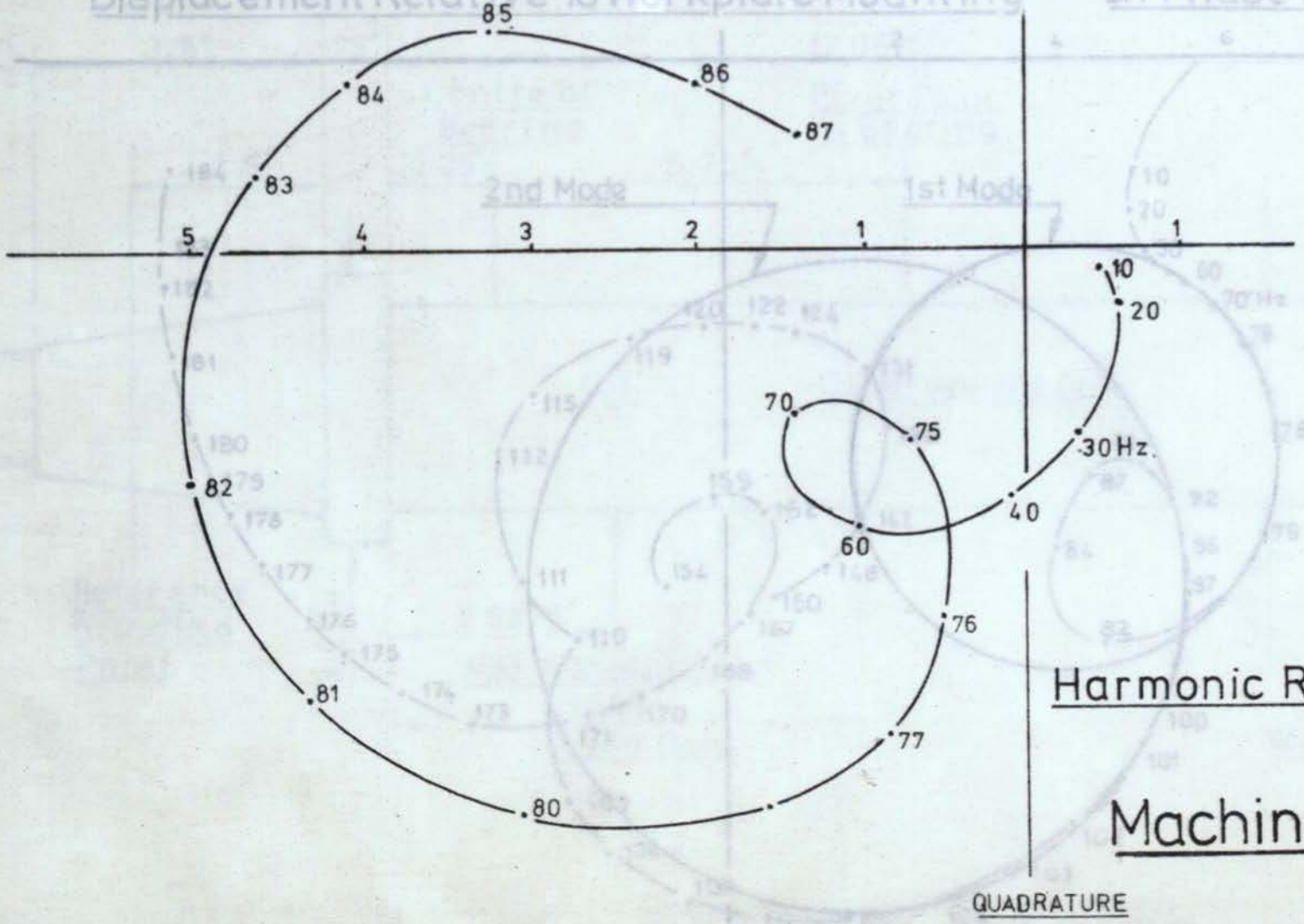

SCALE 1"=0·00001"

Harmonic Response Locus

Machine Tray

Fig 37

Absolute Displacement

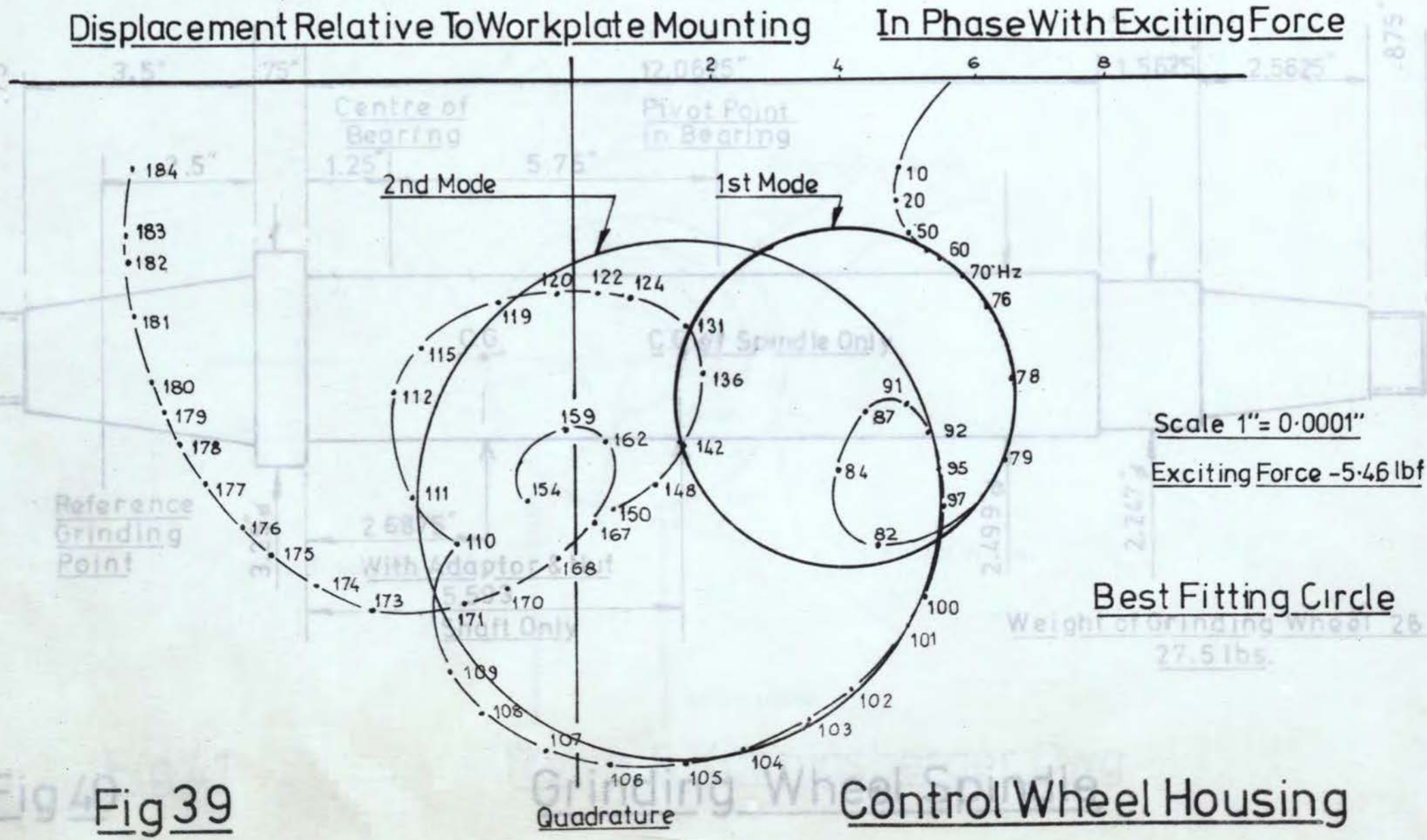
Displacement Relative To Workplate Mounting
In Phase With Exciting Force
2nd Mode
1st Mode
Scale 1" = 0·0001"
Exciting Force -5·46 lbf
Best Fitting Circle
Quadrature
Control Wheel Housing

Fig 39

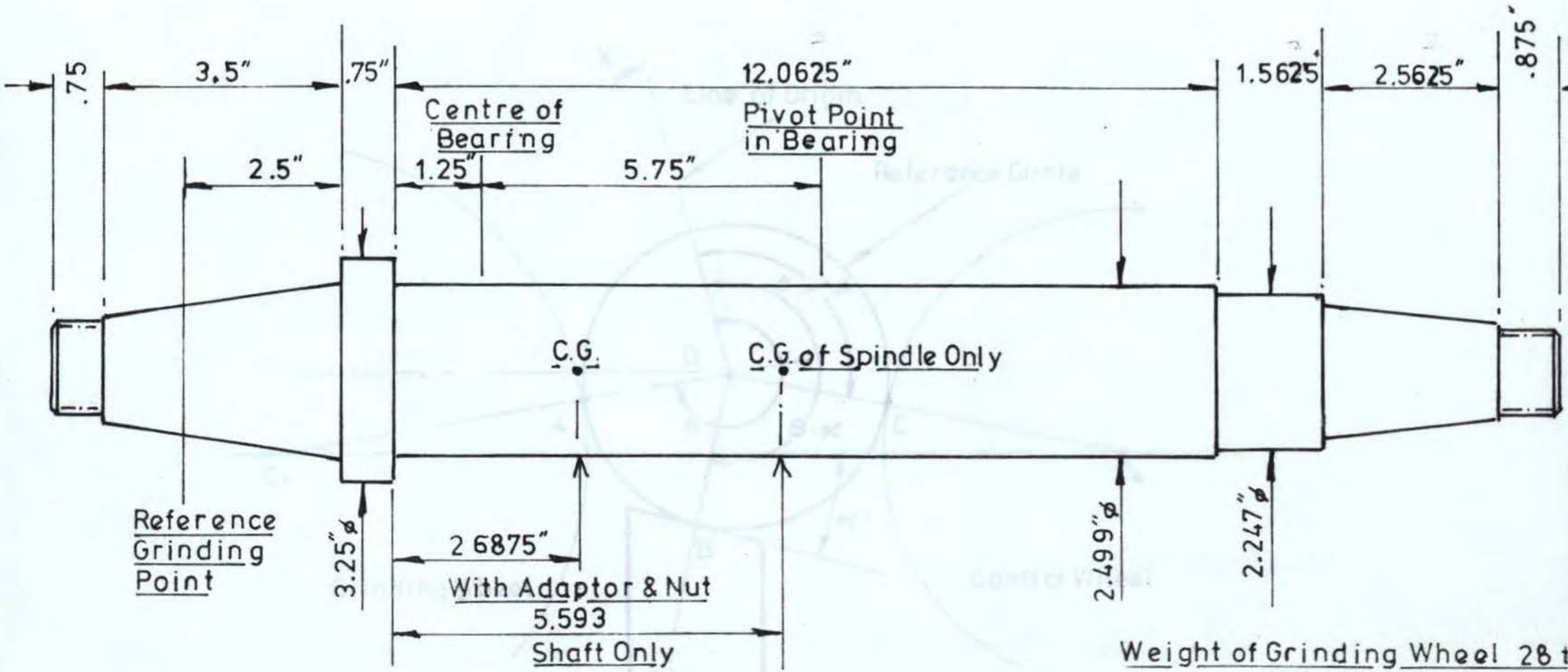

Fig 40 Grinding Wheel Spindle

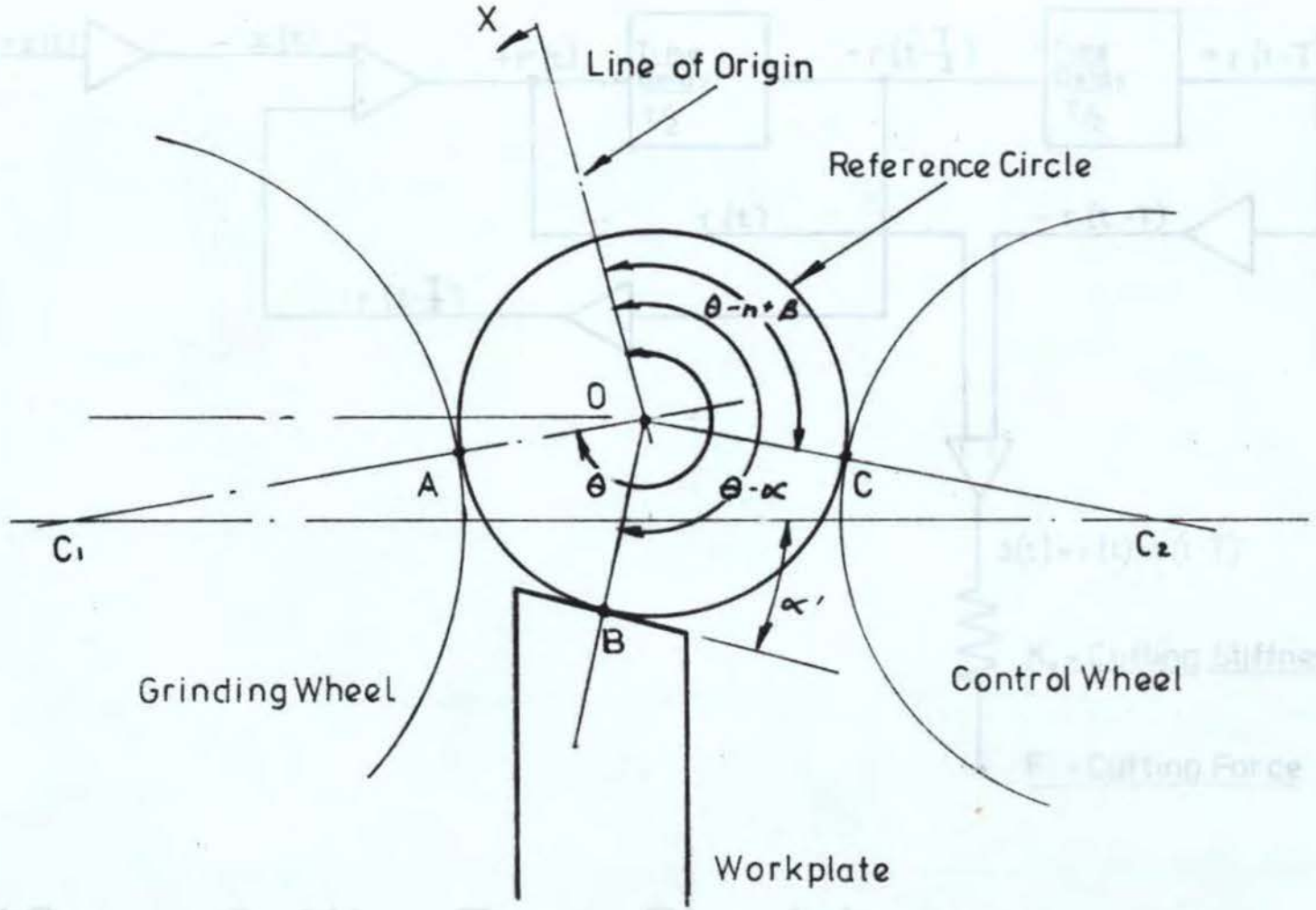

Fig 41 Rowe & Koenigsberger Dwg.

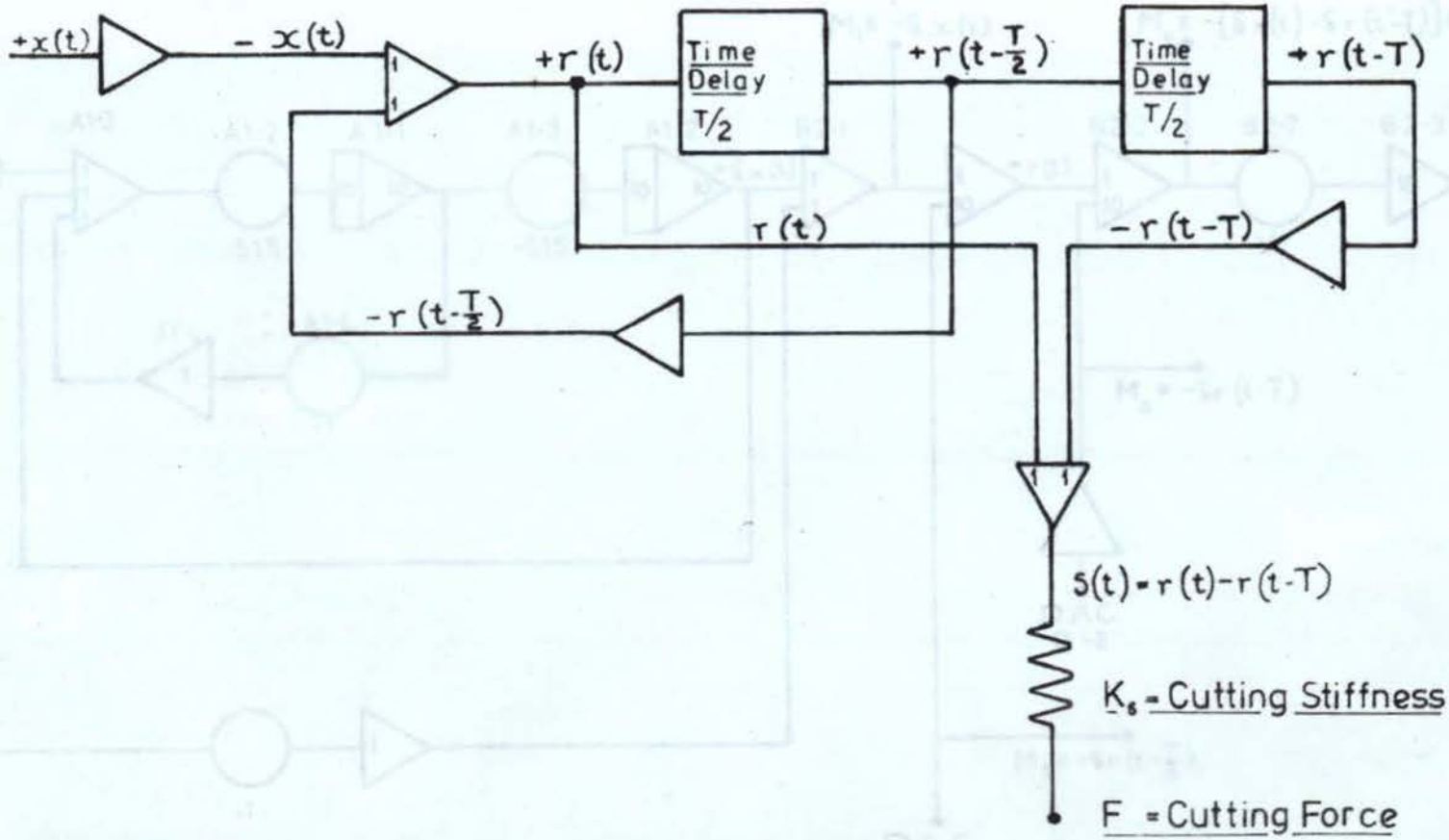

Fig.42 Cutting Force Simulation

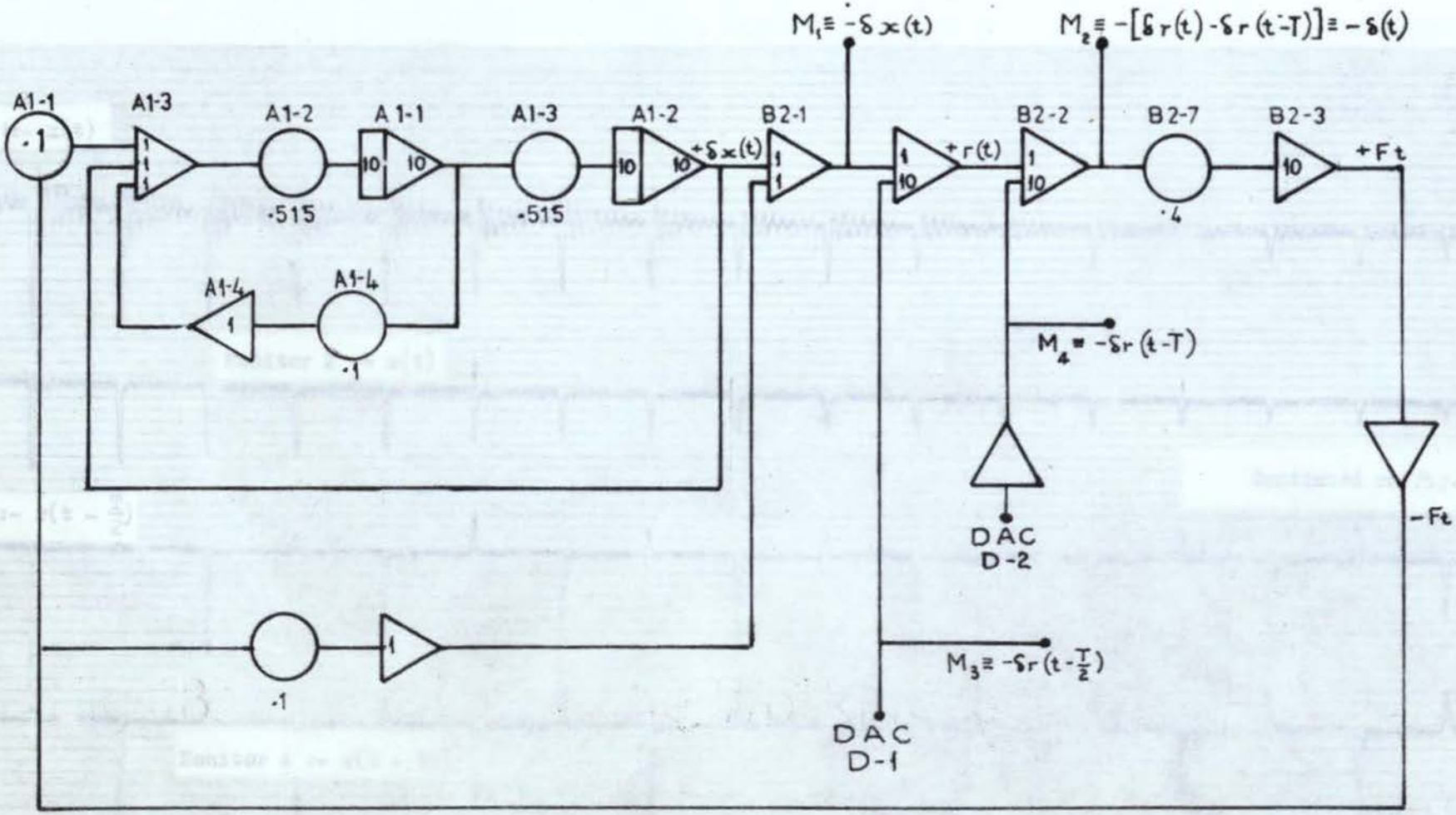

Fig 43 Centreless Grinding Machine Simulation

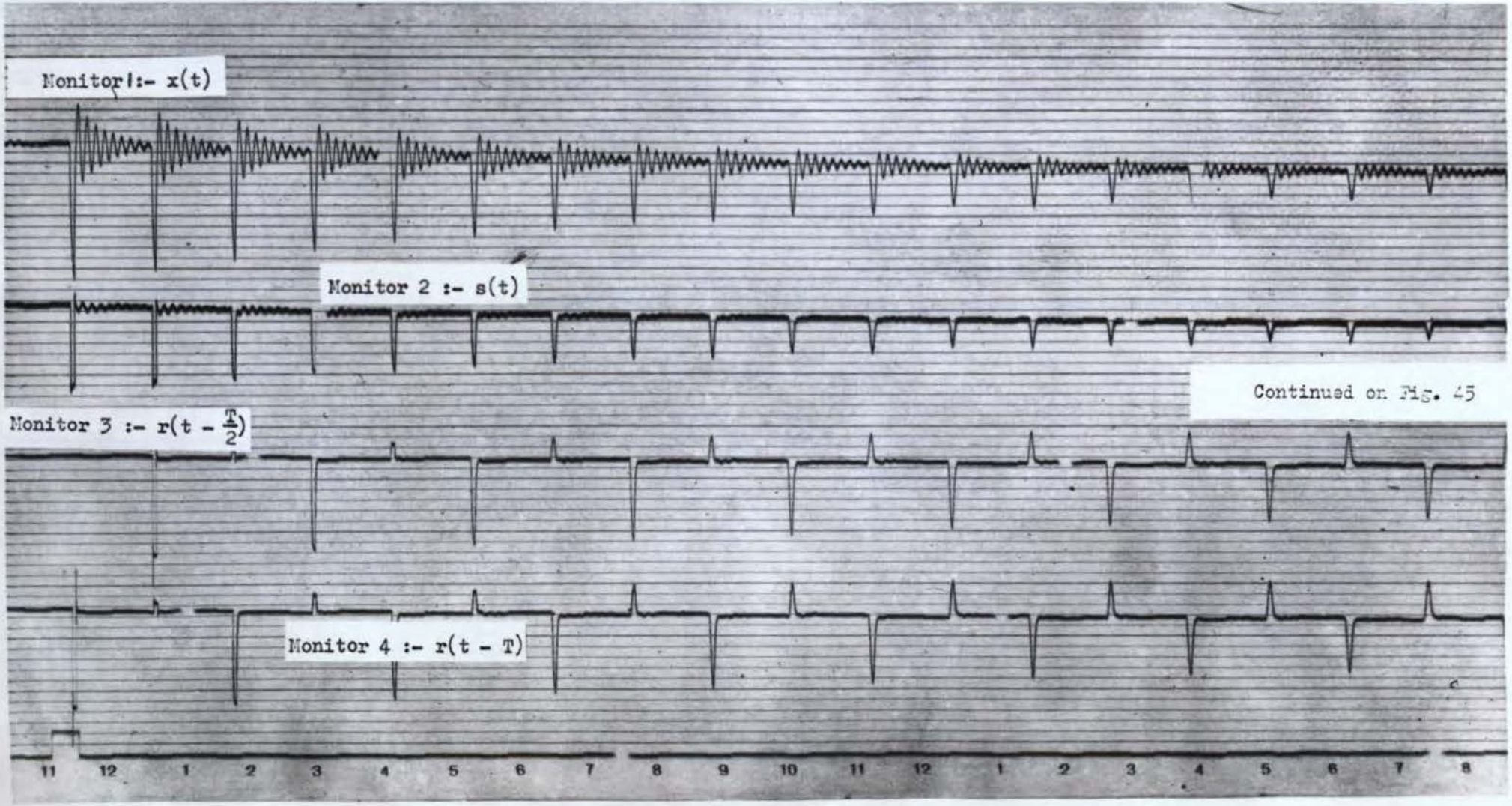

Fig. 44.

Hybrid Computer outputs

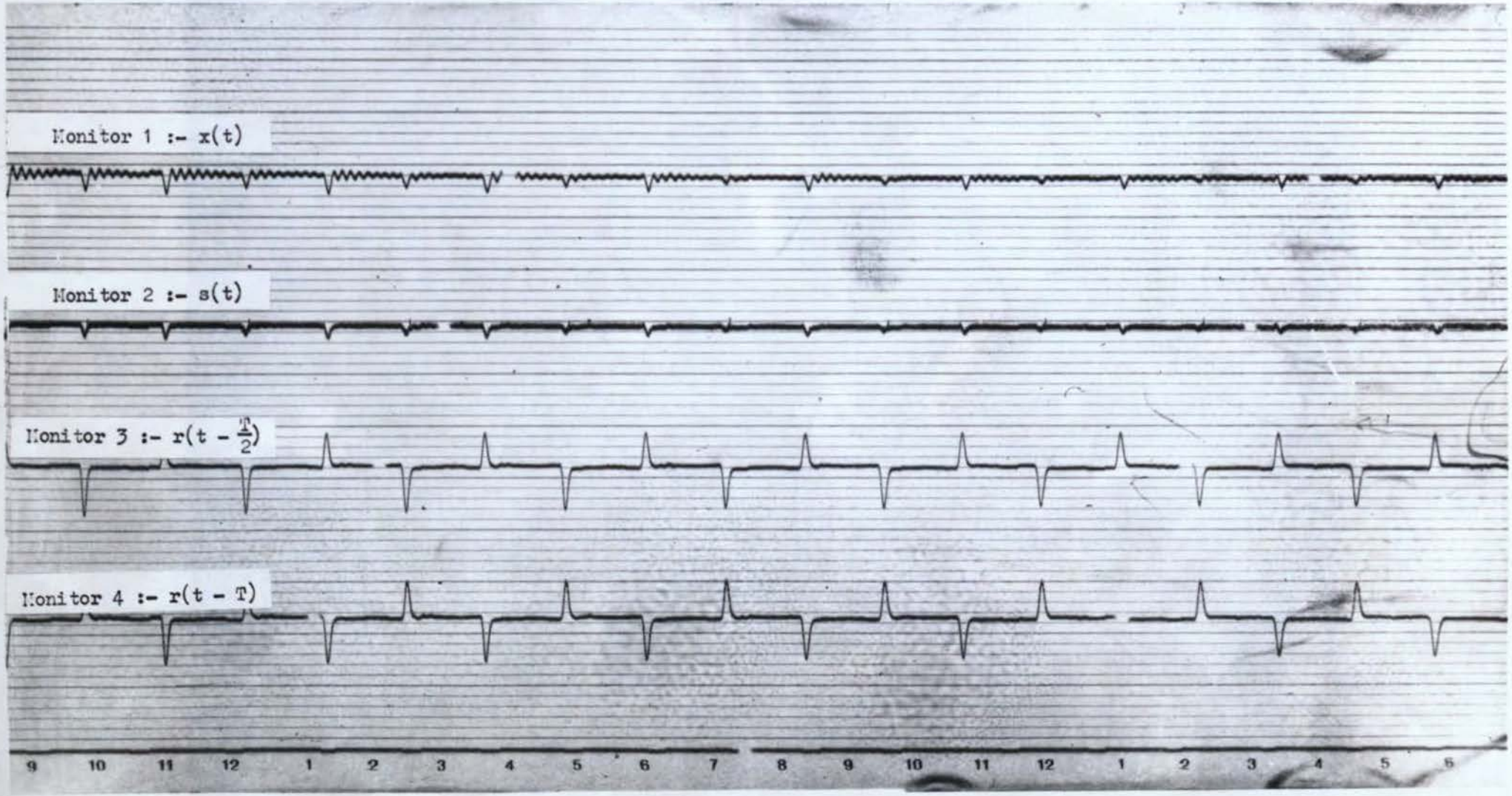

Fig 45

Fig. 44 Continued

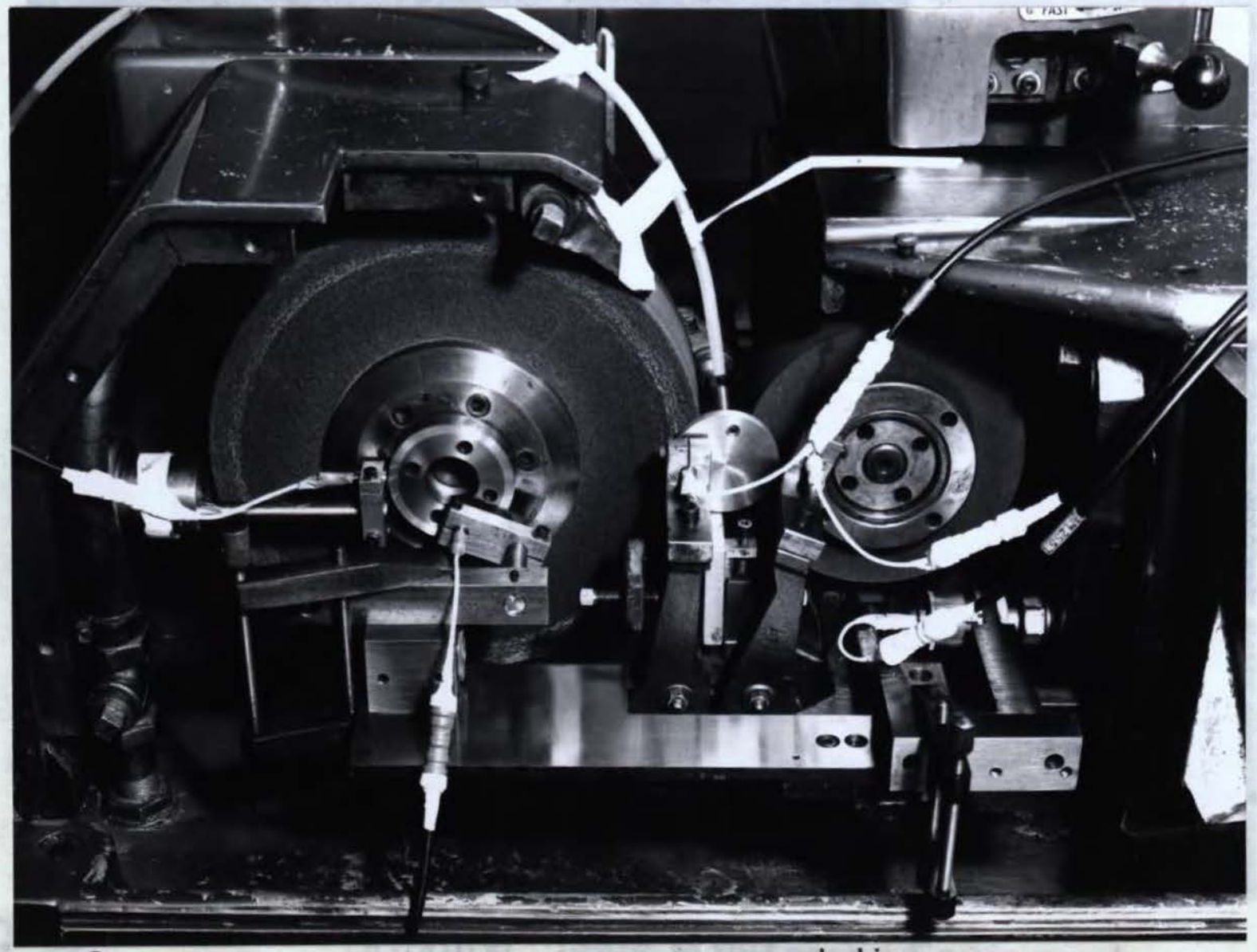

Fig 46 Grinding Test Instrumentation

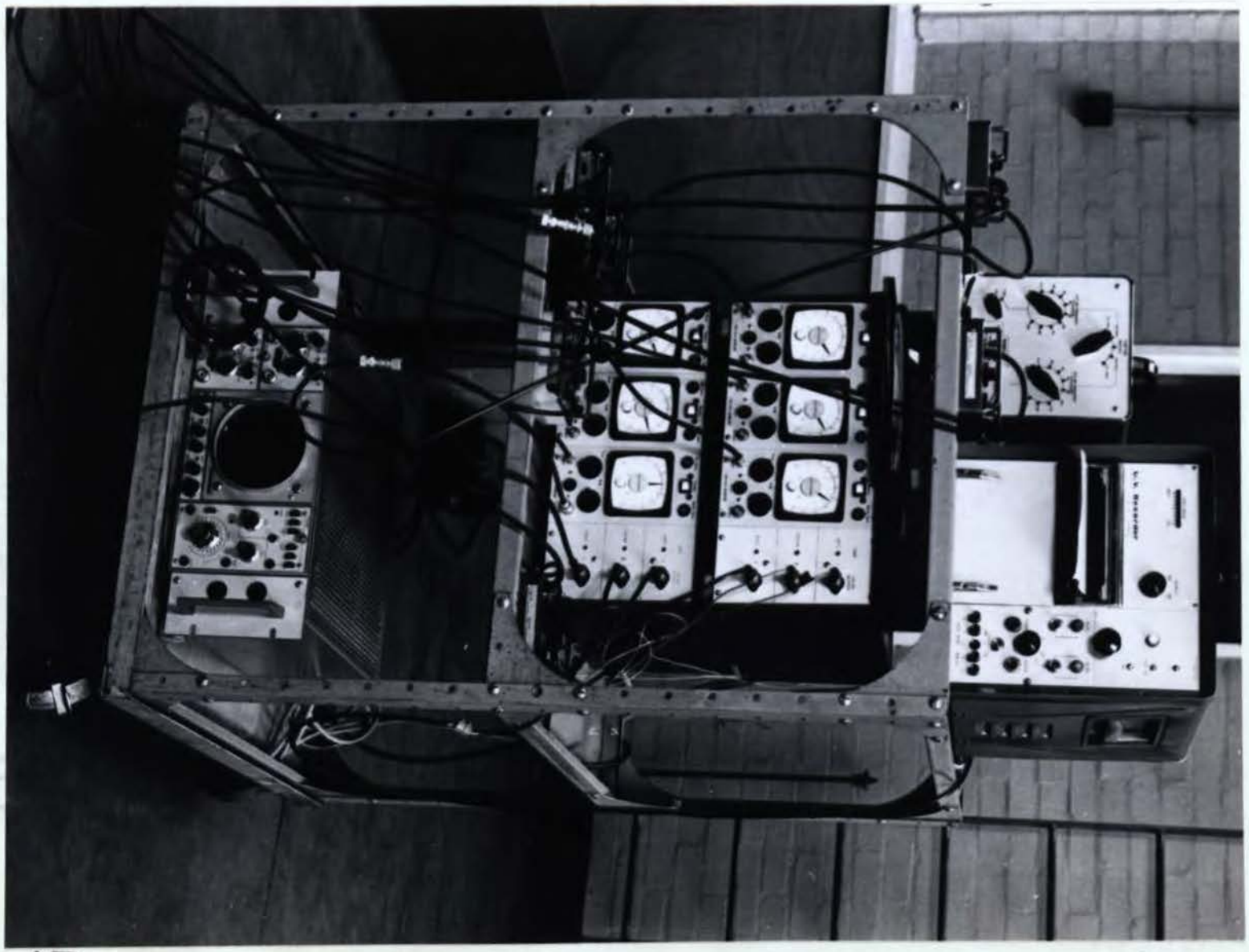

Fig 47 Grinding Tests Monitoring Equipment

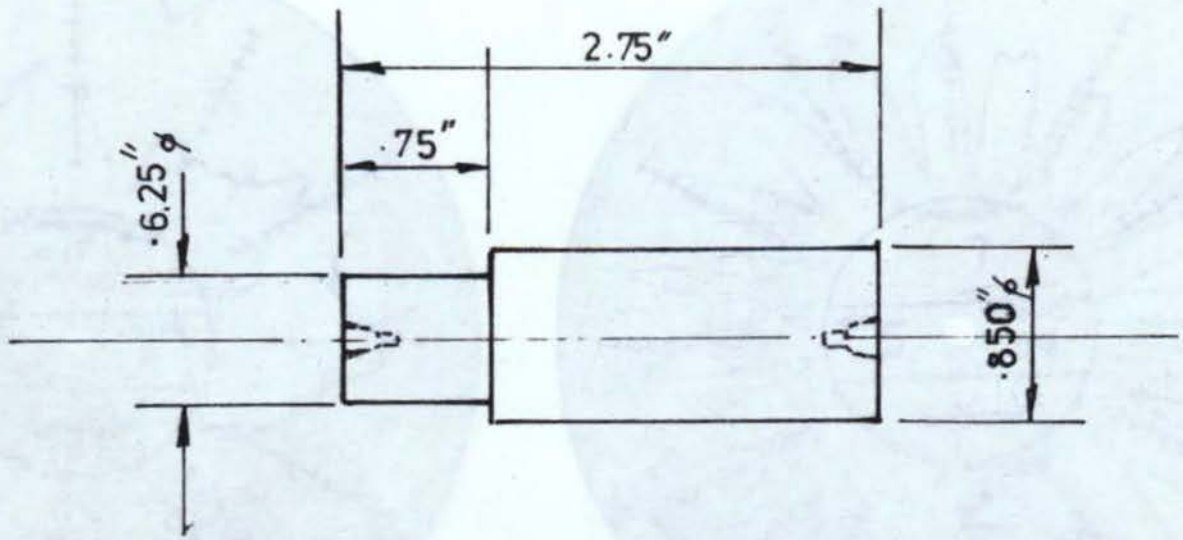

Fig.48. The Workpiece

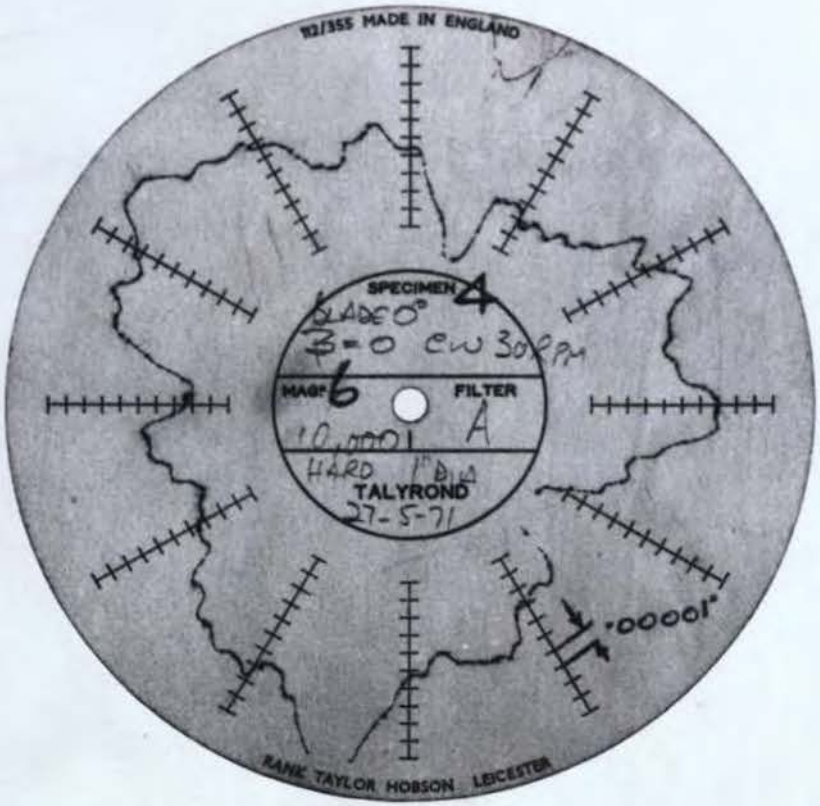

a

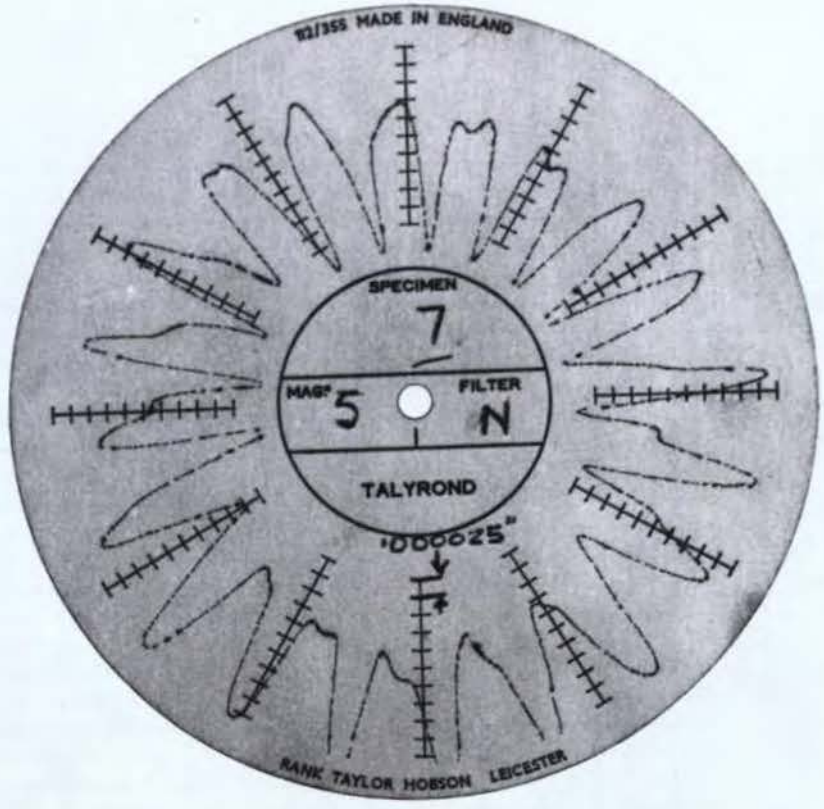

b

Roundness Charts for α, = 0° and β = 0°

Fig 49

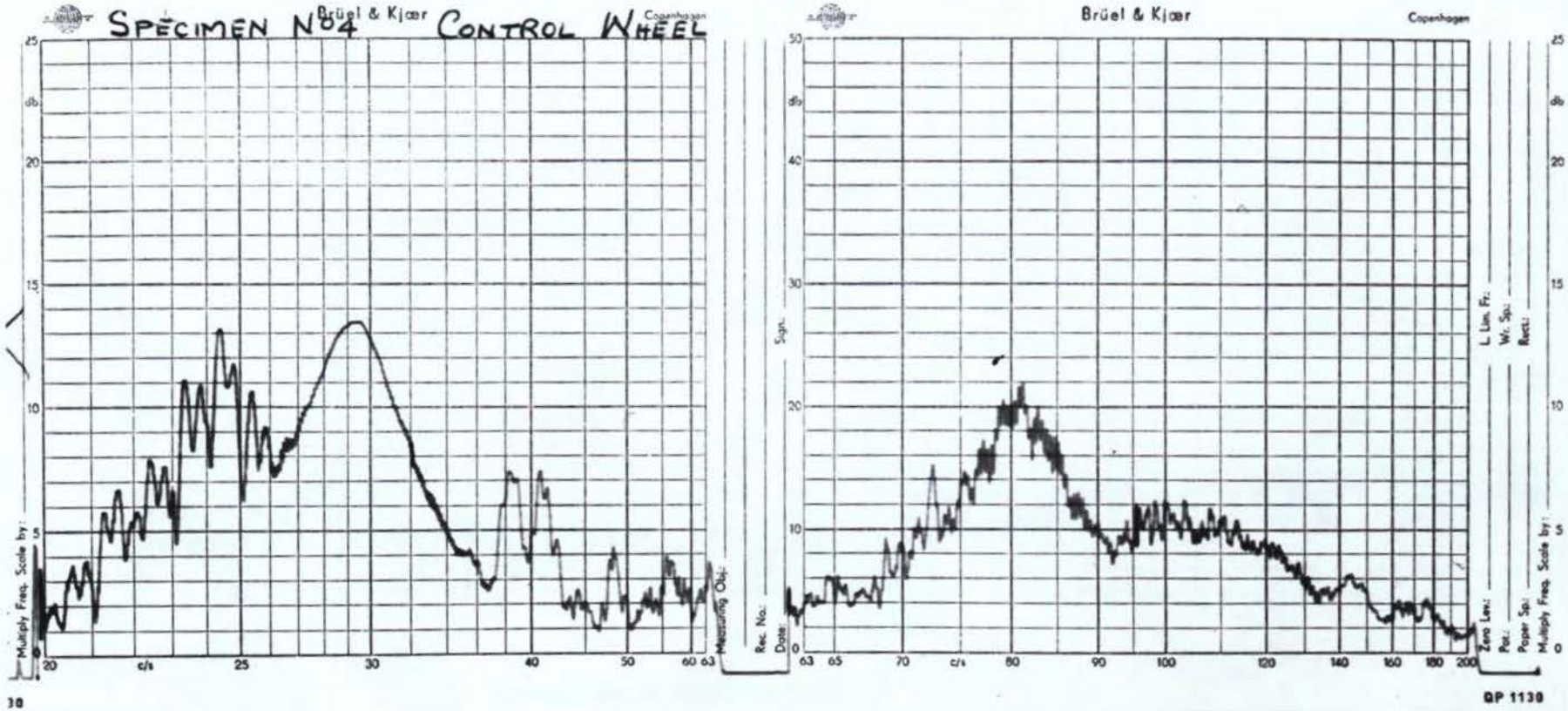

Fig 50

Control Wheel Displacement

Frequency Analyser Chart for $\alpha_1 = 0^\circ$ and $\beta = 0^\circ$

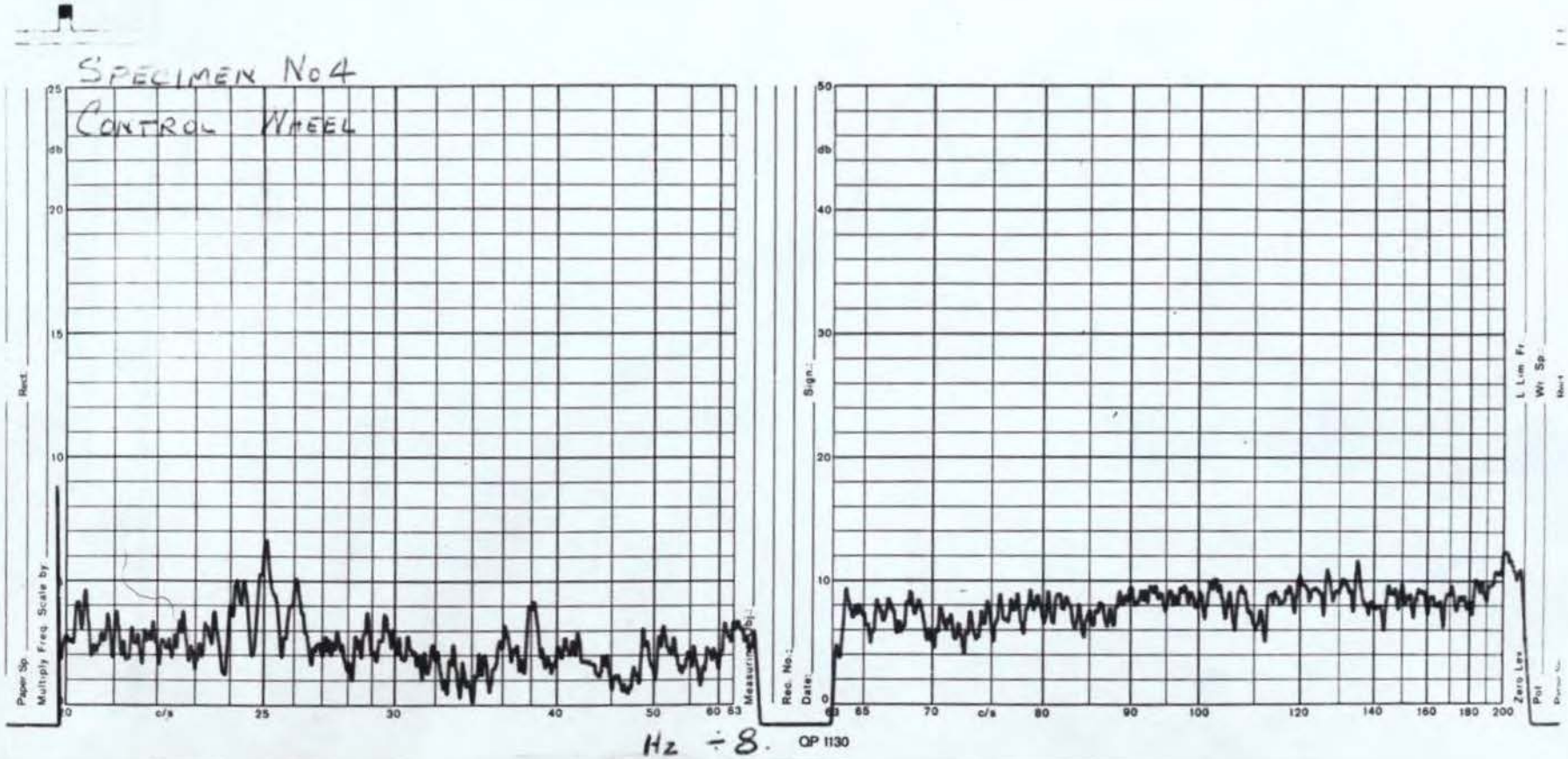

Control Wheel Displacement:

Frequency Analyser Chart for α, = 0° and β=0°
(Frequency ÷ 8)

Fig 51

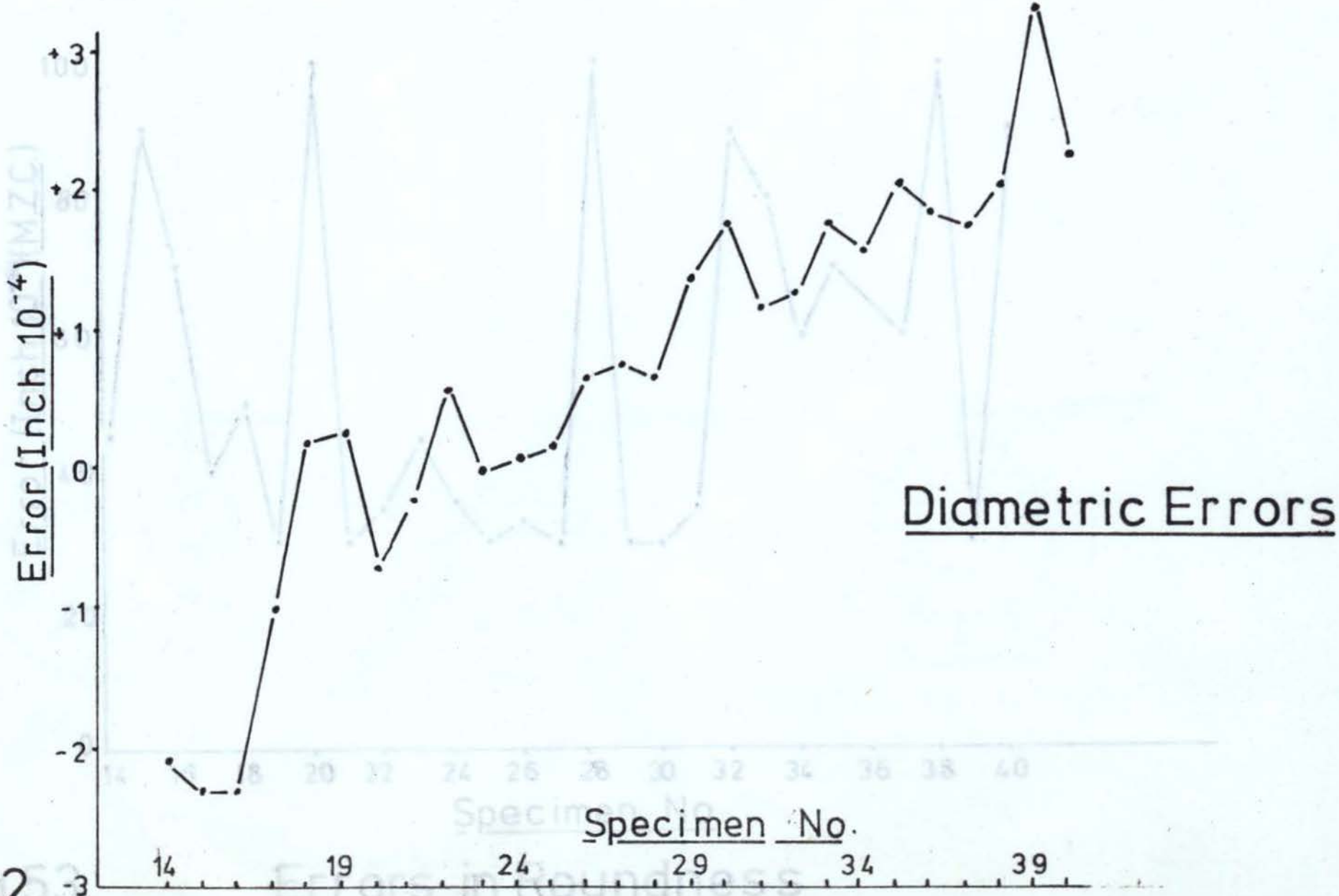
Diametric Errors
Error (Inch 10^{-4})
+3
+2
+1
0
-1
-2
-3
Specimen No.
14
19
24
29
34
39

Fig No 52

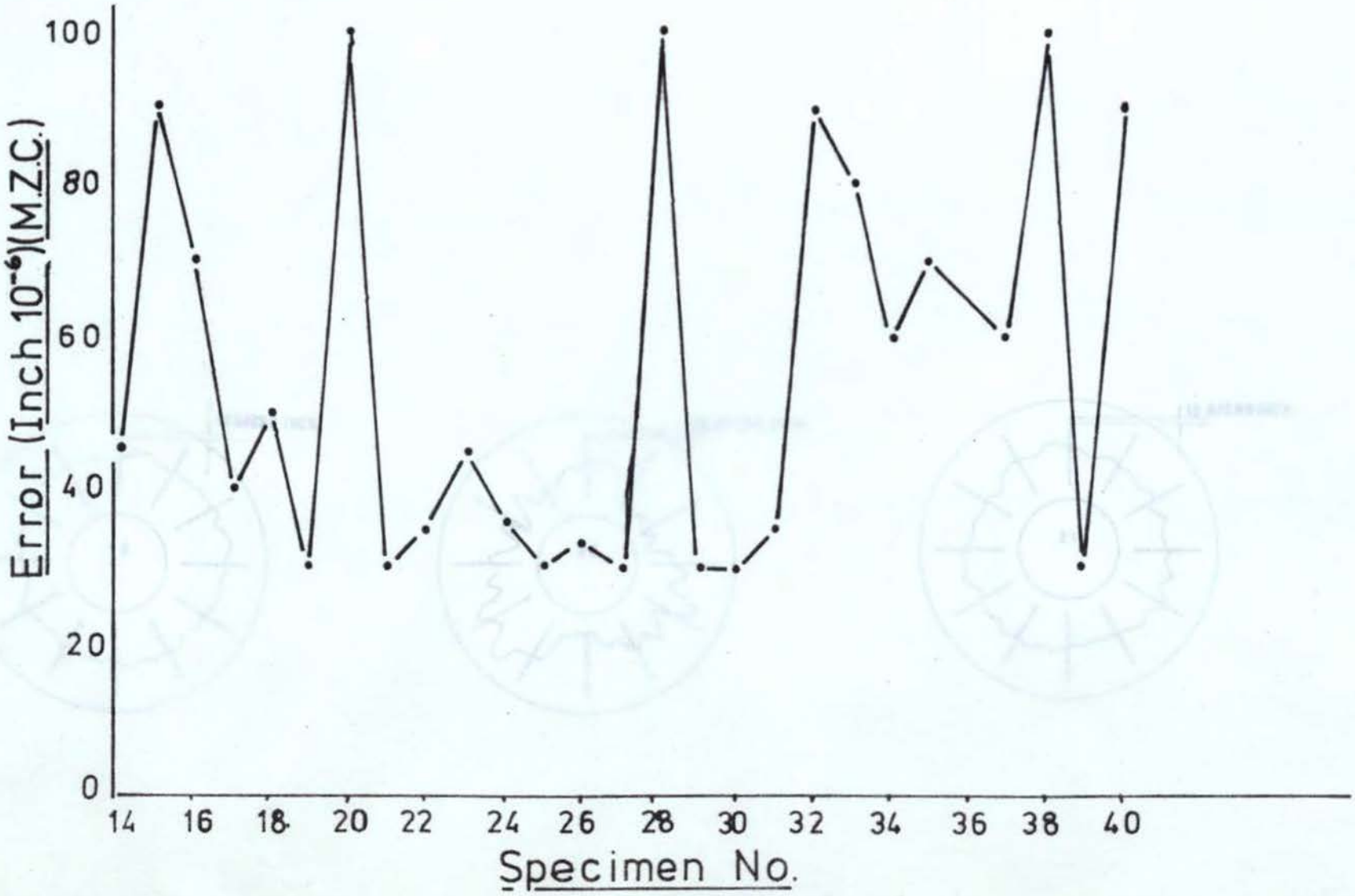

Fig.53. Errors in Roundness

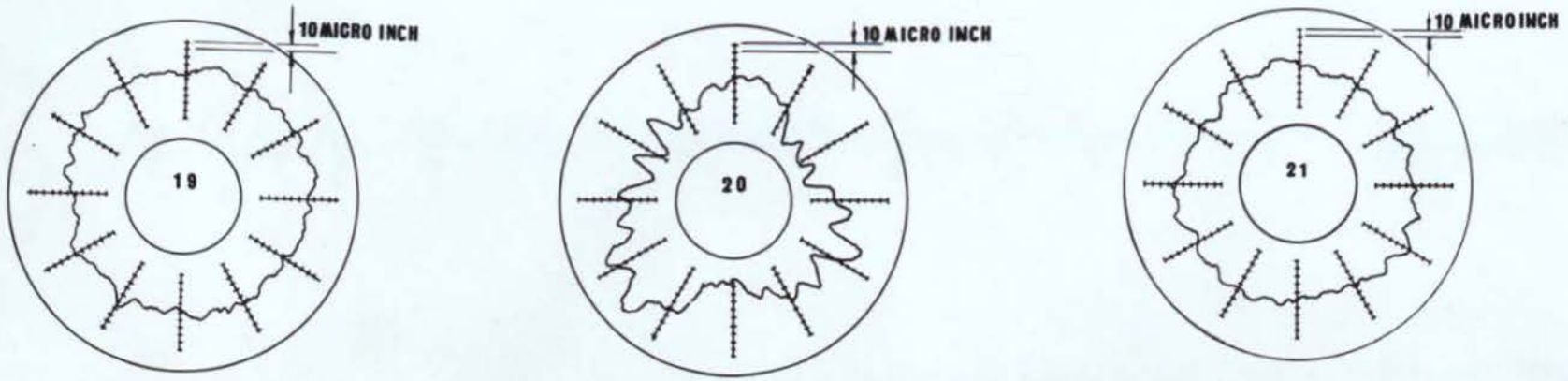

Roundness Charts for α =20° and β = 0°

Fig 54

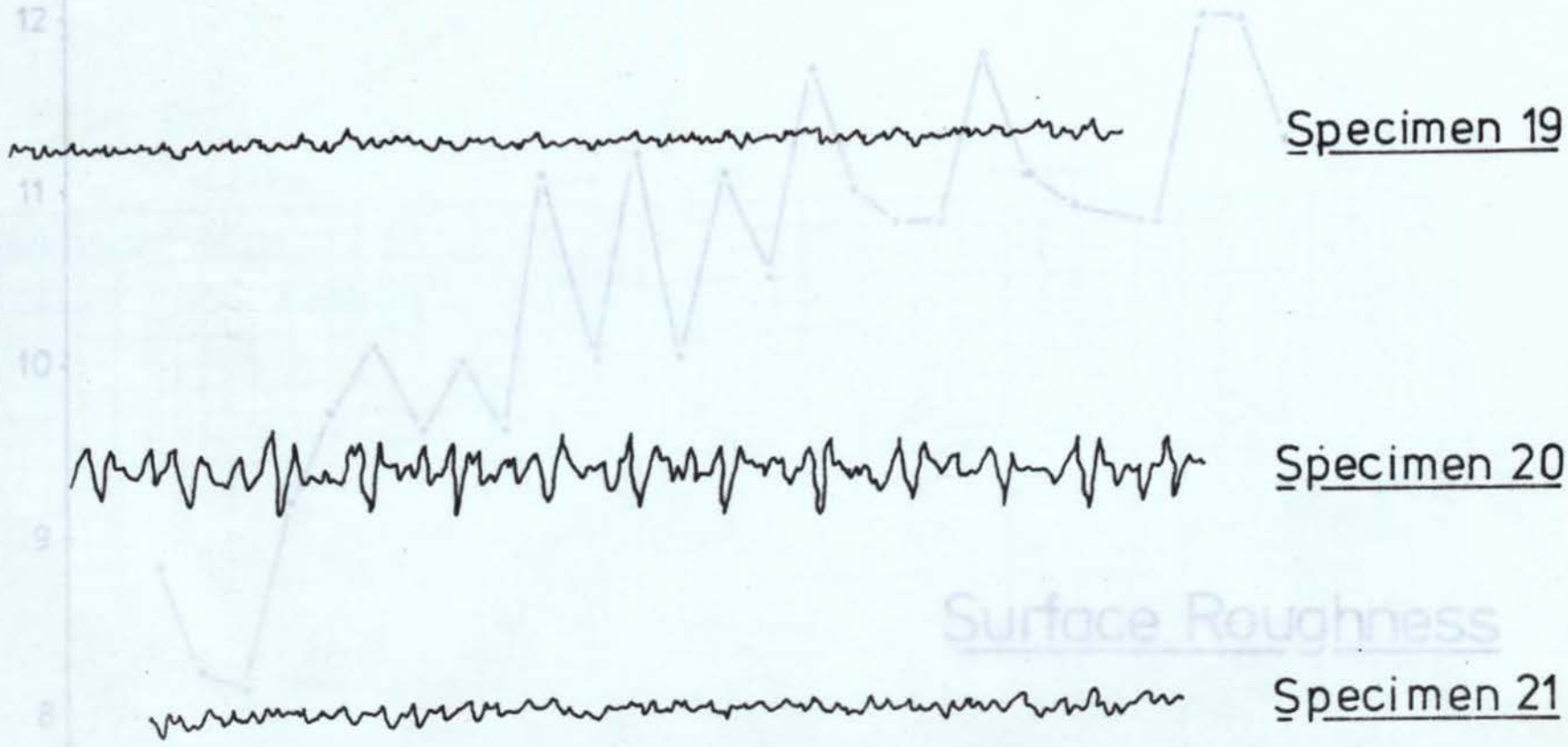

Fig.55. Vibration Levels Whilst Grinding Specimens 19,20,21,

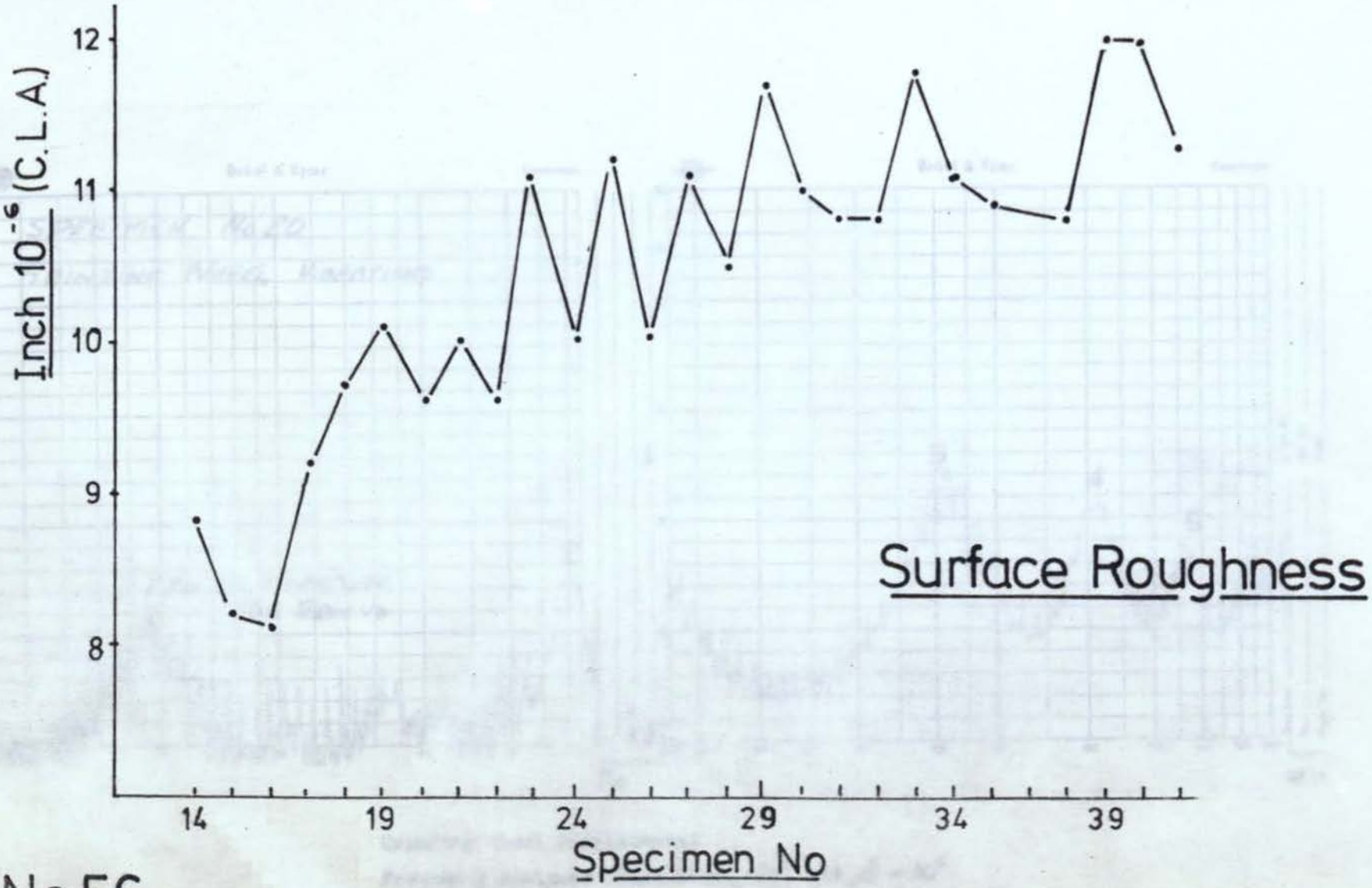
Inch 10^{-6} (C.L.A.)
12
11
10
9
8
14
19
24
29
34
39
Specimen No
Surface Roughness

Fig. No. 56.

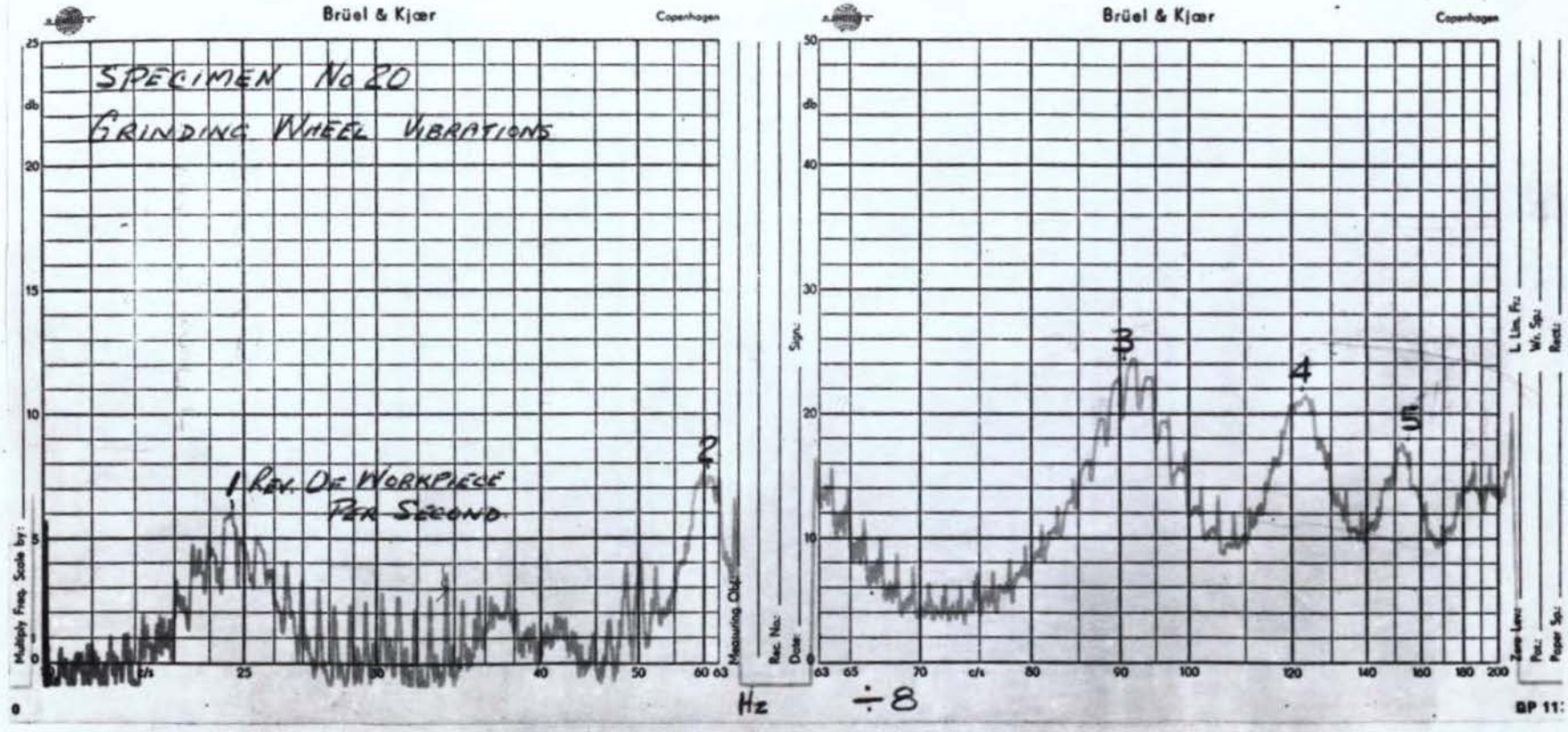

Grinding Wheel Displacement

Frequency Analyser Chart for α = 20° and β = 20°
(Frequency ÷ 8)

Fig 57

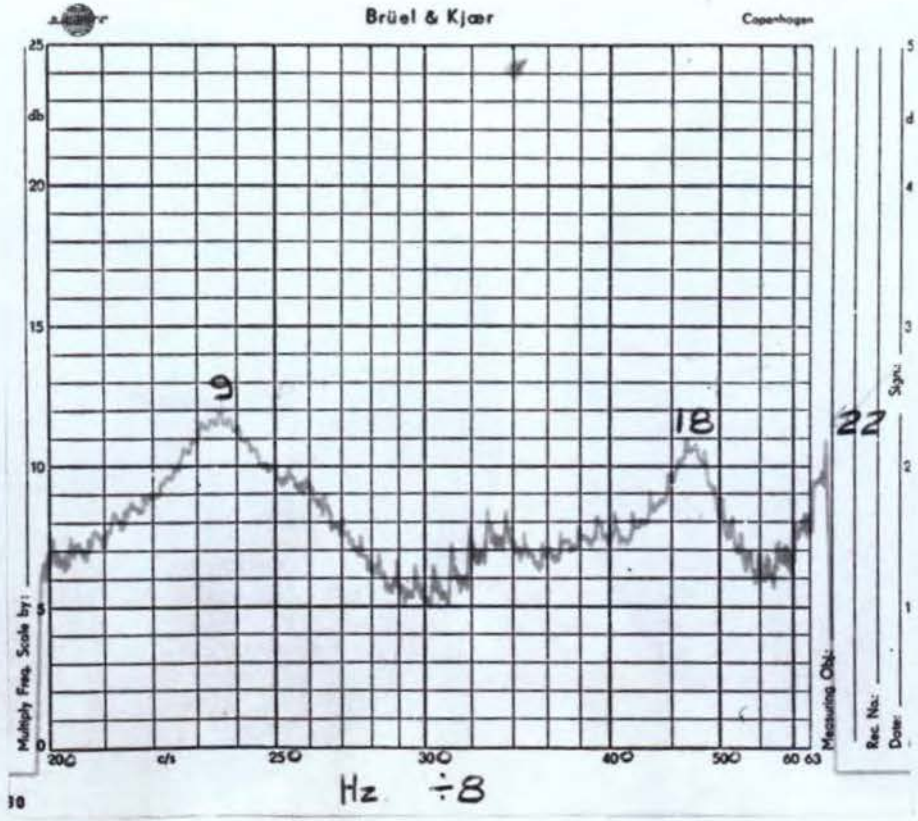

Fig. 57 continued

Fig 58

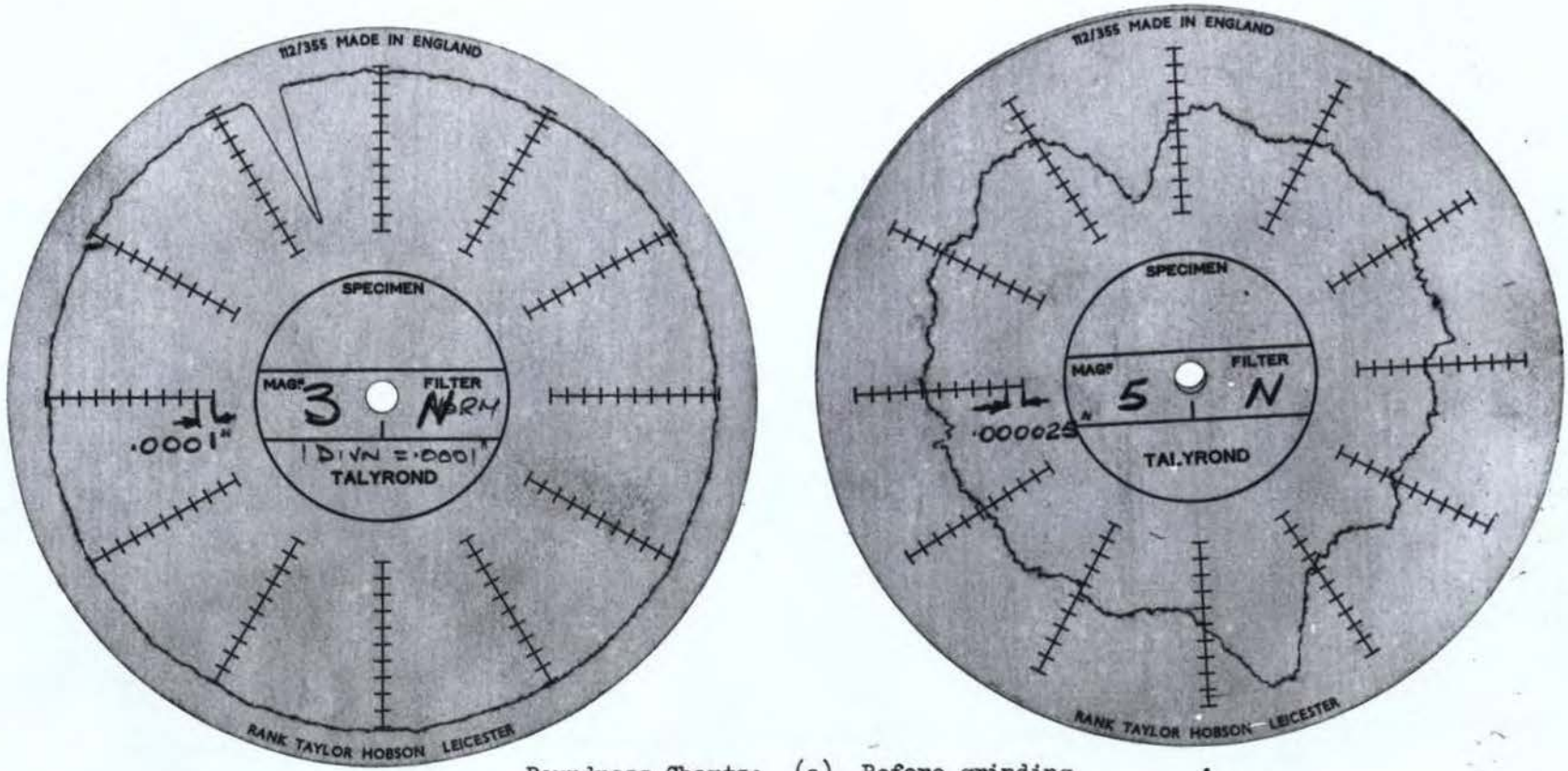

a b

Roundness Charts: (a) Before grinding
(b) After grinding

For α, =30° and β = 0°

Fig 59

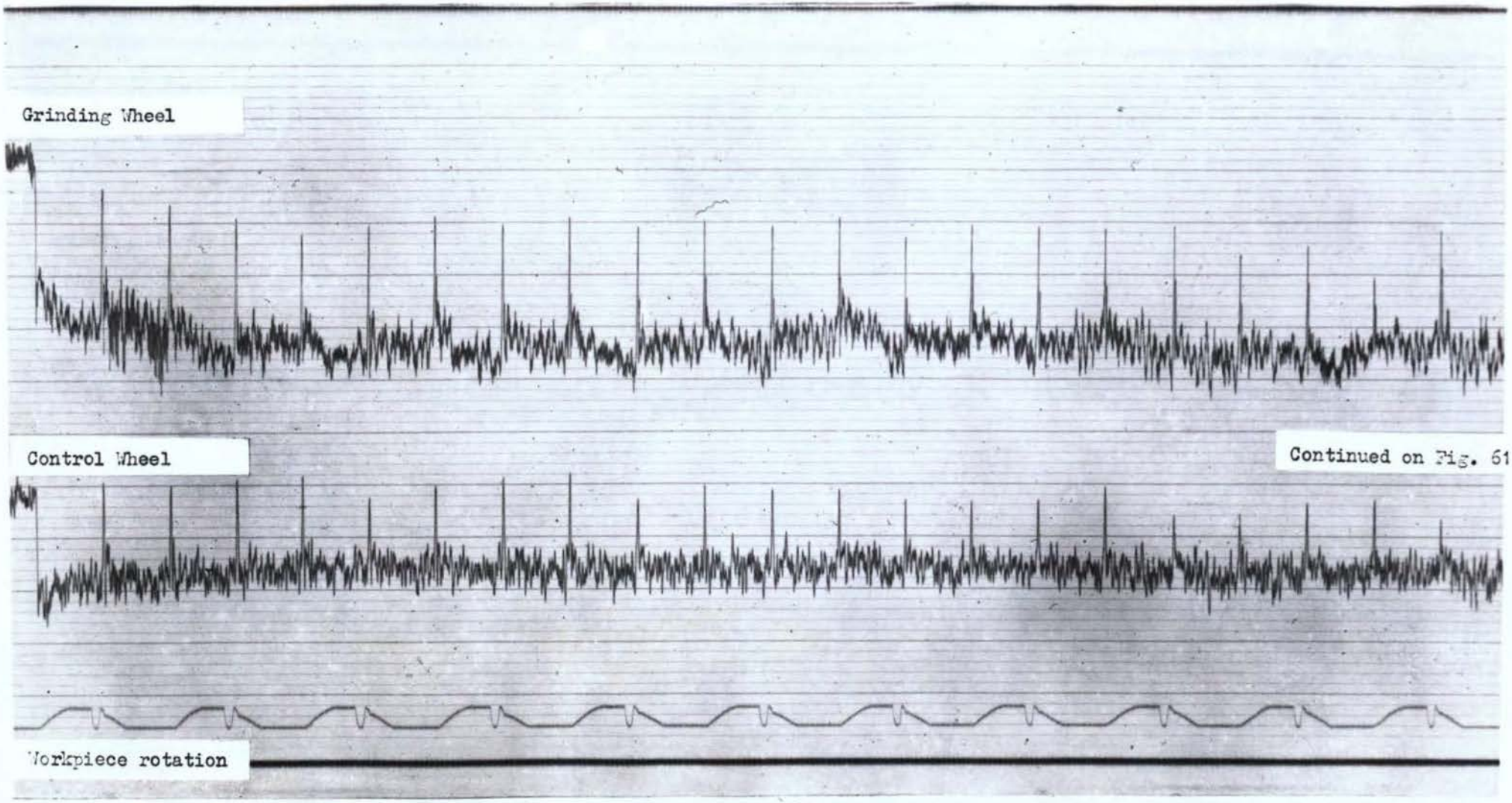

Grinding Test: Grinding wheel deflections
Control wheel deflections
Workpiece rotation

For $\alpha = 30^\circ$ and $\beta = 0^\circ$

Fig 60

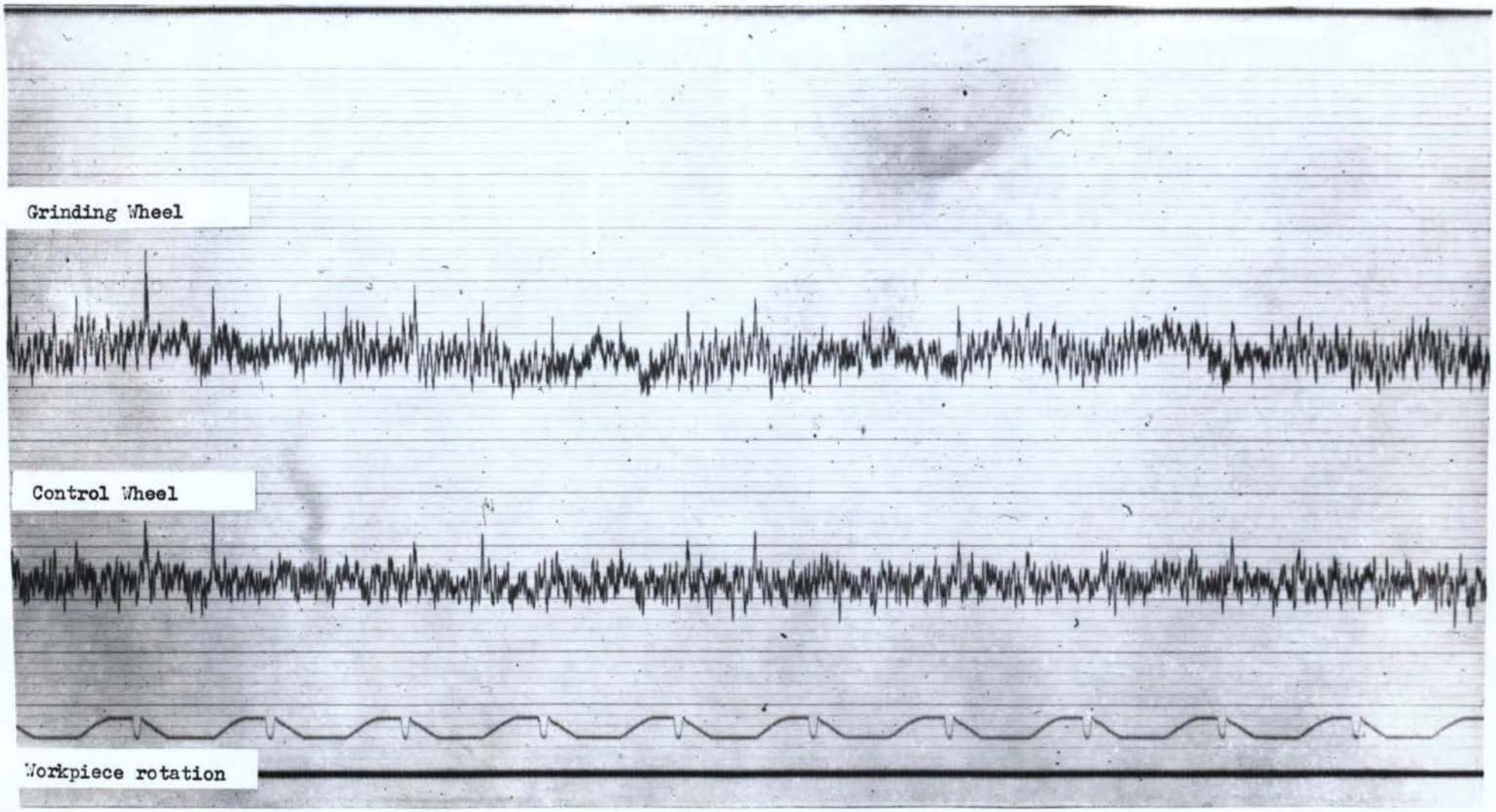

Fig 61

Fig. 60 Continued

Fig 62 Grinding Stiffness Test

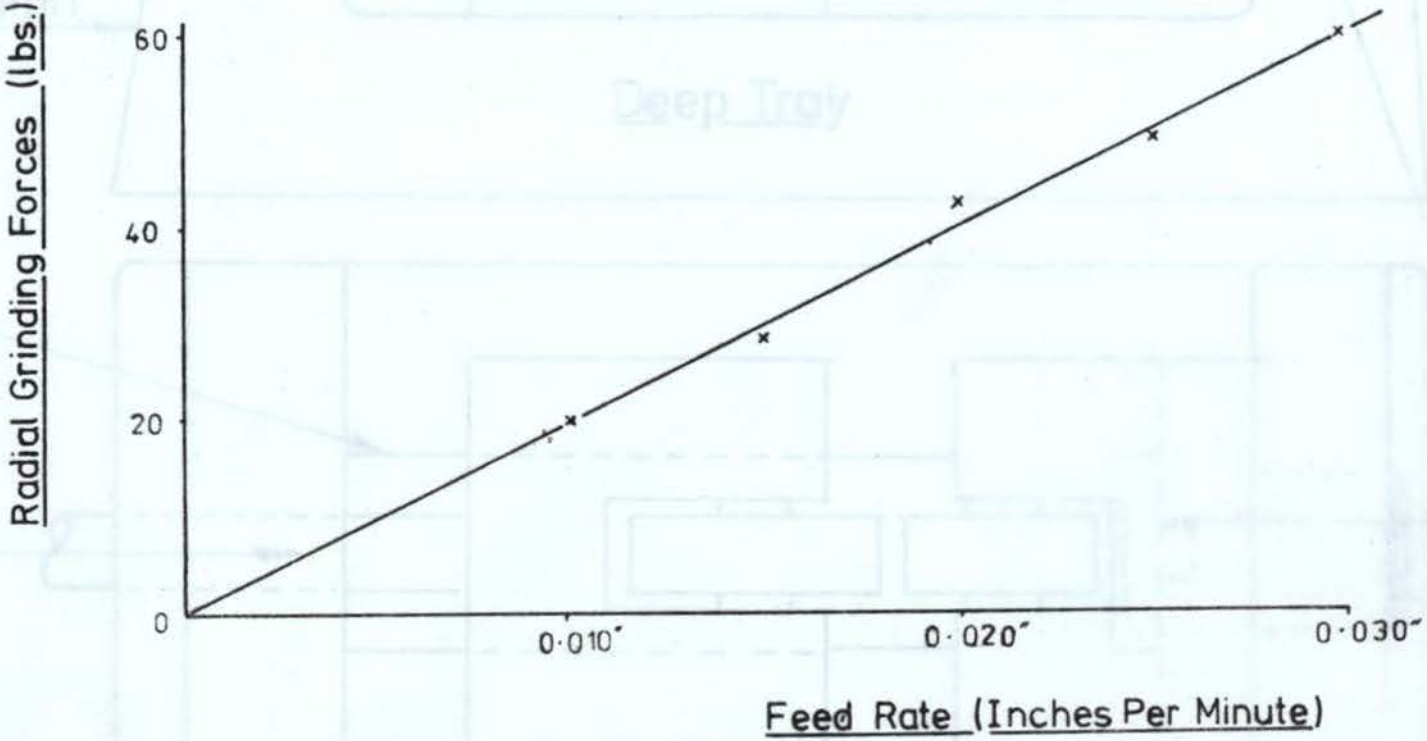

Grinding Forces

Fig.63.

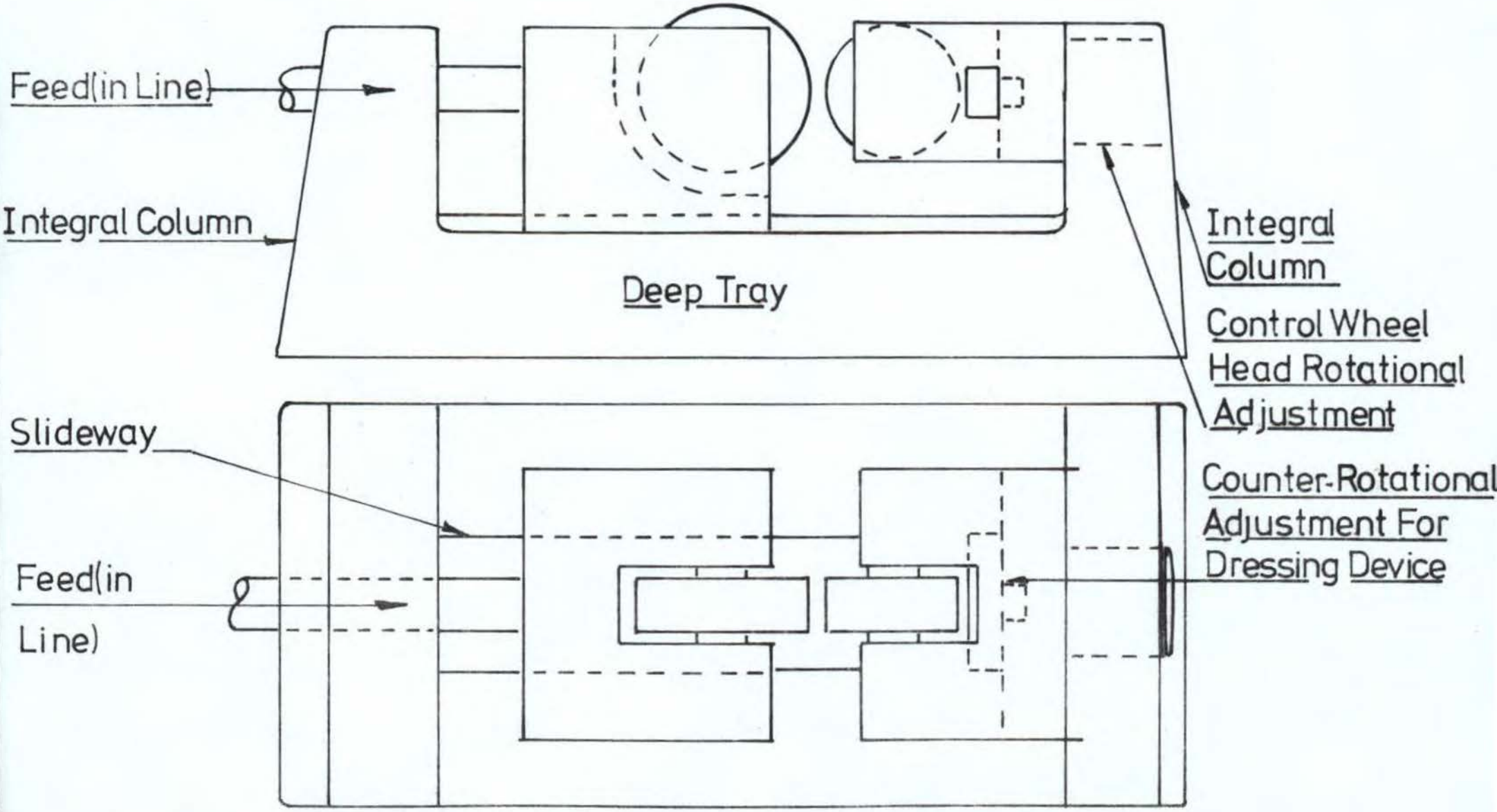

Fig 64. Proposed Design